RESEARCH

UDOT CONNECTING COMMUNITIES

Utah Department of Transportation - Research Division
4501 South 2700 West, Box 148410 - Salt Lake City, Utah 84114-8410

Report No. UT-08.03

DYNAMIC CHARACTERISTICS OF NEW BRIDGES I-15 RESEARCH, PHASE III

TESTING AND MODELING OF THE I-15 FLYOVER, C-846; VINE STREET OVERPASS, C-814; AND CHERRY HILL, C-123 BRIDGES

Prepared For:
Utah Department of Transportation
Research Division

Submitted By:
Utah State University
Dept of Civil & Environmental Engineering
Logan, Utah

Authored By:
Marvin W. Halling, Paul J. Barr,
James A. Bay, Kai H. Hsich,
Michael Hales, Troy Dye, Robert Esplin,
Travis Thurgood, & Austin Ball

August 2006

THIS PAGE INTENTIONALLY LEFT BLANK

DISCLAIMER NOTICE

The authors alone are responsible for the preparation and accuracy of the information, data, analysis, discussions, recommendations, and conclusions presented herein. The contents do not necessarily reflect the views, opinions, endorsements, or policies of the Utah Department of Transportation or the US Department of Transportation. The Utah Department of Transportation makes no representation or warranty of any kind, and assumes no liability therefore.

THIS PAGE INTENTIONALLY LEFT BLANK

UDOT RESEARCH DIVISION REPORT ABSTRACT

1. Report No. **UT-08.03**	2. Government Accession No.	3. Recipients Catalog No.
4. Title and Subtitle DYNAMIC CHARACTERISTICS OF NEW BRIDGES I-15 RESEARCH, PHASE III TESTING AND MODELING OF THE I-15 FLYOVER, C-846; VINE STREET OVERPASS, C-814; AND AND CHERRY HILL, C-123 BRIDGES	5. Report Date 09 August 2006	
7. Authors Marvin W. Halling, Paul J. Barr, James A. Bay, Kai H. Hsieh, Michael Hales, Troy Dye, Robert Esplin, Travis Thurgood, and Austin Ball	8. Performing Organization Report No.	
9. Performing Organization Name and Address Department of Civil and Environmental Engineering Utah State University Logan, Utah 84322-4110	10. Work Unit No. 81F15302 / 8RD0711H 11. Contract No. 04-9150	
12. Sponsoring Agency Name and Address Utah Department of Transportation Research Division 4501 South 2700 West PO Box 148410 Salt Lake City, Utah 84114-8410	13. Type of Report Period Covered Final Report, 2003-2006 14. Sponsoring Agency Code TB00.302	
15. Supplementary Notes		
16. Abstract Several bridges were instrumented with velocity transducers and accelerometers and were vibrated using harmonic forcing and impact forcing. Modal parameters were determined and monitored during the entire process. Finite element models were created for each bridge and calibrated using the field results. The modal parameters from the field were compared with those from the finite element models. In general the models yielded excellent results for the lower modes of the structures. The testing also provides a benchmark for the three bridges tested in order to compare future results.		
17. Key Words condition assessment, structural health monitoring, strong motion instruments, bridge instrumentation, dynamic modal testing, impact testing.	18. Distribution Statement	

19. Security Classification (for this report) Unclassified	20. Security Classification (for this page) Unclassified	21. No. of Pages 117	22. Price

THIS PAGE INTENTIONALLY LEFT BLANK

DYNAMIC CHARACTERISTICS OF NEW BRIDGES
I-15 RESEARCH, PHASE III

TESTING AND MODELING OF THE I-15 FLYOVER, C-846; VINE STREET OVERPASS, C-814; AND CHERRY HILL, C-123, BRIDGES

A Research Report Submitted to the
Utah Department of Transportation

Report UT-08.03

By

Marvin W. Halling
Paul J. Barr
James A. Bay
Kai H. Hsieh
Michael Hales
Troy Dye
Robert Esplin
Travis Thurgood
Austin Ball

Department of Civil and Environmental Engineering
Utah State University
Logan, UT

August 2006

THIS PAGE INTENTIONALLY LEFT BLANK

TABLE OF CONTENTS

DISCLAIMER NOTICE i
UDOT RESEARCH DIVISION REPORT ABSTRACT..... iii
LIST OF FIGURES ix
LIST OF TABLES xi

1.0 EXECUTIVE SUMMARY AND IMPLEMENTATION 1

2.0 INTRODUCTION 5

3.0 LITERATURE REVIEW 7
3.1 Vibrational Excitation 8
3.1.1 Forced Vibration Excitation..... 9
3.1.2 Ambient Vibration Excitation..... 10
3.1.3 Free Vibration 11

4.0 I-15 FLYOVER BRIDGE—C846 13
4.1 Bridge Description 13
4.2 Field Testing 16
4.2.1 Instrumentation 16
4.3 Analytical Modeling 22
4.3.1 Finite Element Modeling 22
4.3.1.1 Stick Model 24
4.3.1.2 Frame Model 25
4.3.1.3 Shell Model 26
4.4 Results 28
4.4.1 Analysis Results from Finite Element Models 28
4.4.1.1 Stick Model 28
4.4.1.2 Frame Model 29
4.4.1.3 Shell Model 30
4.4.2 Analysis Results using System Identification Approaches..... 34

5.0 VINE STREET BRIDGE—C814 45
5.1 Bridge Description 45
5.2 Field Testing 45
5.2.1 Instrumentation 45
5.3 Analytical Modeling 46

5.3.1 Finite Element Model 46
5.3.2 System Identification Method 46
5.4 Results 47

6.0 CHERRY HILL BRIDGE—C123 51
6.1 Bridge Description 51
6.2 Field Testing 53
6.2.1 Instrumentation 53
6.3 Analytical Modeling 55
6.3.1 Finite Element Model 55
6.3.1.1 Stick Model 56
6.3.1.2 Beam Model 61
6.3.2 System Identification Method 64
6.4 Results 65

7.0 CONCLUSIONS 67

8.0 ACKNOWLEDGEMENTS 71

9.0 REFERENCES 73

APPENDICES 81
Appendix A Summary of Test Instruments 83
Appendix B Mass Participation Ratios and Mode Shapes for Stick Model 87
Appendix C General Testing Procedure and Summary of Collected Data Files 91
Appendix D Information for Peak Picking, ERA and ERA-OKID, and FDD Methods 97
Appendix E Frequencies for Forced and Ambient Vibration 99

ACRONYMS 105

LIST OF FIGURES

Figure 4.1 Aerial view of structure C-846. 13
Figure 4.2 Instrumentation of structure C-846. 15
Figure 4.3 Tested portion of section C-846. 15
Figure 4.4 Permanent instrumentation. 19
Figure 4.5 Temporary instrumentation for setup 1. 21
Figure 4.6 Temporary instrumentation for setup 2. 21
Figure 4.7 Temporary instrumentation for setup 3. 21
Figure 4.8 Temporary instrumentation for setup 3. 22
Figure 4.9 Structure C-846 and adjacent structures. 23
Figure 4.10 Stick model. 24
Figure 4.11 Average dimensions of cross-sections. 25
Figure 4.12 Frame model. 25
Figure 4.13 Section view of frame mode in SAP 2000. 26
Figure 4.14 Isometric view of a section of the shell model. 27
Figure 4.15 First ten mode shapes for frame model. 33
Figure 4.16 Eccentric mass shaker. 34
Figure 4.17 Typical forced vibrational seismometer time history. 36
Figure 4.18 Typical forced vibrational accelerometer time history. 36
Figure 4.19 Forced vibration mode shapes 1 through 24 (continued on page 39). 38
Figure 4.20 Vertical and longitudinal mode shapes for modes 1 through 12. 40
Figure 5.1 Orientation and instrumentation setup of Vine Street Bridge. 45
Figure 5.2 First ten mode shapes obtained by ERA. 50
Figure 6.1 Elevation view of Cherry Hill Bridge. 52
Figure 6.2 Skewed girder over bent. 52
Figure 6.3 Eccentric mass shaker. 53
Figure 6.4 Transverse and longitudinal seismometers. 54
Figure 6.5 Instrument locations. 55
Figure 6.6 Stick model. 57
Figure 6.7 Stick model cross-sections. 58
Figure 6.8 Selected modal shapes (continued on page 60). 59
Figure 6.9 Beam model. 61

Figure 6.10 Girder frame cross-section. 62
Figure 6.11 Selected modal shapes (continued on page 64). 63
Figure 6.12 Typical normalized displacement plot.....65

LIST OF TABLES

Table 4.1 Seismometer instrument calibration factors. 17
Table 4.2 Comparisons of testing environment during setups.....18
Table 4.3 Box and channel locations and description (Petty 2001).....20
Table 4.4 Stick model modal periods and participating mass ratios.....29
Table 4.5 Frame Model modal periods and participating mass ratios 30
Table 4.6 Shell Model modal periods and participating mass ratios 31
Table 4.7 Periods comparisons of stick, frame, and shell models. 32
Table 4.8 Average natural frequencies using the peak-picking method. 37
Table 4.9 Dominant direction of modes. 41
Table 4.10 Files taken for three different stages.....42
Table 4.11 Identified natural frequency results at different stages. 42
Table 4.12 Natural frequencies results from FDD and ERA-OKID. 43
Table 4.13 Modal frequency comparison between analytical and field testing models. ...43
Table 5.1 Natural frequency comparison between ERA and HP analyzer. 47
Table 5.2 Natural frequency results for first ten modes.....48
Table 5.3 Natural frequencies and comparisons. 50
Table 6.1 Stick model section properties. 57
Table 6.2 Stick model results. 59
Table 6.3 Beam model sectional properties. 62
Table 6.4 Beam model results. 62
Table 6.5 Cherry Hill Bridge comparison summary. 66

THIS PAGE INTENTIONALLY LEFT BLANK

CHAPTER 1

EXECUTIVE SUMMARY AND IMPLEMENTATION

The transportation system in the USA is experiencing an ever increasing demand for higher levels of performance. These higher performance levels include increased durability, preservation of existing systems, longer design lives for new construction, and issues of security and safety against intentional attack. Since resources are limited, more accurate assessments of the "in-service" condition of structures is becoming increasingly important.

This report discusses the testing and modeling of three bridges in the Salt Lake City Utah area. The first bridge, C-846, is a steel girder flyover where I-80 connects to I-15. The second bridge, C-814, bridges over I-15 on Vine Street. The last bridge, C-123, is an exit ramp off of Utah Highway 89 in Farmington, near the Cherry Hill Resort.

These three bridges were tested using forced and ambient vibrational analysis. Two different non-destructive methods were used to induce vibrations in the bridges. C-846 and C-123 bridges were tested using an eccentric mass shaker. C-814 was tested using a drop weight. In both cases at least 30 velocity transducers were used to acquire data on the response of the bridges. This data was then analyzed using a number of computer programs to determine the natural frequencies, and mode shapes for the different structures. This analysis was then compared to finite element analysis of the structures.

Finite element analyses were also used to determine the natural frequencies and mode shapes for each bridge. The models were then modified to more accurately represent the boundary conditions and structural properties.

I-15 Flyover Bridge, C846

For Bridge C-846, three levels of model were created; namely, a stick model, a frame model and a shell model. Each of these models were compared to the results of the forced and ambient vibration testing. For the first 5 modes, the forced vibration testing results were within 14 % of the results from the shell model.

Based on the comparison between the field testing and computer based finite element model, the stick model provides some basic geometry and material properties about the testing structures. In general, the frame model provides results with enough accuracy to be used to quickly verify the structural dynamic parameters. For research purpose, the shell model is recommended because it provides better precision of the testing structures. Mode shapes and modal frequencies for 10 modes were determined using each of the three models discussed. The field testing consisted of sinusoidal forced vibration testing and ambient vibration testing.

When comparing the first five modal frequencies of the more detailed shell model with the results from the forced vibration testing, the largest difference in frequencies was 14%. The first three modes were within 4% when comparing the model with the field results.

Vine Street Bridge, C814

This bridge was field-tested using both forced vibration testing as well as ambient vibration testing. The forcing used was a 4000 lb drop weight normally used for geotechnical site testing. This study is the first time that the authors are aware of this type of testing on a healthy, in-service highway bridge. In order to not damage the bridge or the bridge deck, the drop weight was lifted only approximately 4 inches off the deck and was dropped on a one inch thick neoprene pad.

The finite element model was compared with the results of both the forced vibration testing and the ambient vibration testing. Each comparison was made with the first 10 identified modes. The identified modal frequencies from the forced vibration testing differed from the model by at most 11% whereas the same comparison with the ambient data differed by at most 7%. These modal correlations are extremely good, particularly since the drop weight excited predominantly vertical modes.

Cherry Hill Bridge, C123

The Cherry Hill bridge was field-tested using the sinusoidal shaker as well as ambient vibration. The bridge was modeled using both a stick as well as a beam type model. The first 4 modal frequencies obtained from the forced vibration testing differed by up to 14% from those obtained from the beam finite element model. The relatively large differences may be attributed to concrete deck thicknesses that differed substantially from the specified thicknesses and affected both the bridge stiffness as well as the mass.

The ability of using different system identification methods have been demonstrated in this report. The natural frequencies and mode shapes can be identified using many system identification methods. ERA and peak picking methods have been successfully applied to forced vibration data. On the other hand, the dynamic properties of the testing structure can be extracted using ERA-OKID and FDD methods.

Results presented in this research reveal that both methods (ERA-OKID and FDD) can be applied to ambient and forced vibration data. Also, these methods provide similar results in modal frequencies using field-collected data.

Based on the results presented in the I-15 Flyover chapter, it appears that using an overlap in digital data processing did not produce better results. The results between the tests using the overlap compared to the results without the overlap are very similar. Some normalized variations were slightly higher while others were slightly lower. The

difference was so insignificant that there were no benefits found to use an overlap in future analysis.

Statistical analysis was also done to determine if temperature has an effect in the ranges of the natural frequencies. The temperatures ranged from -6°C to 28°C. The average natural frequencies were found for files with temperatures from -6°C to 0°C, from 0°C to 14°C, and from 14°C to 28°C. According to the results presented in the third chapter, the effect of temperature on the natural frequencies of the bridges is inconclusive at this time.

This research has been able to better identify the natural frequencies of the bridge while giving future researchers a better idea of the ranges of natural frequencies that can be expected over the course of a year. The natural frequencies determined here will be used in future analysis to identify changes to the dynamics of the structures. Although it appears that some natural frequencies have shifted slightly, further analysis is needed to identify whether the shifts are due to the normal ranges of natural frequencies or to changes in the structural dynamics of the bridge. Some variations in natural frequencies may be due to white noise, or the lack of ambient excitation to the bridge. These natural frequencies will give a good basis for future testing and analysis of these bridges.

For computer modeling, many different assumptions were used to create the models as explained throughout the text. Variations of these assumptions caused slight variations in the modal characteristics of each of the models. Many of the assumptions are based on the geometry and material properties of the structure. While the geometry and material properties were derived from the as-built plans, it is likely that the actual geometry and material properties vary slightly from the assumed design values.

Implementation

The anticipated implementation of the current research is in the area of continued investment into long term monitoring of the transportation system for the State of Utah. The results described in this report are optimistic that the investment of money into instrumentation and monitoring of the infrastructure will lead to better information regarding the function and health of the system and will facilitate decision making in the future. The future health of the system will be affected by slow moving damage (age deterioration of components) which is encompassed in the overall goals of asset management, as well as faster acting damage such as earthquake, impact, scour, wind, or other damage mechanisms.

The authors strongly recommend that the Utah Department of Transportation support an ongoing program of health monitoring instrumentation including an assortment of sensors. These instruments should include strong motion arrays (accelerometers), geotechnical monitoring devices for settlement, slope stability, bridge pressures, etc., and other structural and pavement embedded and non-embedded devices.

The closely monitored systems in the future will lead to a more “intelligent” management of the state’s transportation infrastructure.

CHAPTER 2

INTRODUCTION

Thousands of large scale civil structures such as high-rise buildings, highway bridges, dams, heavy industry complexes, and nuclear facilities have been built all over the world in the past century. These civil structures are aging and many are reaching the end of their design lives. In addition, many structures encounter severe environmental conditions such as hurricanes or earthquakes during their service lives. To be able to ensure the public safety, engineers must be able to monitor structural performance. Therefore, the capability of obtaining basic structural parameters using generalized system identification methods can be very valuable and desirable.

In the field of non-destructive evaluation and damage detection, there is a continued interest in the utilization of vibrational techniques. Structural damage will result in permanent changes in structural stiffness, changes in the distribution of stiffness, and changes in relevant material properties. These changes may be detected in the study of the dynamic behavior of the structure. Because of the direct relationship of mass, damping, and stiffness of a multi-degree-of-freedom to the natural frequencies, modal shapes, and modal damping values, many studies have been directed at using these properties for the purpose of structural health monitoring.

Periodic visual inspection of highway structures is intended to identify and prevent failures. Typically, inspections are cursory in nature and do not contribute significantly to the knowledge of the health of a structure, but instead only call attention to minor maintenance issues. It is required for inspectors to understand at what point a structure could fail. Damage in the early stages of development may go unnoticed and cracks in load-bearing members could enlarge to hazardous proportions between inspection intervals (Biswas, Pandey and Samman, 1990).

While not every failure can be prevented, structural health monitoring provides the possibility to discover and prevent many failures or provide warning of impending failure. The goal of bridge testing is to maximize the structure performance and minimize the public safety risk. This can be difficult to achieve by conventional methods due to intricacies or accessibility of the structure, such as offshore platforms, long span bridges, and even tall buildings. Not only are these and many other types of structures difficult to thoroughly inspect, it is also dangerous to have people investigate them.

Therefore, an improved system to monitor and inspect these structures needs to be developed. A step in the direction of this effort is developing an understanding of how to adequately model these structures using computer-modeling techniques. The focus of this work is the development of a computer model of each full-scale bridge which has been calibrated using field determined properties to provide a baseline for future comparison.

In the long term, computer models should be able to directly link to the sensors to determine the healthy condition of the civil structures by analyzing their natural frequencies and other modal parameters. Development of quick warning from each civil structure should be done for large or important civil structures. A communication network should be developed to frequently update the structural health information. Online information for general public awareness could be developed in real time.

CHAPTER 3

LITERATURE REVIEW

In the field of non-destructive evaluation and damage detection, there is a continued interest in the utilization of vibrational techniques. Vibration testing has been used for many years to assess dynamic characteristics of structures. Advances in technology have made the availability of instrumentation much more accessible than it was only a few years ago. Structural health monitoring implements these technologies in much the same way as a physician uses his instruments to detect problems in a human body.

Structural damage generally will result in permanent changes in structural stiffness, changes in the distribution of stiffness, and changes in relevant material properties. These changes may be detected in the study of the dynamic behavior of the structure. Because of the direct relationship of mass, damping, and stiffness of a multi-degree-of-freedom to the natural frequencies, modal shapes, and modal damping values, many studies have been directed at using these properties for the purpose of structural health monitoring.

Damage usually changes the physical properties such as mass or stiffness of the structure. The localization and quantification of damage evaluations are based on the measured difference in stiffness in different stages. The authors first utilized system identification (SI) techniques as mentioned in the previous section to obtain eigenstructure which includes the eigenvalues and eigenvectors of a system.

The methodology used includes a mathematical model and computer finite element model. The computer model is constructed and used to simulate the problem. The natural frequencies and modal shapes are then obtained from the structures accompanying a finite element model to determine if the structure is in a healthy condition. The natural frequencies of a structure will depend on its materials and geometry. The natural frequencies may be excited by trucks moving on the highway, strong wind, and so on. Thanks to the modern technology, natural frequencies can be obtained by installing sensors at certain locations.

Vandiver (1975) used the changing modal frequency to detect the damage in an offshore structure. Loland and Dodds (1976) used the relative change of natural frequencies to predict the location of the structural damage in North Sea. Liu and Yao in 1978 used modal analysis to determine the dynamic behavior of offshore structures. Cawley and Adam (1979) used changing natural frequency to determine the damage location in a two-dimensional structure. Tsai and Yang (1988) pointed out that if one can determine the engenvalues and eigenvectors of a system, then the mass, stiffness, and damping matrices of the system are simply the products of the eigenvalue and eigenvector matrices. Turner and Pretlove (1988) found that ambient vibrations produced by traffic could be used to find the natural frequencies of a bridge and changes in the

frequencies of as little as 5% could indicate significant structural damage. Spyrakos et al (1990) found a solid correlation between dynamic properties and the amount of damage. Stubbs and Osegueda (1990) developed an approach to detect damage. The approach was based on the sensitivity of changing modal frequencies. Salane and Baldwin (1990) performed testing on a singe-span bridge model that was tested before and after the flange of its steel beam was cut. A three-span bridge was also tested after fatigue load testing. For both tests the natural frequencies of each identified mode significantly decreased.

Sannan, Biswas and Pandey (1991) investigated a scale model of a typical highway bridge to determine the changes of modal parameters as related to crack propagation in the girders. The method used was found to be useful in identifying relatively small cracks as well as approximating the location of the crack. Pandey and Biswas (1994) used changes in flexibility to detect damage in structures. They also found that structural damage can be found from changes in natural frequencies. Changes in a structure are made evident by modifying the modal parameters such as natural frequencies, modes of vibration and modal damping. Alampalli, Fu, and Dillon (1995) investigated the sensitivity of measured modal parameters and concluded the modal frequencies may be used to identify the existence of damage in highway bridges. Liu (1995) performed an identification and damage detection study on a truss structure using modal data. Measured natural frequencies and modal shapes of a structure were used in the identification process.

Stubbs and Kim (1996) developed a methodology to localize and estimate the severity of damage in structures without baseline modal parameters. The writers utilized changes in mode shapes of structures to locate and estimate severity when only post-damage modal parameters are available. Salawu (1997) summarized a review for damage detection by frequency changes. Farrar and Doebling (1998) showed the fundamental frequency changed on the order of 5 percent during a 24 hour testing period. Oh and Jung (1998) proposed an improved damage detection assessment algorithm based on the method of system identification. The characteristics of a structure are defined in terms of the stiffness, damping, and mass matrices in a finite element formulation. Zhao and DeWolf (1999) presented a demonstration showing that modal flexibility was more sensitive than natural frequency and modal shapes in damage detection. Ren and De Roeck (2002) established the relation between damage and change of structural dynamic characteristics such as structure stiffness by using an experimental program of a reinforced concrete beam.

3.1 Vibrational Excitation

The civil engineering structures such as a pedestrian walkway between two connected buildings, commercial buildings, industrial complexes, and highway bridges can be tested by three major ways: forced vibration, ambient vibration, and free vibration. Structural vibration monitoring using a known vibration source has several significant advantages when compared with monitoring using ambient vibration sources. Just as a

monitoring scheme is designed to capture certain aspects of the potentially faulty behavior of a structure, the excitation can also expose desired aspects or behavior of the structure.

The reasons for the use of ambient excitation are varied, but its benefits include low cost, less disruption to traffic and function, availability of long-term excitation, and in some cases, more appropriate frequency band to the structure. Factors which make the use of ambient excitation less than ideal include the variability in amplitude, duration, direction, frequency content, and difficulty in accurately measuring the excitation.

3.1.1 Forced Vibration Excitation

Forced vibration is one of the available experimental procedures used to excite a structure. Forced vibration is very popular for small structures and mechanical systems. The input forces can be accurately measured using this approach. The main concept of forced vibration is to apply a force of sufficient magnitude to the structure in order to produce useful response amplitudes and lead to more major excitation of the modes of vibration.

Forced vibration can be divided into two areas: the first one is that the tested structure attached to the ground undergoes a displacement such as a simulated earthquake vibration. The second one is a force applied to the tested structures. For example, a force generated by an eccentric mass shaker can be a popular approach. Salawu and Williams (1995) conducted full-scale forced vibration tests before and after structural repairs on a multi-span reinforced concrete highway. A hydraulic vibrator was used to artificially excite the bridge. Nielson, Womack, and Halling (1999) performed a forced vibration test on a nine-span bridge using a shaker machine. The natural frequencies and the associated mode shapes of the bridge were obtained. Halling, Muhammad, and Womack (2001) performed seven forced vibration tests on an isolated single span of freeway overpass structure. The results showed that dynamic response is sensitive to changes in mass, damping, and stiffness of a structure.

In addition to the above, Aktan et al. (1997) and Catbas and Aktan (2002) used truck load as the excited force for highway bridges. Womack, Halling, and Bott (2001) used a fully loaded dump truck for steel girder bridge testing. Chotickai and Bowman (2006) also performed a similar test.

Eccentric mass shakers often use large rotating eccentric masses to produce a sinusoidal vibration in one horizontal direction in order to produce sinusoidal vibration. The sinusoidal inputs usually offer a much higher signal-to-noise ratio, thus it can reduce the possibility of contaminating the results with other sources of excitation. Applications of utilizing eccentric mass shaker on highway bridges can be found in Kramer, De Smet, and Peeters (1999a), Kramer, De Smet, and De Roeck (1999b), Kim and Stubbs (2003). McManus, Hamilton, and Puckett (2003) used an eccentric-mass oscillator to find the

dynamic characteristics of a cantilevered traffic signal structure. Applications used on buildings can be found in Jennings, Matthiesen, and Hoerner (1971) and Yu et al. (2005).

Impact testing utilizes an impact hammer to excite the testing structure. It works like an ordinary hammer. The weight of an impact hammer can be adjusted to allow different force levels to be input to the structure. One holds the impact hammer in much the same way as one holds a regular hammer and quickly strikes the structure being tested. Care should be taken to assure the hammer hits the structure only once. The advantage of using impact hammers is that they are fast to use and relatively inexpensive. The impact hammer usually does not attach to the testing structure so it does not alter its dynamic characteristics. When conducting non-destructive testing, care should be taken so the hammer does not hit the structure too hard or damage it. An example for impact testing on a highway bridge in Utah can be found at Halling, Muhammad, and Womack (2001). In addition, a concrete frame and columns were studied using a shaking table (Dolce et al. 2005, Benavent-Climent 2005).

3.1.2 Ambient Vibration Excitation

Ambient vibration to tested structures happens naturally in different environments and it is typically considered random. Ambient vibration could include vibrations due to wind, traffic, micro-seismicity, water, and other driving sources. Ambient vibration is often used for long-term structural health monitoring. Gentile and Cabrera (1997) performed a theoretical and experimental investigation of a cable-stayed bridge after a major repair. The experimental program included both traffic-induced and free vibration measurements.

DeWolf, Culmo, and Lauzonn (1998) presented different monitoring approaches in the assessment of Connecticut's bridges. Long-term bridge monitoring information caused by ambient vibration was collected and analyzed. Structural vibration monitoring is often carried out utilizing ambient vibrations for the excitation of a structure.

Many studies have been conducted by utilizing a variety of ambient excitation sources. Examples of studies which use the following sources of ambient excitation include wind (Abdel-Ghaffar and Scanlan 1985a, 1985b, Jones and Scanlan 2001, Xu, Xia and Yan 2003); seismic activity (Chang and Lin 2004); automobile or train traffic (Huang 2001, Kou and DeWolf 1997, Li, Su and Fan 2003, Calcada, Cunha and Delgado 2002, Xu, Ko and Zhang 1997, Xu et al. 2003, Harik et al. 1997, Chang, Chang and Zhang 2001, and Ren et al. 2004, Heckl, Hauck and Wettschureck 1996, Yang, Yau and Hsu 1997, Li and Su 1999, Kaynia, Madshus and Zackrisson 2000, Degrande and Schillemans 2001, Yang et al. 2004b, Museros and Alarcon 2005, Paolucci and Spinelli 2006; waves or tidal fluctuations (Vandiver 1975, Loland and Dodds 1976, and Liu and Yao 1978); and industrial ground vibration from adjacent industries, etc.

Utilizing some knowledge and some assumptions regarding the excitation, the data analysis is very important. Common assumptions regarding the excitation and

system identification include stationary, white, and unidirectional or pre-determined multidirectional. There have been a great number of different analysis procedures developed to extract the modal characteristics of structures. Frequency Response Functions (FRFs) are usually used prior to running a modal identification algorithm. Even though there are many identification algorithms available, FRFs are still the most popular approach.

A wind load testing for a tall building can be found at Yue et al. (2005). Similar research can be found in (Xu and Kwok 1993, Chen and Yuan 2000, Wu and Pan 2002, Yang et al. 2004a, Wu, Lu and Hsu 2006) In addition, several studies on wind speed effects can be found in Tschanz and Davenport 1983, Gioffre et al. 2000, Chen and Kareem 2005, Hanzlik et al. 2005, Vickery and Skerlj (2005). A database based study on wind effect estimation on industrial complexes was presented by Hanzlik et al. (2005) and Rigato, Chang, and Simiu (2001). A case study of floor vibration induced by walking can be found in Hanagan (2005). Similar studies on man-induced vibration can be found in Wheeler 1982, Bachmnann 1992, Fujino et al 1993, Wilkinson and Knapton 2006. A fatigue damage analysis using truck loading for a steel girder bridge can be found in Wang et al. (2005).

3.1.3 Free Vibration

Free vibration occurs when the tested structures are displaced from their original position of rest, then released. The response is then measured as the structures vibrate freely. The amplitude usually decreases gradually depending when the energy dissipated into the system. A detailed description of free vibration testing about Z24 bridge can be found in Kramer, De Smet, and Peeters (1999a); and Kramer, De Smart, and De Roeck (1999b). In general, free vibrations occur in flexible systems when a body moves away from its original or at-rest position. The internal forces tend to move the body back to its at-rest position and the restoring forces are in proportion to the displacement. The acceleration of the body is directly related to the force on the body. The body moves in a simple harmonic motion.

In real civil structures, energy may be lost due to internal losses such as friction and heat generation. As a result, the magnitude of the free vibration response of a system will weaken with time. Free vibration techniques have been successfully applied to different civil structures. Cunha, Caetano, and Delgado (2001) utilized the sudden release of a 60-metric ton mass suspended from the deck of a large cable-stayed bridge to measure the free vibration. Chang and Lin (2004) used pulling and suddenly releasing to test a full-scale steel frame structure for free vibration test. Eberhard and Marsh (1997a) and Eberhard and Marsh (1997b) perform a displacement induced free vibration test by applying transverse loads to the bent of a three-span reinforced concrete bridge.

Nakash ima et al. (2005) performed a pushover analysis on a three story full-scale steel moment frame building.

CHAPTER 4

I-15 FLYOVER BRIDGE—C846

4.1 Bridge Description

The bridge tested and modeled is an overpass bridge on the 21st South Interchange of I-15 in Salt Lake City, Utah. The bridge is a connector from westbound I-80 to westbound SR-201. The bridge includes four individual structures containing a total of 25-spans with a total length of 1.14 km (3741 ft). The instrumentation and modeling was confined to a single 13-span structure with two expansion joints shown in Figure 4.1.

Figure 4.1 Aerial view of structure C-846.

Because modal parameters of the structure under consideration are highly dependent on the geometry and material properties that comprise the bridge, the structure is described in this chapter at length. Structure C-846 is a 13-span 722.65-meter long reverse curve steel girder bridge constructed during the I-15 Interstate corridor reconstruction project and was completed in 2000.

The spans are constructed of a transversely post-tensioned concrete deck supported by three steel girders. Reinforcing steel is epoxy-coated M284. Structural

steel is ASHTO M270M Grade 345. The strength of the cast-in-place concrete is f'_c = 28 MPa (4060 psi) with a 5% silica fume content (by weight). The steel girders are continuous, bearing on concrete-filled steel pipe piles. The bearing soils consist of extremely deep soft sediments.

The structure serves the purpose of connecting commuters traveling westbound from I-80 to the State of Utah's State Road 201 (SR-201), by crossing over I-15. Located among a number of other freeway interchanges, the structure traverses over the top of all but one providing a structure built on very tall columns. Of these columns, the minimum height is 12.61 meters and the maximum height is 23.80 meters, measured from the top of their respective foundations to the bottom of the bent cap.

Several structures in the 21st South Interchange were considered. It was decided to choose a structure with the number one priority to be placed on its research significance. The location of the selected bridge proved to be very difficult to access and instrument, but the selected bridge did provide the desired characteristics. The structure only carries traffic on two lanes in one direction, and is therefore a rather narrow structure with an outside deck width of 12.92 meters. The width, height and length characteristics, combined with the relatively light mass of the structure, result in a structure that is well suited for dynamic testing. The instrumentation was limited to the center portion of structure C-846 as can be seen in Figure 4.2.

Since the instrumentation is limited to structure C-846, this text will refer to bents and locations without identifying the structure; it is inferred that it is structure C-846. The numbering of the bents on structure C-846 begins at the south end of the structure C-846 and increments with the bridge northward. For more detailed information on this bridge and the instrumentation, refer to Petty (2002). Figure 4.3 shows the tested portion of the structure.

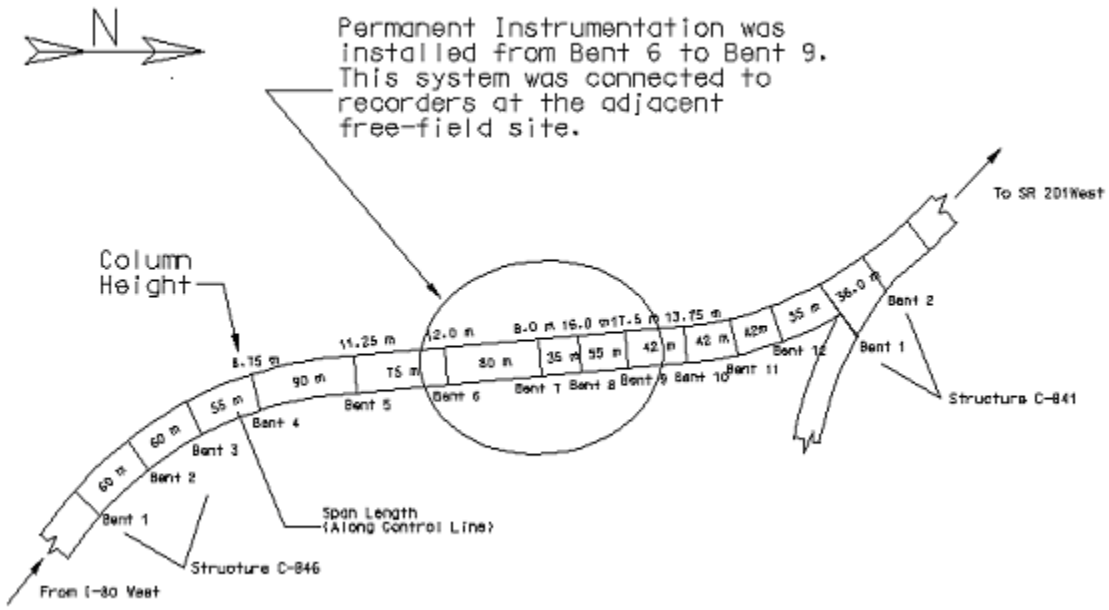

Figure 4.2 Instrumentation of structure C-846.

Figure 4.3 Tested portion of section C-846.

4.2 Field Testing

The location of instruments along a structure is critically important to effectively and efficiently discover possible mode shapes. Permanent, free field, and temporary sensor arrays were used to acquire data. Past research done by Jeffrey Hodson on a bridge located and tested in Switzerland influenced the decision to include more vertical seismometers than previously planned (Hodson, 2001). Due to the limited number of vertical seismometers available, three different setups were utilized to allow for greater coverage along the structure by these vertical instruments. The vertical instruments were moved, but the other instruments remained in the same position.

Over a three-year period, both ambient and forced vibration testing have been performed. The forced vibration excitation source was an eccentric mass shaking machine. This shaker was placed on a bridge bent below the deck so as to avoid interrupting traffic during testing. The ambient sources include traffic, wind, micro-seismicity, and other ground vibration sources. The results are presented in the later discussion section.

4.2.1 Instrumentation

The layout of the instrumentation was designed qualitatively to best determine the structural dynamics of the bridge. The channels were placed in the longitudinal, vertical, and transverse directions. Table 4.1 gives a summary of all the instruments used in this research along with their relative position on the structure.

Testing the same structure three different times permitted most of the transverse and longitudinal temporary instruments as well as all the permanent instruments to provide repeated data. This created an opportunity to compare how the resonant frequencies changed given a different type of testing environment. These comparisons will be discussed later. Table 4.2 illustrates the difference in temperature and traffic conditions between the three testing setups.

Past research has shown that only instruments within relatively close proximity of the forcing machine measure strong dynamic vibration. This structure contains instruments that are approximately 180 meters apart. Ideally, the shaker would need to be relocated along the bridge in order to encompass all the instruments within its forcing influence. Unfortunately, limited road closures and time restraints prevented this from occurring. To make the best of the situation the shaker was located in the middle of the structure on bent 7. The eccentricity of the masses was adjusted causing the forcing direction to be at a 45 degree angle relative to the axis of the bridge as shown in Figure 4.4.

Table 4.1 Seismometer instrument calibration factors.

Serial #	Bridge Reference	Volts/mm/sec	Natural Frequency	Damping
2317	T1	0.2723	0.98	0.289
2314	T2	0.2799	0.96	0.302
2319	T3 T29	0.2735	0.97	0.298
2321	T4	0.2763	0.99	0.284
2309	T5 T30	0.2755	0.96	0.288
2322	T6 Lground	0.2691	0.99	0.278
2320	T7	0.2663	0.97	0.284
2308	T8 T31	0.2696	1	0.273
2311	T9	0.2698	0.98	0.284
2312	T10	0.2702	0.96	0.301
2327	T11	0.2724	0.97	0.285
2326	T12	0.2729	1.01	0.278
2325	T13	0.2647	1	0.287
2324	T14	0.2694	0.97	0.294
2323	T15	0.2758	0.98	0.297
2304	T16	0.27	0.96	0.288
2303	T17	0.2718	1	0.278
2306	T18 L3	0.2765	1	0.292
2307	T19	0.2761	0.98	0.289
2315	T20 Tground	0.2703	1	0.292
2313	T21	0.2678	1	0.271
2316	T22	0.2696	0.98	0.287
2298	T23	0.2723	0.97	0.295
2299	T24	0.2689	1.01	0.268
2302	T25	0.2721	0.99	0.281
2301	T26	0.276	0.98	0.288
2300	T27	0.267	1	0.268
2305	T28 L4	0.2687	0.98	0.285
2310	L2	0.2738	0.97	0.29
2318	L1	0.2761	1	0.29
2293	V2 V4 V7	0.2694	0.97	0.29
2296	V3 V5 V13	0.2706	0.99	0.269
2297	V8 V15	0.2683	0.96	0.281
2294	V9 V10 V14	0.2769	0.99	0.288
2295	V6 V11	0.2711	0.96	0.298
2292	V1 V12 V16	0.2706	0.97	0.287

Table 4.2 Comparisons of testing environment during setups.

Setup	Date	Time	Cars/min	Weather
1	11 Jun 2001	3:15 am	None	Unknown
1	11 Jun 2001	9:25 am	Unknown	Rainy & cold
2	13 June 2001	5:30 pm	Unknown	12ºC
2	13 June 2001	6:00 pm	23	14ºC
2	13 June 2001	7:30 pm	Unknown	12ºC
2	13 June 2001	11:50 pm	None	12ºC
2	14 June 2001	1:00 am	Unknown	11ºC
2	14 June 2001	2:30 am	none	11ºC
2	14 June 2001	10:00 pm	14	16ºC
2	15 June 2001	5:00 am	Unknown	14ºC
2	15 June 2001	6:30 am	18	14ºC
3	19 June 2001	11:00 am	15	20ºC
3	19 June 2001	1:45 pm	23	24ºC
3	19 June 2001	3:45 pm	29	25ºC
3	20 June 2001	9:00 pm	13	25ºC
3	20 June 2001	11:30 pm	None	unknown
3	21 June 2001	2:15 am	none	22ºC

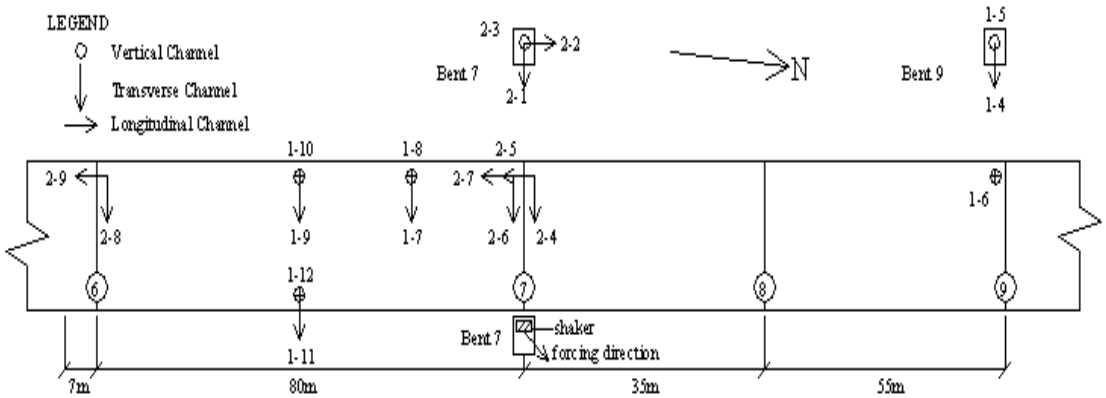

Figure 4.4 Permanent instrumentation.

The permanent array of instruments consists of 18 structural channels connected to two Kinemetrics K2 Recorders at an adjacent free field site. The Kinemetrics K2, hereafter referred to as simply K2, is a self-contained multiplexing digital recorder that is capable of recording up to twelve EpiSensor channels at sample rates of 50, 100, 200, or 250 sps. One of the K2s contains an additional internal tri-axial accelerometer. All of the instruments are Kinemetrics EpiSensors (strong motion accelerometers). Due to the limited number of channels available, only the spans from Bent 6 to Bent 9 of the structure were instrumented. The spans between these bents comprise the majority of the center "straight" section of the bridge.

This research used two types of accelerometers; namely FBA-11s and EpiSensors manufactured by Kinemetrics Inc. Both types of accelerometers came with mounting devices making the installation procedure simpler than the seismometers. The EpiSensors were permanently mounted to the bents and underside of the deck to be used in the long-term monitoring of the structure. For those instruments mounted upside down on the deck, the direction of the vertical and longitudinal directions did not match those instruments on the bents. These were noted so their directions could be changed during the analysis portion of the research. Figure 4.5 represents a typical mounting of an EpiSensor used in the testing.

The eighteen structural channels are made up of a total of nine structural instruments; one tri-axial ES-T (three channels), seven bi-axial ES-Bs (fourteen channels), and one uni-axial ES-U (one channel). The layout of the instruments was designed qualitatively to best determine the structural dynamics of the bridge. Each structural instrument was placed in a protective box. The channels were placed in three directions; longitudinal, vertical, and transverse. Several channels were located on bents of the bridge, and the others were placed at various locations under the deck of the bridge.

Table 4.3 gives the box and channel locations and descriptions. Appendix A gives a summary of all of the instruments used, both permanent and temporary.

Table 4.3 Box and channel locations and description (Petty 2001).

Instrument				Channel	
Box #	Location	Type	Connection Information	Number**	Orientation
1	On Bent 9	ES-B	Connected directly to K2 with cable #1	1-4	Transverse
				1-5	Vertical
2	On deck above Bent 9	ES-U	Junctioned at Instrument 1	1-6	Vertical
3	On Bent 7	ES-T	Connected directly to K2 with cable #2	2-1	Longitudinal
				2-2	Transverse
				2-3	Vertical
4	On deck above Bent 7 on north side of expansion	ES-B	Junctioned at Junction Box*	2-4	Longitudinal
				2-5	Vertical
5	On deck above Bent 7 on south side of expansion	ES-B	Junctioned at Junction Box *	2-6	Longitudinal
				2-7	Vertical
6	On deck at ¼ span from Bent 7 to Bent 6	ES-B	Junctioned at Junction Box*	1-7	Transverse
				1-8	Vertical
7	On deck at midspan between Bents 6 & 7 (west side)	ES-B	Junctioned at Junction Box*	1-9	Transverse
				1-10	Vertical
8	On deck above Bent 6	ES-B	Junctioned at Junction Box*	2-8	Longitudinal
				2-9	Transverse
9	On deck at midspan between Bents 6 & 7 (east side)	ES-B	Junctioned at Junction Box*	1-11	Transverse
				1-12	Vertical

* Junction Box is located on Bent 7

** First number in channel number indicates the recorder number

Figure 4.5 Temporary instrumentation for setup 1.

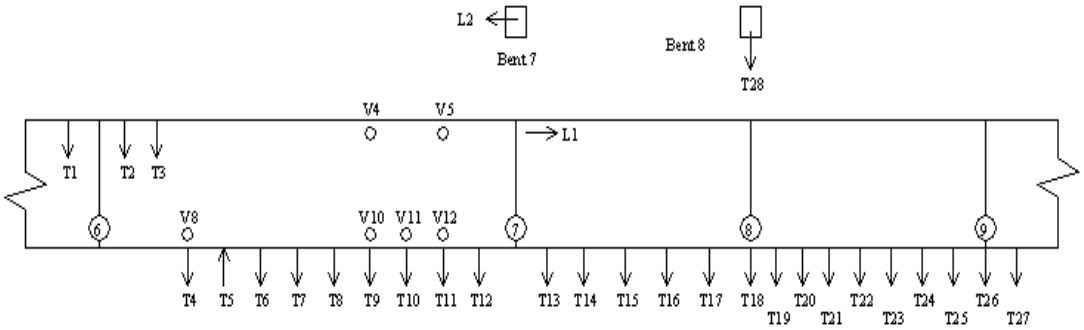

Figure 4.6 Temporary instrumentation for setup 2.

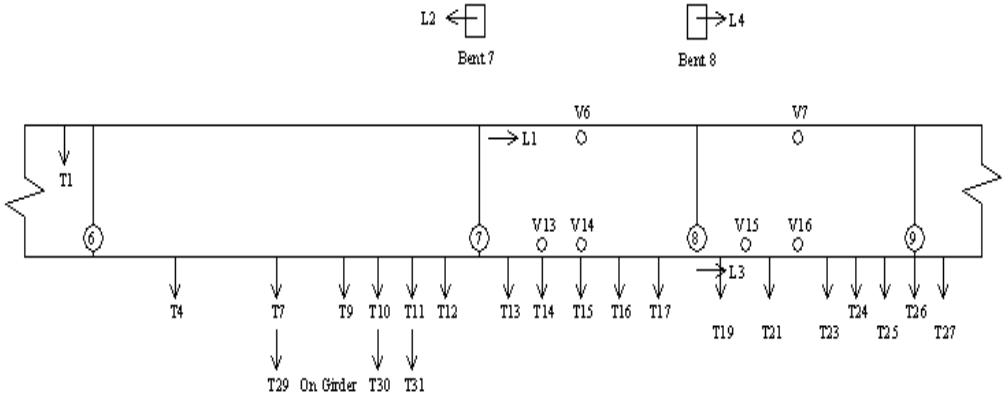

Figure 4.7 Temporary instrumentation for setup 3.

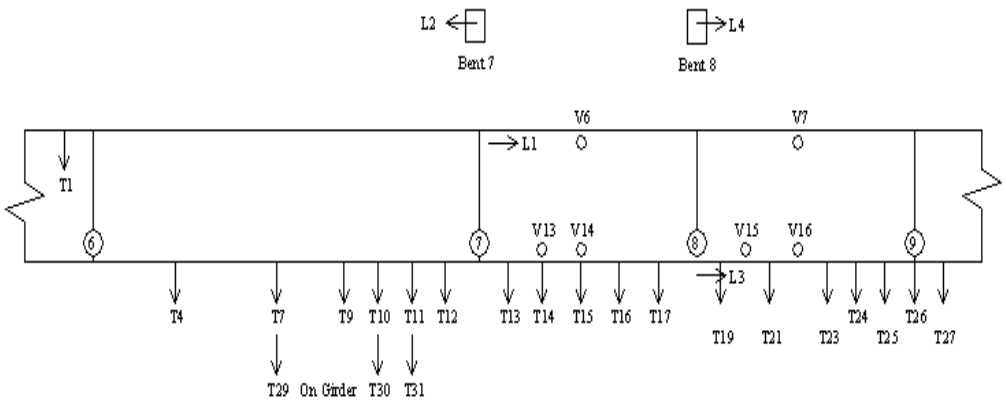

Figure 4.8 Temporary instrumentation for setup 3.

4.3 Analytical Modeling

The section of analytical modeling is divided into two subsections. The first subsection discusses the finite element modeling from software chosen, model consideration, and model comparison. The second subsection discusses the system identification methods which were applied to the field collected data, including forced and ambient vibration data.

4.3.1 Finite Element Modeling

The computer model was created using commercially available structural analysis software, SAP 2000 (CSI, 1997).

Three approaches were used to model the bridge. Each is described briefly in this introduction and further developed in later chapters. The first method used a very simple "stick" type of model that consisted only of frame elements. The purpose of this model was to gain a quick overview of the dynamic characteristics of the first few modes of the model as compared to the bridge, and to examine the usefulness of using such a model. The other two methods were used to gain more detailed information about the comparison of the models to the bridge. The first of these two models used frame elements for all of the members except the deck. The deck was modeled using shell elements. The second model utilized shell elements for the webs and flanges of the girders, deck, diaphragms, and stiffeners; and frame elements for the transverse cross bracing, piles, bent columns and bent caps.

The parts of the bridge that were modeled encompassed nearly every part of the structure. The components used in each model are described along with that model. Generally, the components used in the model included the deck, girders, diaphragm stiffeners, bearing stiffeners, intermediate web stiffeners, intermediate transverse cross bracing, bent caps, bent columns, footings and piles. The bridge rail was not included in

the model because the author felt that the stiffness and mass associated with the bridge rail would not significantly contribute to the model.

From the aerial view of Structure C-846 (Figure 4.1), it is observed that it is not an isolated structure. It connects with other bridge structures at each end as shown in Figure 4.9. Because the other structures express influence to the dynamic properties of C-846, additional modeling was used to determine the significance of influence these structures exhibited on C-846. The structures adjacent to C-846 are similar in design and the details of modeling each of the structures was done in a similar manner to C-846. The full lengths of structures C-849 and C-847 are not shown in Figure 4.9. The length of each structure that exhibited influence on C-846 is the portion of each of the adjacent structures that is shown.

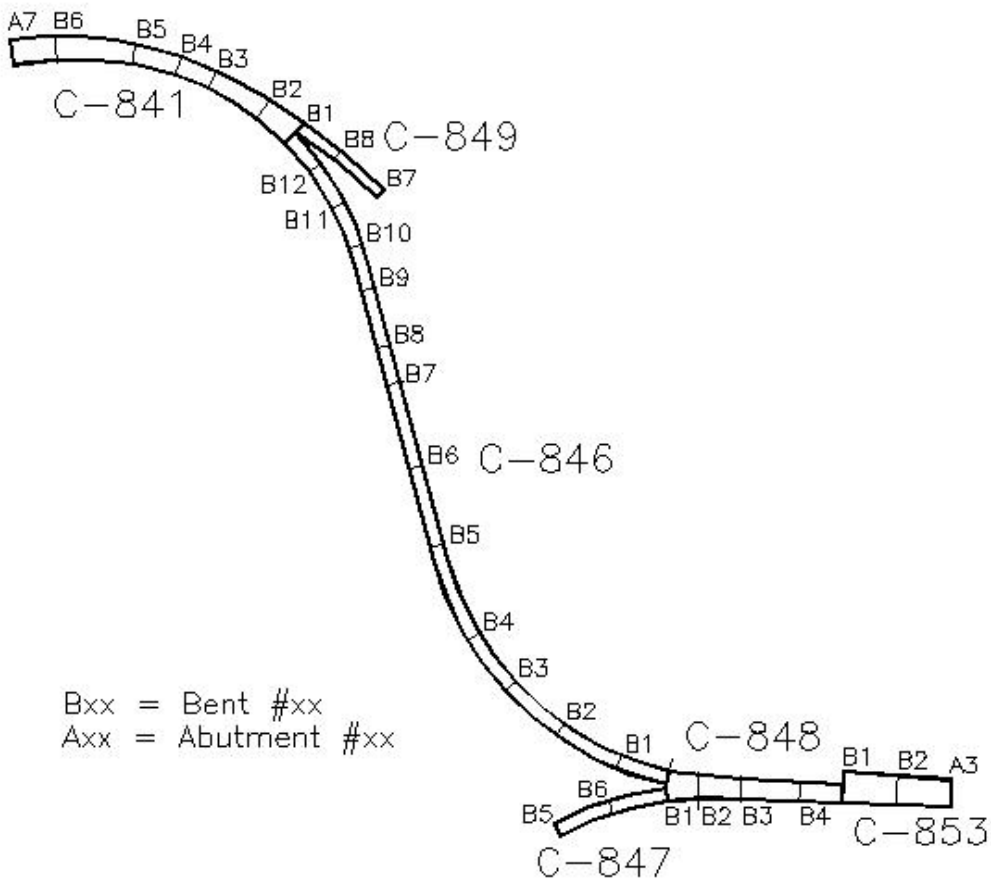

Figure 4.9 Structure C-846 and adjacent structures.

4.3.1.1 Stick Model

The simplest of models that can be used to investigate the dynamic behavior of a bridge is a stick model, as shown in Figure 4.10. The name of this model refers to the fact that this type of model consists of little more than the most basic geometry of the bridge with the stiffness parameters tied to it. Because the computer modeling software lumps the mass of elements at the joints, the model essentially consists of a series of frames whose periods are affected by the stiffness of each adjoining frame. This type of model is often used by practicing engineers to obtain the most basic of dynamic characteristics of the bridge, but provides little research value beyond an initial investigation of the approximate first mode of the structure.

In fact, the periods obtained from this type of model (or any other, for that matter) can actually be somewhat misleading if the mode shapes are not also considered. For example, if the intent is to understand the period of a mode in the transverse direction, but the mode shape is not viewed, then the possibility exists that the period being examined is actually a vertical period. It should also be noted that torsional modes are not well exhibited by this type of model.

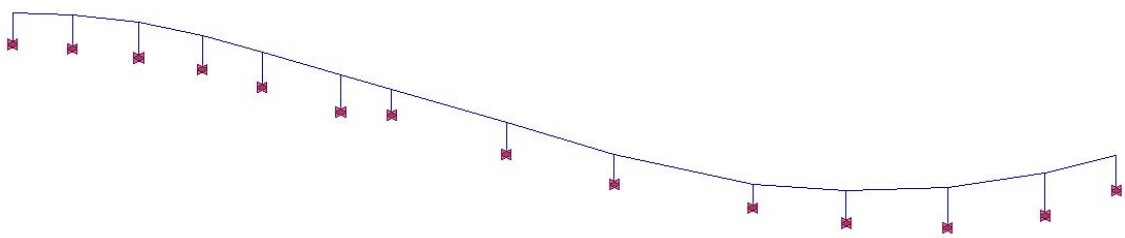

Figure 4.10 Stick model.

This model was created for structure C-846 using the geometry previously described and further structure properties detailed in Appendices A. An average of the girder dimensions was used in conjunction with the deck geometry to provide a cross-section that was used in each of the horizontal frame elements. The cross-section used is shown below in Figure 4.11.

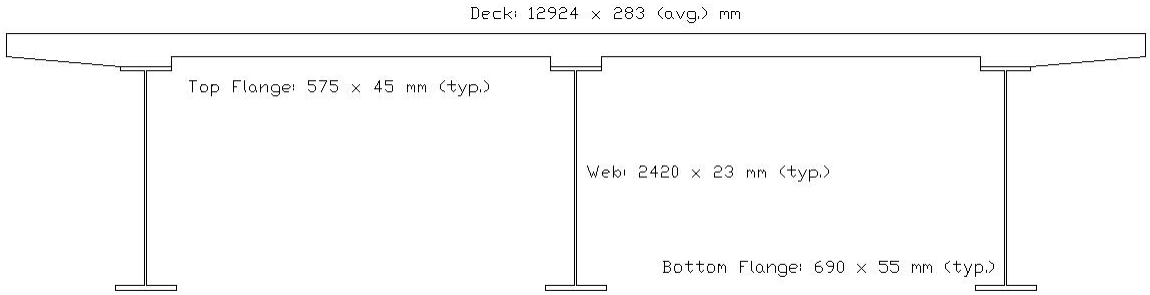

Figure 4.11 Average dimensions of cross-sections.

4.3.1.2 Frame Model

The frame model (see figure 4.12) is similar to the stick model in that frame elements are used for all girders and bents. The frame model differs from the stick model in that, instead of using a single line to represent the superstructure, the girders were detailed individually. To keep the model simple, the intermediate cross-braces between the girders were not modeled. The deck was modeled as shell elements, though the elements are relatively large. This type of model allows considerably more freedom in changing the properties of the model. It also allows a much better display of the torsional modes.

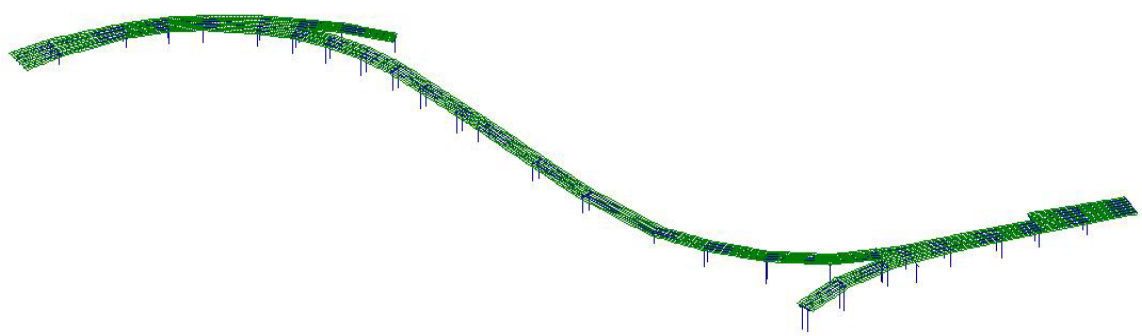

Figure 4.12 Frame model.

Because the model was composed of relatively few elements and was, therefore, relatively easy to adjust, this model was used to investigate boundary conditions and assist in calibration of the shell model. This will be discussed in greater depth in the shell model chapter.

Despite the additional detail that is available with this type of model, it still has limitations. Accurately describing the geometry of the structure is the most significant limitation. The model relies on using the center line geometry of each frame element. Because of this, links are used to connect parts of the model together to place elements in

their most correct positions. The links were given negligible mass and assigned large stiffness values such that they were used to allow connections between different parts of the model without unduly influencing the output. A cross section of the structure showing the spatial relationship of the link connection between frame and shell elements is shown in Figure 4.13.

This model was used to help determine the influence of the surrounding structures. Because the model is relatively simple, it was very easy to quickly add sections of adjacent structures and analyze new models.

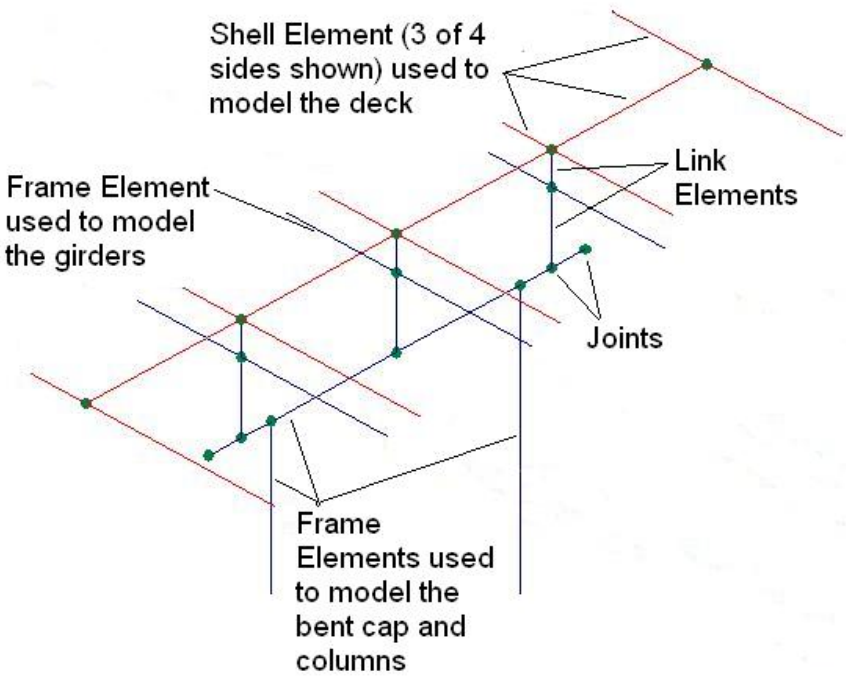

Figure 4.13 Section view of frame mode in SAP 2000.

4.3.1.3 Shell Model

The most significant difference between the shell model and other models is that the shell model most accurately reflects the geometry of the bridge. The model is made more detailed by decreasing the element size and increasing the number and type of element that is used to model a bridge part. This is particularly evident where the girders are concerned. In the stick and frame models, the girders were modeled as frame elements, but in the shell model, the girders are modeled as assemblies of shell elements as described below. More accurate geometry allows for better refinement of the boundary conditions.

The shell model for which results were reported after calibration was completed was composed of 80,840 joints, 71,337 shell elements, and 2,532 frame elements. Since the model had so many elements, material properties could be applied more precisely and accurately to individual elements. For these reasons, the shell model is the most accurate of the models, and was the model most fully developed for this study. Because of the large number of elements, the model required considerable processing time.

The details of each portion of the model of the bridge are explained here. Figure 4.14 shows an isometric view of a midspan section of the bridge as it appears in SAP 2000. The lower left half is shown without the deck for clarity. The three steel girders are on the bottom with the concrete deck above. In this view, the web stiffeners are located on the sides of the girders at the same points where the intermediate cross-bracing laterally stiffens the girders. The steel girders, web stiffeners, diaphragm stiffeners and deck were modeled using shell elements. Lateral bracing elements, links between the deck and the girders, columns, bent caps and links between the bent caps and girders were created using frame elements.

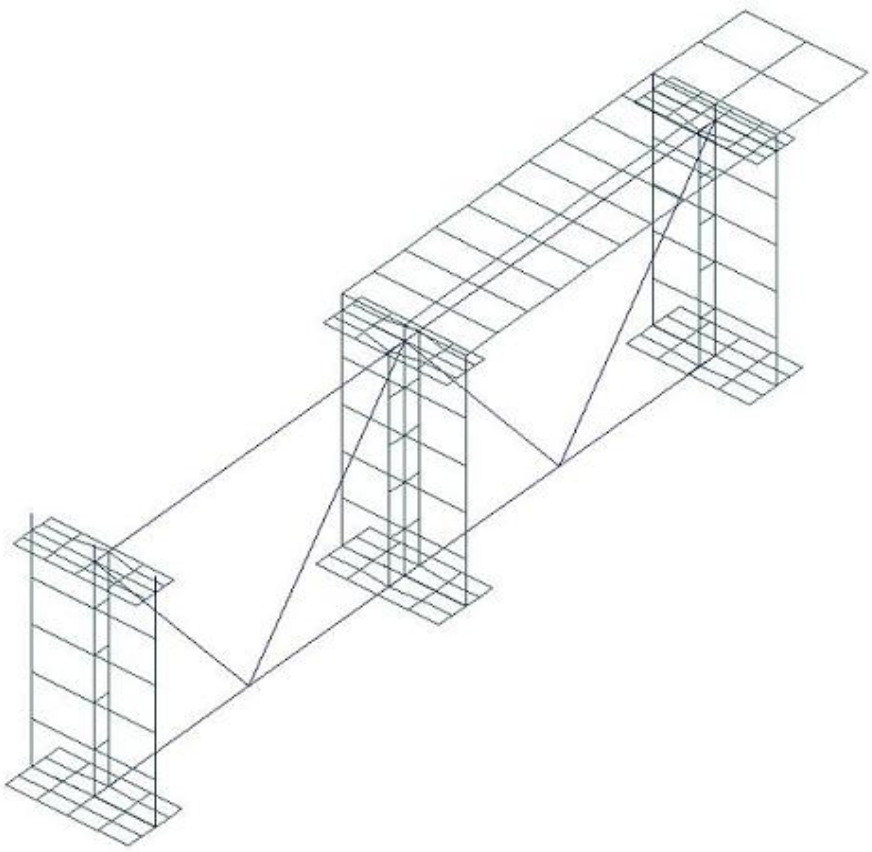

Figure 4.14 Isometric view of a section of the shell model.

The deck of the structure was modeled as a mesh of shells with a width of 24 elements along the whole length of the structure. Each of these elements was assigned a thickness of 255 mm. The material properties of the deck were assigned as noted previously.

4.4 Results

The section of discussion followed the set up of analytical modeling. It is divided into two subsections. The first subsection presents the analysis results from finite element models. There are three different finite element models shown. They are stick, frame, and shell models. The results of period and mass participating ratio for each mode (for different models) are shown and summarized. The periods for three finite element models are then compared. Selected model shapes are also shown. The second subsection presents the analysis results using system identification methods. The forced vibration data and ambient vibration data were collected and analyzed. Different system identification methods are used for the analysis. Since the excitation methods were mentioned in the previous section, the forced vibration using eccentric mass shaker is introduced and ambient vibration is briefly discussed. The selected results of natural frequencies and mode shapes are presented. Finally, the natural frequencies comparisons for the long term monitoring are presented.

4.4.1 Analysis Results from Finite Element Models

4.4.1.1 Stick Model

The first method used a very simple “stick” type of model that consisted only of frame elements. The purpose of this model was to gain a quick overview of the dynamic characteristics of the first few modes of the model as compared to the bridge, and to examine the usefulness of using such a model. The stick model results for first ten modes are summarized. The periods and associated modal participating mass ratios are shown below in Table 4.4.

Table 4.4 Stick model modal periods and participating mass ratios.

Mode	Period	UX	UY	UZ
Number	Sec	Unitless	Unitless	Unitless
1	1.12	4.000E-01	3.800E-01	3.135E-14
2	0.97	5.300E-01	4.000E-01	6.305E-16
3	0.83	7.937E-03	2.824E-02	5.381E-15
4	0.76	2.226E-02	1.700E-01	1.393E-13
5	0.61	9.624E-03	2.798E-03	1.400E-12
6	0.59	9.018E-04	1.031E-03	3.933E-12
7	0.58	4.165E-04	1.191E-04	1.791E-12
8	0.56	1.643E-04	9.207E-04	1.116E-14
9	0.56	7.588E-04	1.598E-05	2.249E-12
10	0.52	5.194E-04	1.585E-04	5.483E-12

The results of this model indicate that the model may be useful for providing information about the first few modes of the structure, but the relatively unchanged periods and insignificant mass ratios of later modes demonstrate that little more information can be obtained from the higher modes of the model. Also, the extremely small amounts of mass participation in the Z-direction show that this rather simple model does not adequately represent vertical modes. Extended results and “stick’ mode shapes for the modes reported above are shown in Appendix B.

4.4.1.2 Frame Model

The frame model is used to gain more detailed information about the comparison of the models to the bridge. This model used frame elements for all of the members except the deck. The deck was modeled using shell elements.

There are several disadvantages of using such a simple model for research. The first of these is the lack of refinement. Because the program lumps masses at the joints, less accurate mode shapes are obtained. To remedy this problem, the model could be divided into a greater number of elements to obtain a more refined mode shape and more precise period.

The frame model provided results with enough accuracy to be used to quickly verify whether a set of boundary conditions would be worth considering on the shell model. For most practical applications, the frame model provides sufficient accuracy, but for research purposes, the shell model allows a degree of precision that would be impossible to obtain with a simpler model.

Mass participation ratios of the final model would have to be examined carefully to ensure that the mode under consideration is valid and derived from the behavior of the whole structure, rather than from only a portion of the structure. The identified periods for the first ten modes are presented in Table 4.5. Also, the corresponding first ten mode shapes for frame models are shown in Figure 4.15.

Table 4.5 Frame Model modal periods and participating mass ratios

Mode	Period	UX	UY	UZ
Number	Sec	Unitless	Unitless	Unitless
1	0.87	1.300E-01	2.000E-01	6.291E-07
2	0.83	2.086E-02	1.500E-01	5.460E-08
3	0.77	5.541E-02	1.721E-02	3.128E-07
4	0.75	8.179E-03	2.800E-01	1.767E-06
5	0.71	1.185E-02	4.760E-03	7.031E-07
6	0.66	3.948E-06	3.048E-04	1.133E-05
7	0.66	1.461E-03	9.589E-02	2.689E-05
8	0.65	1.348E-06	4.315E-05	5.355E-06
9	0.62	9.585E-02	1.058E-03	3.066E-05
10	0.60	2.773E-03	1.798E-02	5.138E-04

This model differs from the stick model in that it is expanded to include not only structure C-846, but five adjacent structures as well. The dimensions used for each of the girders were an average of the girder dimensions of each girder line in each span. This significantly increased the accuracy of modal periods and modal shapes obtained because the girders were better represented. In addition, the bents were also considered in more detail. Each bent was modeled by using the appropriate number of columns and a bent cap. The increased definition of the structure also added to the accuracy of the model. The deck is modeled as shell elements connected to the girders by links. Web and bearing stiffeners and cross braces were not included in this model.

4.4.1.3 Shell Model

The third model utilized shell elements for the webs and flanges of the girders, deck, diaphragms, and stiffeners; and frame elements for the transverse cross bracing, piles, bent columns and bent caps.

The most significant difference between the shell model and other models is that the shell model most accurately reflects the geometry of the bridge. The model is made more detailed by decreasing the element size and increasing the number and type of element that is used to model a bridge part. This is particularly evident where the girders are concerned. In the stick and frame models, the girders were modeled as frame elements, but in the shell model, the girders are modeled as assemblies of shell elements

as described below. More accurate geometry allows for better refinement of the boundary conditions.

One of the most important factors that was considered in modeling this bridge was the boundary conditions. As shown by the variations of the shell model, significantly different results can be obtained by small variations in the boundary conditions. The results of periods and mass participating ratios for the shell element model are summarized in Table 4.6.

Table 4.6 Shell Model modal periods and participating mass ratios

Mode	Period	UX	UY	UZ
Number	Sec	Unitless	Unitless	Unitless
1	0.87	5.000E-04	2.600E-03	6.400E-03
2	0.74	1.850E-02	3.800E-01	0.000E+00
3	0.70	4.870E-02	5.800E-02	0.000E+00
4	0.69	0.000E+00	0.000E+00	1.750E-02
5	0.66	0.000E+00	2.000E-04	7.100E-03
6	0.58	7.400E-03	4.380E-02	0.000E+00
7	0.56	4.660E-02	1.740E-02	0.000E+00
8	0.54	3.560E-02	4.360E-02	1.000E-04
9	0.53	5.170E-02	2.310E-02	0.000E+00
10	0.48	7.910E-02	1.660E-02	0.000E+00

In order to understand the relationships between different models, the ratios between different models are summarized in Table 4.7. While comparisons between the stick and frame, frame and shell, and stick and shell models are not a direct correlation, the model results do establish a very reasonable baseline for future research. Exactly matching the periods obtained by finite element models is not a feasible consideration based on the information provided for creating the model. There are virtually an infinite number of combinations of variables that could be considered and adjusted to correlate the model with the field results. This could be countered to some degree by taking samples of the materials from various locations on the bridge and including the data in the model.

Table 4.7 Periods comparisons of stick, frame, and shell models.

Mode	Stick (1)	Frame (2)	Shell (3)	(1)/(2)	(1)/(3)	(2)/(3)
	Period (sec)			Ratio		
1	1.12	0.87	0.87	1.28	1.28	1.00
2	0.97	0.83	0.74	1.17	1.31	1.12
3	0.83	0.77	0.70	1.07	1.19	1.11
4	0.76	0.75	0.69	1.01	1.10	1.09
5	0.61	0.71	0.66	0.87	0.93	1.07
6	0.59	0.66	0.58	0.89	1.01	1.13
7	0.58	0.66	0.56	0.88	1.03	1.17
8	0.56	0.65	0.54	0.87	1.04	1.20
9	0.56	0.62	0.53	0.89	1.04	1.17

One of the greatest advantages that the stick and frame models have over the shell model is the lesser number of elements. In the case of the stick model, there were only 27 elements which made it very easy to find and correct errors. Even the frame models have a fairly limited number of elements and error correction is not difficult. In the case of any of the shell models, however, there are more than 154,000 elements. While many parts of the model were checked repeatedly for errors, undoubtedly some error has been introduced into the model. Also, each portion of the model was not subjected to the same scrutiny simply because those parts of the model created near the end of the process received less scrutiny.

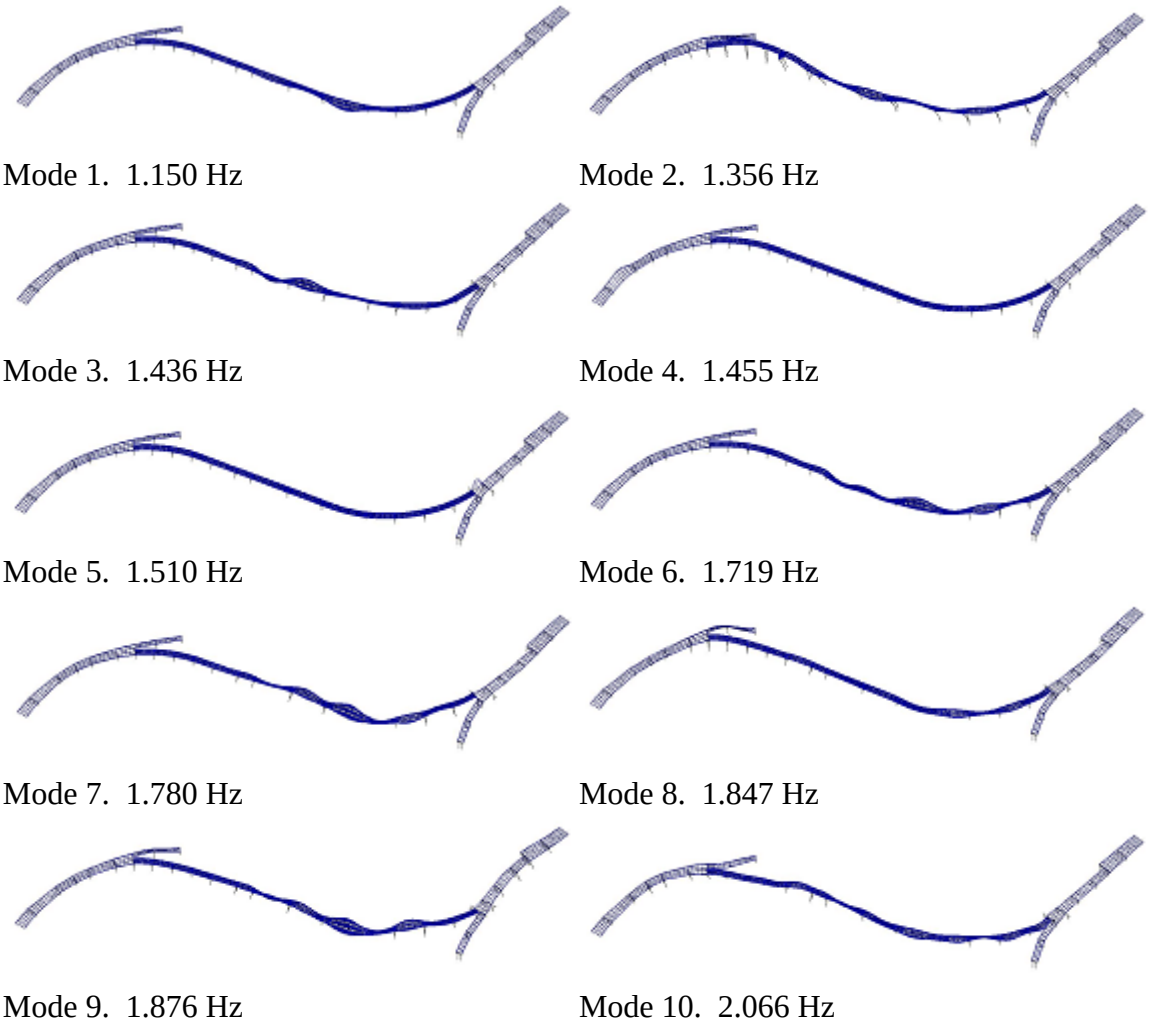

Figure 4.15 First ten mode shapes for frame model.

4.4.2 Analysis Results using System Identification Approaches

Two excitations were used for this bridge and data were collected. The forced vibration data are used in comparing the data sets and natural frequencies. The long term source of data is the ambient vibration data. The idea of the forced vibration testing is introduced and the identified natural frequency results using system identification method (peak picking) are presented. Then, the recorded ambient vibration data are analyzed using two different system identification methods: frequency domain decomposition (FDD), and eigensystem realization algorithm with an observer Kalman filter identification (ERA-OKID). All of the data taken to this point will be compared to determine if the ranges of natural frequencies have been shifting with time.

For the forced vibration testing, the structure was tested using an eccentric mass shaker to produce a sinusoidal vibration in one horizontal direction. The shaker was used to produce vibrations at frequencies between 0.75 and 20 Hz (Dye, 2002). The permanent instruments as well as a variety of setups of temporary instruments were used in the forced vibration testing. The eccentric mass shaker is shown in Figure 4.16.

Figure 4.16 Eccentric mass shaker.

Forced vibration testing was performed three different times to allow for minor adjustments to the vertical instrument array. The testing procedure was nearly identical for all three setups. Table C.2 in Appendix C shows the general testing procedure followed for each setup. Forcing was applied at frequencies between 0.75 to 20.00 Hz. The data was collected at 200 samples per second for a 10.24 second period. An interval of ten seconds was created to allow the shaker time to ramp up to the next frequency step and stabilize. Table C.3 in Appendix C summarizes all the collected data files for the forced vibration testing.

During the forced vibration testing, the data acquisition systems were used simultaneously to include all possible instruments in the collection of data. Two problems were encountered in order for the data from both systems to be used simultaneously in the analysis. First, the frequency of the eccentric mass shaker needed to be relayed to both systems. This was accomplished by sending the shaker channel signal to both systems via an interconnecting cable. Second, the two acquisition systems needed to be synchronized. The digital recorders recorded data in real time while the portable system paused its recording between frequency steps to allow for the structure to receive stationary forcing. This was solved by sending a voltage spike from the portable system to the digital recorders the instant the portable system commenced data recording. The data from the digital recorders was later modified to save only those data points immediately after the voltage spike and up to the length of the sample block. This process allowed for an additional 18 instruments to be used towards better definition of the mode shapes of the structure.

The forced vibration data consisted of time histories for each seismometer and accelerometer. Figures 4.17 and 4.18 show typical time histories for seismometers and accelerometers, respectively. It is observed that the accelerometer signal is noticeably noisier than the seismometer signal. The raw data format was tab delineated with each column representing an instrument channel. All the field data was transferred from the data acquisition systems to compact discs until it was ready for analysis.

The peak-picking method found peaks on the normalized displacement plots which correlated with natural frequencies. Detailed information about peak-picking method can be found in Appendix D. This method resulted in 82 transverse, 12 longitudinal, and 24 vertical natural frequency measurements for each mode. Some variation was noted within these mode measurements. As shown in past research, variations in natural frequencies can occur due to environmental conditions or structural damage, so numerous measurements of natural frequencies aid in precisely calculating a structure's natural frequency. By averaging these 118 values, a fairly precise natural frequency measurement can be documented. Table 4.8 shows the average values for each of the natural frequencies as determined through peak-picking of the normalized displacement plots. The dominant directional mode for each natural frequency will be discussed in the next section.

In addition, the correlation between the model and field data also depends on the interpretation of the field data. Depending on the method used to interpret data (Peak Picking Method), the type of data collected (ambient or forced vibration) or other external factors (temperature, exact age and condition of structure, etc.), the correlation between the field testing and the model will vary. Despite these issues, the lower modes, in particular, of the shell model reasonably represent those expressed by the actual structure and it is reasonable to expect that a model of this level of detail would be quite useful in understanding the relationship between localized damage and changes in the dynamic characteristics of the bridge.

Possibilities for the discrepancies between the field data and the model results could also be attributed to the interpretation of data. The method used to interpret data may have caused the interpreter of the data to interpret a separate mode as part of another mode. Another possible cause for the discrepancies could be that the modulus of concrete increases with increasing frequency.

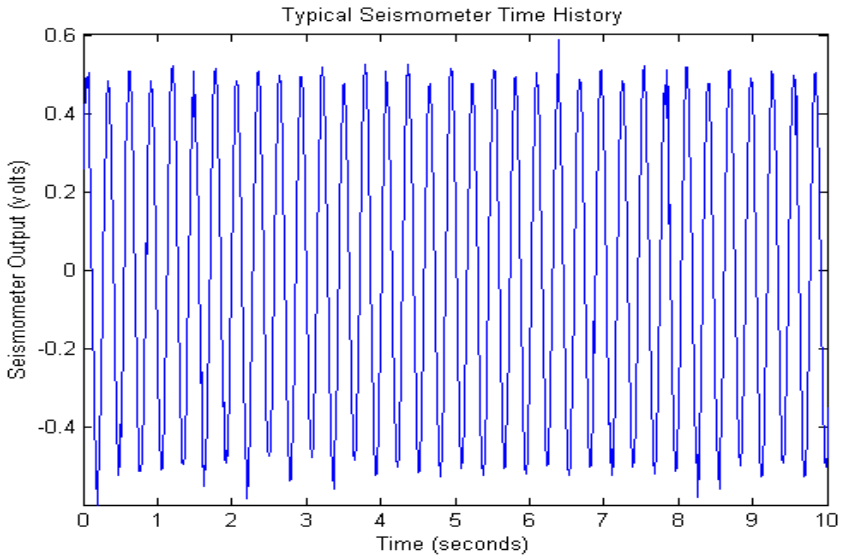

Figure 4.17 Typical forced vibrational seismometer time history.

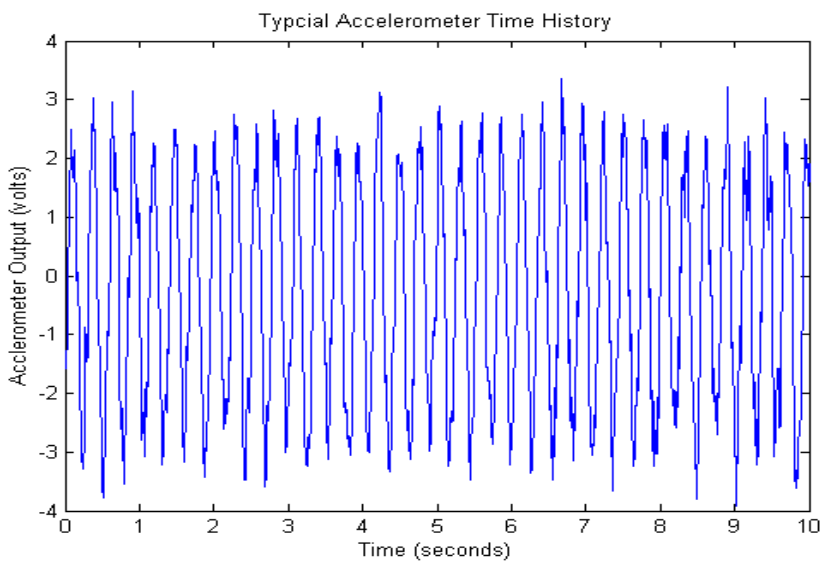

Figure 4.18 Typical forced vibrational accelerometer time history.

Table 4.8 Average natural frequencies using the peak-picking method.

MODE	NATURAL FREQUENCY (Hz)	MODE	NATURAL FREQUENCY (Hz)
1	1.11	14	4.25
2	1.31	15	4.72
3	1.49	16	5.17
4	1.58	17	5.58
5	1.76	18	6.15
6	1.92	19	7.30
7	2.25	20	8.98
8	2.37	21	10.70
9	2.70	22	11.75
10	3.07	23	13.00
11	3.32	24	14.29
12	3.49	25	15.59
13	3.72	26	17.08

A typical mode shape is produced by using instrument displacement values along with their corresponding relative phase angles at a given natural frequency. For the forced vibration data, the displacement values were considered in the positive direction when their corresponding relative phase angle was between –90° and 90°. The sign became negative when the relative phase angle measured between –180° and –90° or 90° and 180°. Most of the time these phase ranges produced fairly smooth mode shapes, but it was noted that there were exceptions. Sometimes it was more accurate to compare two channels that were physically close to each other on the bridge to determine if one was 180° out of phase from the other. If this occurred it was assumed that the two channels had displacements in opposite directions. Using this latter criterion throughout the length of the bridge it could be seen that the mode shapes increased in smoothness. These displacement values were then applied to the structure at the appropriate instrument locations. The plot of the displacement along each measured location of the structure produced the mode shape for a given natural frequency. Figure 4.19 shows the corresponding forced vibration produced modes with their corresponding natural frequency.

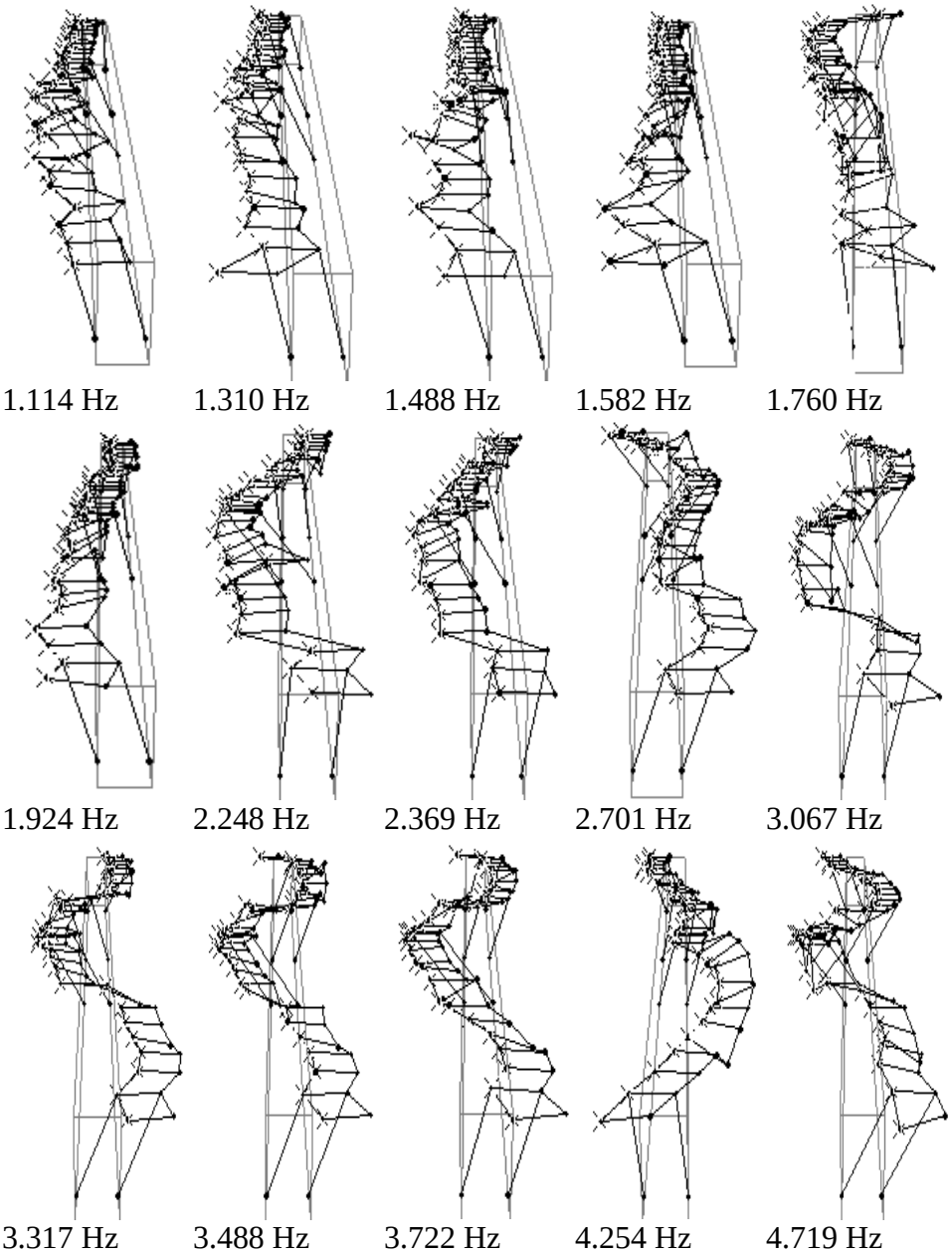

Figure 4.19 Forced vibration mode shapes 1 through 24 (continued on page 39).

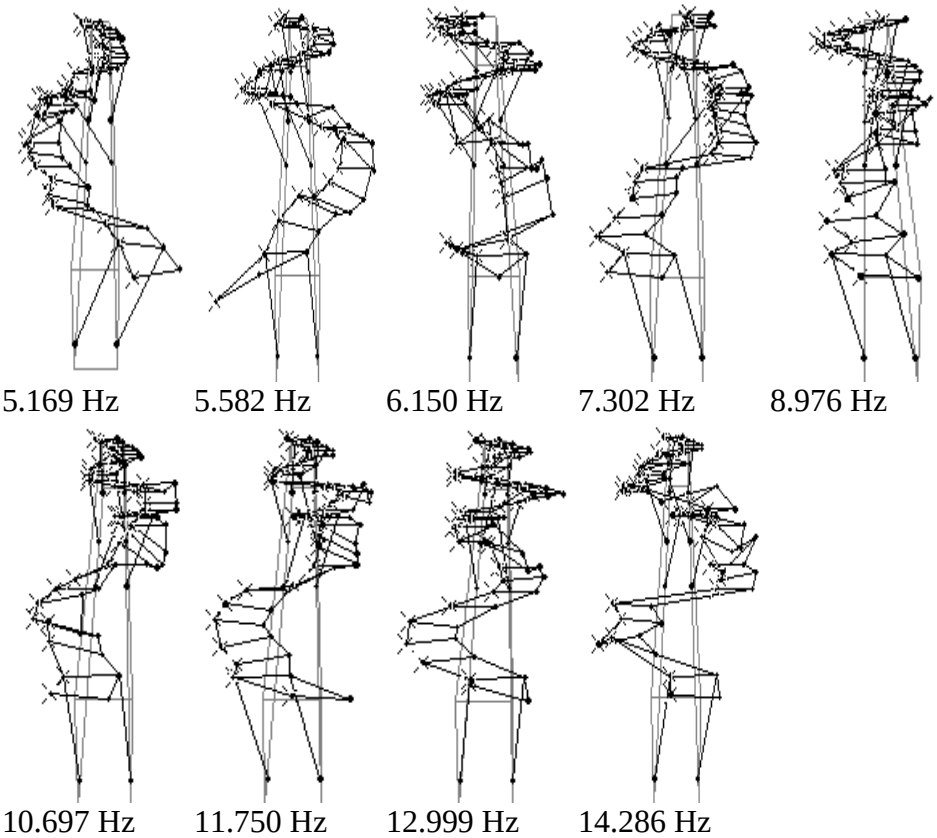

Figure 4.19 Forced vibration mode shapes 1 through 24 (continued from page 38).

It is observed that certain mode shapes appeared similar in the transverse direction. This could be caused by several things. The first could be that different vertical and longitudinal modes are present in the similar transverse modes. The second reason could be that the entire I-80 Flyover Bridge has several different transverse modes, but the limited number of instrumentation views these as the same transverse mode. In order to explain this situation, vertical and longitudinal modes needed to be found. Figure 4.20 shows the first 12 different longitudinal and vertical modes.

Table 4.9 summarizes the dominant direction for each mode. The vertical modes were more difficult than the transverse modes to differentiate between for several reasons. First, there were not enough vertical instruments to describe the shapes in detail. Most of the decision-making between vertical mode shapes stemmed from comparing bridge sections of two different modes. Second, the interaction between lateral and vertical deflections was at times dependent upon each other. For example, if all the bridge moved east, the deck would act as a stiff structure and tilt east with the lateral deflection. This relationship made it difficult to accurately conclude if the deck had torsional bending.

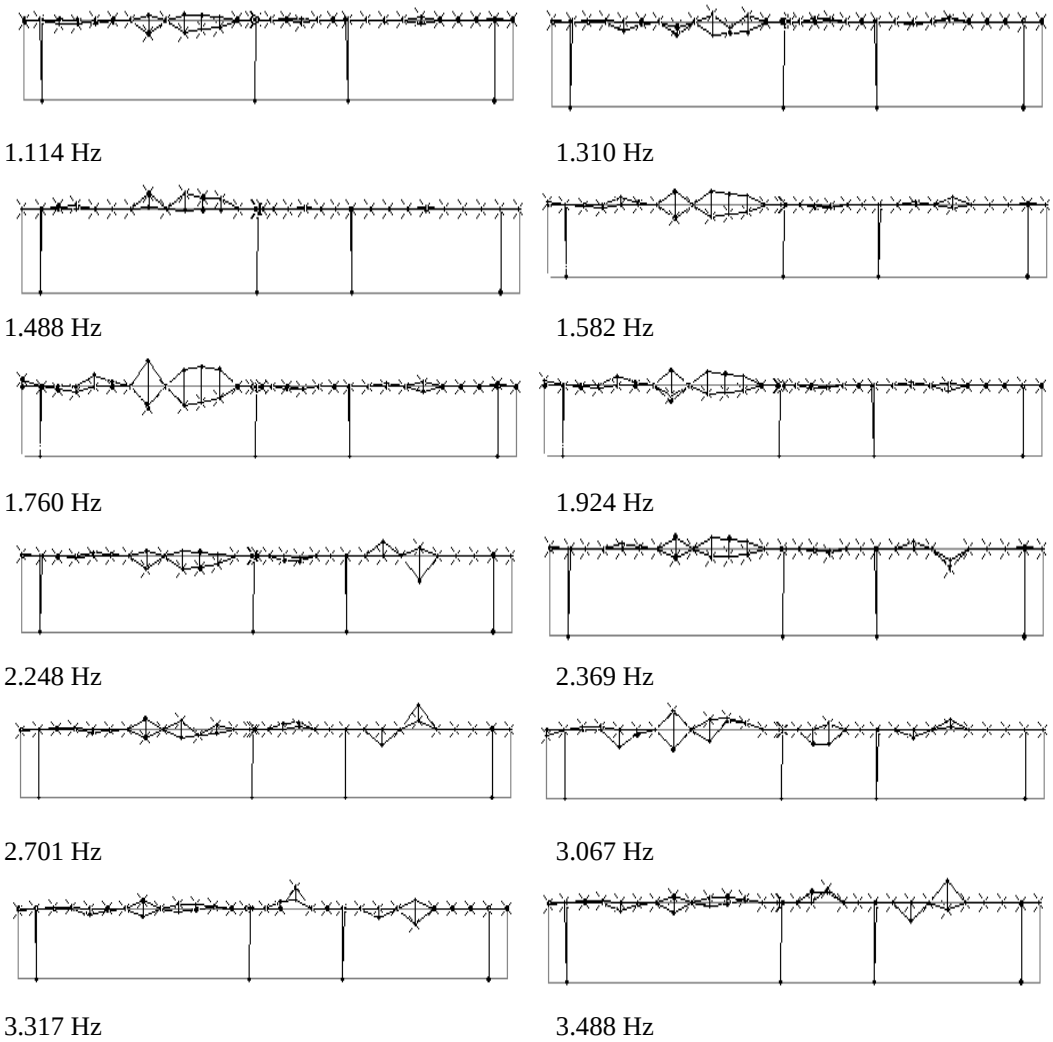

Figure 4.20 Vertical and longitudinal mode shapes for modes 1 through 12.

Table 4.9 Dominant direction of modes.

MODE	NATURAL FREQUENCY	DOMINANT DIRECTION	MODE	NATURAL FREQUENCY	DOMINANT DIRECTION
1	1.11	Vertical	14	4.25	Vertical
2	1.31	Longitudinal	15	4.72	Vertical
3	1.49	Vertical	16	5.17	Vertical
4	1.58	Transverse	17	5.58	Transverse
5	1.76	Transverse	18	6.15	Vertical
6	1.92	Transverse	19	7.30	Vertical
7	2.25	Vertical	20	8.98	Transverse
8	2.37	Transverse	21	10.70	Vertical
9	2.70	Vertical	22	11.75	Vertical
10	3.07	Transverse	23	13.00	Transverse
11	3.32	Vertical	24	14.29	Vertical
12	3.49	Vertical	25	15.59	Vertical
13	3.72	Vertical	26	17.08	Vertical

Ambient vibrations were considered to be those occurring in the bridge's natural environment. Wind, traffic on the bridge, surrounding traffic, and nearby construction are assumed to be the major causes of ambient vibrations. The ambient vibrations were considered to be stationary white noise. As mentioned previously, some ambient vibration data were collected and analyzed using a frequency decomposition method (Hodson, 2001).

The ambient vibration data collected after June 2001 were analyzed using an overlap of 4096, or half of the FFT (Hales 2002). It was hoped that by using the overlap the peaks or natural frequencies would become more prominent, which in turn would narrow the natural occurring range of frequencies.

The selected ambient vibration data were also analyzed using Eigensystem Realization Algorithm with an Observer Kalman Filter Identification (ERA-OKID). This method is popular for the control engineers to identify the modal parameters, such as natural frequencies, phase angles, and model shapes. More information about ERA-OKID can be found in Appendix D.

There are three different sets of ambient vibration data recorded. The stage 1 data was recorded in June, 2001. There are 45 data sets recorded. The ambient vibration analysis can be found in Dye (2002). The data was collected by the temporary instruments. The stage 2 data was collected in August and September, 2002. There are 25 data sets collected. The data was recorded by the permanent instruments. In addition, there are 11 data sets collected in the early 2002. The stage 3 data was collected on April 23rd, 2004. Table 4.10 shows that the time data was taken and used for the long term health monitoring. A summary table for the identified natural frequencies with

covariance is shown in Table 4.11. The forced vibration data collected on June, 2001 is analyzed by peak picking method. By observation, the percent variations are less than 4 percent, except the ninth mode. The ambient vibration data collected during 2001 and 2002 are analyzed by FDD method. It is observed that the covariance of variation is less than 5 percent. The identified natural frequencies yield reasonable results because the covariance of variation is small. To better understand the relationships between different system identification methods with different vibration data sets, the comparison results of the identified natural frequency between FDD and ERA-OKID methods are shown in Table 4.12. Since the ambient data analyzed using ERA-OKID were collected on April, 2004, a small percent shift on natural frequencies, especially the first mode, is anticipated. The shift may cause by the environmental changes during the testing period.

Table 4.10 Files taken for three different stages.

	Stage 1	Stage 2	Stage 3
Data Type	Ambient	Ambient	Ambient
Time Taken	June, 2001	September, 2002	April, 2004
System Identification Method	FDD	FDD	ERA-OKID

Table 4.11 Identified natural frequency results at different stages.

	Data Sets	Mode 1	Mode 2	Mode 3	Mode 4	Mode 5	Mode 6	Mode 7	Mode 8	Mode 9	Mode 10
ForVib(Hz) (June, 2001)	45	1.11	1.31	1.48	1.58	1.76	1.92	2.24	2.37	2.69	3.06
COV (%)		4.00	3.14	1.26	1.80	1.63	1.01	1.62	1.52	4.07	1.85
AmbVib(Hz) (June, 2001)	45	1.10	1.35	1.46	1.58	1.77	1.93	2.22	2.38	2.67	3.04
COV (%)		1.25	1.18	0.63	1.10	2.84	1.47	2.54	2.24	2.55	1.78
AmbVib(Hz) (Aug-Dec, 2001)	25	1.09	1.33	1.45	1.58	1.75	1.91	2.20	2.35	2.70	3.04
COV (%)		1.92	1.22	1.55	2.94	2.39	1.95	2.05	1.20	4.13	3.33
AmbVib(Hz) (Jan-Apr, 2002)	11	1.15	1.31	1.46	1.59	1.78	1.94	2.16	2.38	2.72	3.09
COV (%)		2.37	4.54	2.08	1.42	2.25	1.74	4.99	2.87	4.91	2.69
AmbVib(Hz) (Apr, 2004)	1	1.18	1.37	1.52	1.62	1.77	1.95	2.10	2.31	2.53	3.11
COV (%)		NA	NA	NA	NA	NA	NA	NA	NA	NA	NA

Table 4.12 Natural frequencies results from FDD and ERA-OKID.

Mode	FDD Forced (Hz)	FDD Ambient (Hz)	ERA-OKID Ambient (Hz)	(2)/(1)	(3)/(1)
1	1.11	1.12	1.18	1.01	1.0631
2	1.36	1.33	1.37	0.98	1.01
3	1.47	1.46	1.53	0.99	1.04
4	1.59	1.59	1.62	1.00	1.02
5	1.77	1.76	1.77	0.99	1.00
6	1.94	1.92	1.95	0.99	1.01
7	2.23	2.20	2.11	0.99	0.95
8	2.38	2.37	2.32	1.00	0.97
9	2.67	2.70	2.53	1.01	0.95
10	3.05	3.06	3.11	1.00	1.02

By simple observation, we find that the ratios show good agreement between FDD forced vibration frequency and FDD ambient vibration frequency. The similar ratio results can be found for FDD forced vibration frequency and ERA-OKID ambient vibration frequency.

Since typical analytical results for forced and ambient vibration are shown in the previous chapter, the compressive results of the statistical analysis of all the recorded frequencies for both forced and ambient vibration analysis can be found in Appendix E. The statistical results were plotted showing the mean natural frequencies with their accompanying standard deviations. The average natural frequency, the standard deviation, and the coefficient of variation are shown to give a better perspective of the natural frequencies.

To better understand the relationships between analytical model and field testing model, the natural frequencies identified by the FDD method using forced vibration data are compared with the modal frequencies from frame and shell models. The selected results and ratios are summarized in Table 4.13. The largest percent difference observed is around 20 percent.

Table 4.13 Modal frequency comparison between analytical and field testing models.

Mode	FDD Forced (Hz) (1)	Frame (Hz) (2)	Shell (Hz) (3)	(2)/(1)	(3)/(1)
1	1.11	1.15	1.15	1.04	1.04
2	1.36	1.20	1.35	0.89	0.99
3	1.47	1.30	1.43	0.89	0.97
4	1.59	1.33	1.45	0.84	0.91
5	1.77	1.41	1.52	0.80	0.86

THIS PAGE INTENTIONALLY LEFT BLANK

CHAPTER 5

VINE STREET BRIDGE—C814

5.1 Bridge Description

The Vine Street overpass bridge, C-814, structure is a two-span steel girder and concrete deck bridge located in the Salt Lake City area. This bridge serves as the connector of the Vine Street overpass to I-15. This bridge is relatively new in service. The length of the bridge is 80 meters with 18 meters in width. This bridge has two lanes with a pedestrian walkway in each east and west direction. The elevation difference is 2 meters and the skew ratio is less than 8 percent. In addition, this highway bridge is fairly straight and the length to width ratio is large. The orientation of the bridge is shown in Figure 5.1.

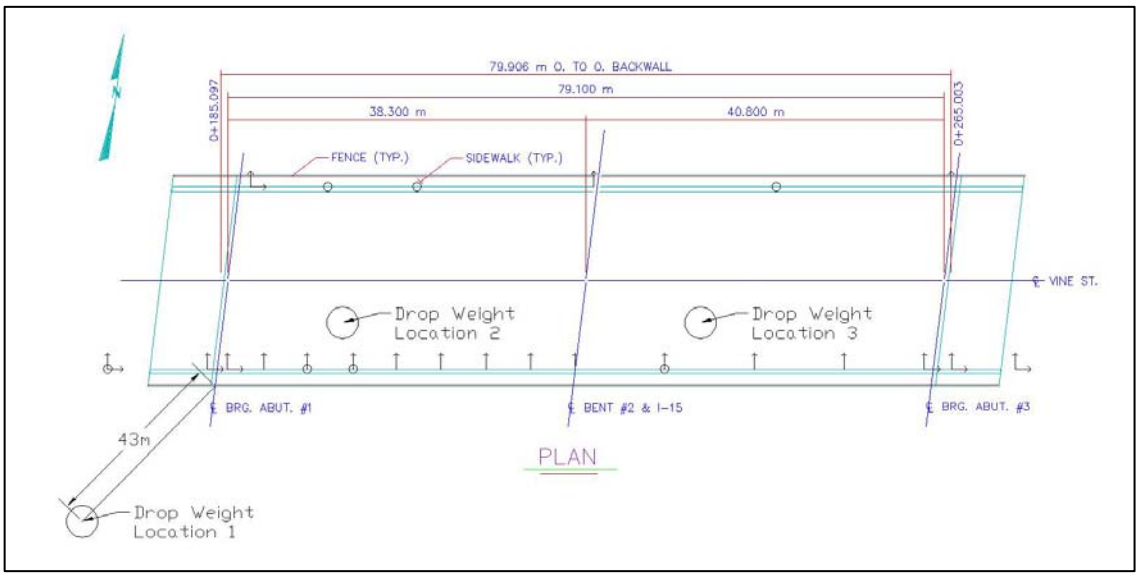

Figure 5.1 Orientation and instrumentation setup of Vine Street Bridge.

5.2 Field Testing

5.2.1 Instrumentation

There are 6 vertical channels, 8 longitudinal channels, and 20 transverse channels designed to perform for testing. A total of 34 temporary instruments were used in the two different testing stages. The temporary instrument array was designed in 2 setups which primarily improve the coverage of vertical motion in the test section of the bridge. The temporary array is covered on the top of the pedestrian walkway. Only the vertical instruments channel 28 and channel 29 were moved during the second setup, but the

other transverse and longitudinal instruments remained in the same position. See above instrumentation figure for typical temporary layout of instrumentation for setup 1.

The forced and ambient vibration testing procedures are almost identical for two different setups. This forced vibration of the Vine Street Overpass Bridge was excited by a 4000 lbs drop weight. The weight is carried by a special designed mobile trailer. The first drop weight location was at approximately 23 meters from the southwest corner of the bridge. The second drop weight location was at approximately the quarter-point of the west span, while the third location was at the quarter-point of the east span

The other drop location is one fourth of the bridge from the west side. The forced vibration was tested in the late afternoon. The forced vibration data was taken by an HP digital analyzer. The measurements recorded by the analyzer are self-windowed. In addition, there are two vertical channels used to record vertical forced vibrational motion.

5.3 Analytical Modeling

5.3.1 Finite Element Model

The finite element modeling (FEM) is performed by SAP 2000, which is commercially available finite element software. This FEM was accomplished through the use of the shell, frame, and solid elements. The shell elements are used for the steel plate girder and concrete deck. The frame elements are used for the bents, braces and cross connections. The parapet was modeled by the solid elements. A total of 29,488 shells were used to model the plate girders, and concrete deck. A total of 1407 frame elements were used for the bent and bent caps as well as the intermediate cross-bracing between girders. An aspect ratio less than 4:1 was maintained for most of the shells.

5.3.2 System Identification Method

The testing procedure is almost identical for each setup. This bridge was excited by using a 4000 lbs drop weight and ambient vibrations. The drop weight was dropped at the quarter-point of the bridge, approximately 45 meters from the end. Forced vibration and ambient vibration data were collected and recorded separately using a PC-based data acquisition system. The data was taken at 200 samples per second. They were analyzed by ERA-OKID method. In addition, there are two vertical channels used to record vertical forced vibrational motion and the data was analyzed by an HP analyzer. The analysis result was used to help determine the mode shapes and to compare the frequencies.

5.4 Results

Eigensystem realization algorithm (ERA) and Eigensystem realization algorithm with an observer Kalman filter identification (ERA-OKID) methods were used for the analysis. The ERA method was used to analyze the collected forced vibration data. ERA-OKID was utilized on the analysis for the ambient vibration data. The forced vibration data is the data collected when a 4,000 pounds concrete cylinder impacted the bridge. During the testing period, an HP analyzer was used to identify the natural frequencies. The identified natural frequencies using ERA is compared to the results from the analyzer. Note the sample data length (4096 points) for ERA is not equal the data length (1024) used by the analyzer. The selected natural frequencies and model shapes using ERA-OKID to deal with ambient vibration are identified.

The comparison results of forced vibration between ERA analysis and digital analyzer (FFT analysis) are summarized in Table 5.1. Note that only the forced vibration data analyzed by ERA was compared with analyzer's result. It is observed that the results of the identified natural frequencies are close to each other. The largest difference is 6 percent which occurred on the third mode. For other modes, the percent difference is less than 4 percent.

Table 5.1 Natural frequency comparison between ERA and HP analyzer.

	ERA_forced (1)	Analyzer (2)	(2)/(1)
	Frequency (Hz)	Frequency (Hz)	Ratio
Mode1	1.84	1.88	1.02
Mode2	2.05	2.06	1.00
Mode3	2.95	2.77	0.94
Mode4	3.13	3.13	1.00
Mode5	4.03	3.91	0.97
Mode6	4.19	4.18	1.00
Mode7	5.13	5.31	1.04
Mode8	5.99	6.09	1.02
Mode9	6.40	6.39	1.00
Mode10	7.17	7.16	1.00

ERA-OKID approach was used to identify both natural frequencies and model shapes from ambient vibration data. The ERA-OKID method used the known input and measured output for data analysis. Natural frequencies and model shapes were obtained using both methods. The comparison results are summarized in the results section of this case. To better understand the dynamic properties of the testing bridge, this bridge also was modeled using commercially available finite element model software. The natural frequencies results from the finite element model were recorded. Table 5.2 summarizes the modal frequency results and provides the variation for the first 10 modes. To better understand the dynamic properties of the testing bridge, this bridge also was modeled

using commercially available finite element model software. The natural frequencies results from the finite element model were recorded. The modal frequencies are compared with field-tested ambient vibration data analyzed by ERA-OKID method and results from the finite element model. The corresponding mode shapes obtained by ERA-OKID are shown in Figure 5.2.

It is observed that the frequency differences are less than 7 percent for most modes. Based on the identified natural frequencies, the generated finite element model is close to the real structure. In addition, the modal frequency comparisons from the finite element model, forced vibration data, and ambient vibration data are summarized in Table 5.3. This table also provides the calculated percent difference.

Table 5.2 Natural frequency results for first ten modes.

	FEM	ERA-OKID	ERA-OKID/FEM
	Freqency (Hz) (1)	Freqency (Hz) (2)	Ratio (2)/(1)
Mode 1	1.84	1.71	0.93
Mode 2	2.05	2.05	1.00
Mode 3	2.94	2.96	1.01
Mode 4	3.13	3.05	0.97
Mode 5	4.40	4.08	0.93
Mode 6	4.48	4.20	0.94
Mode 7	5.05	5.21	1.03
Mode 8	6.43	6.04	0.94
Mode 9	6.59	6.39	0.97
Mode 10	7.03	7.03	1.00

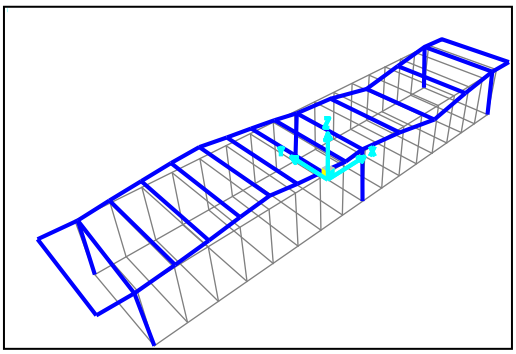

Mode1-- 1.71 Hz [C-814 bridge].

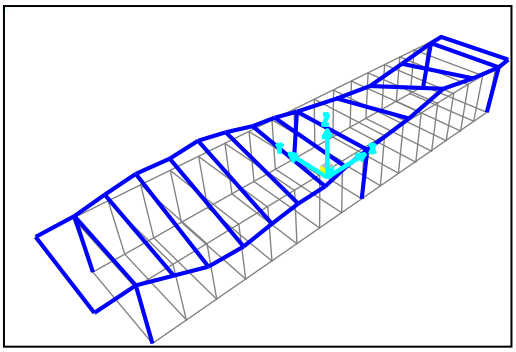

Mode2-- 2.05 Hz [C-814 bridge].

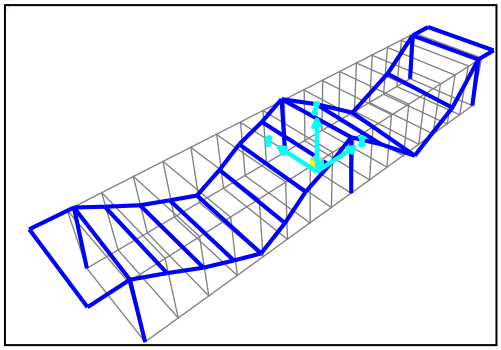

Mode3-- 2.96 Hz [C-814 bridge].

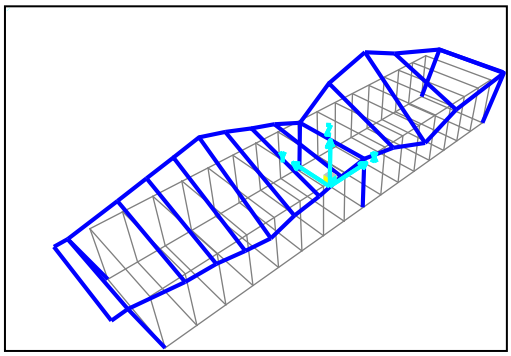

Mode4-- 3.05 Hz [C-814 bridge].

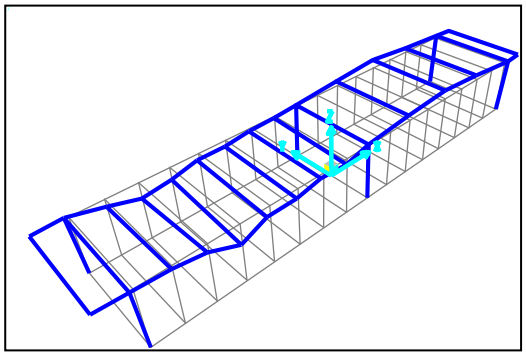

Mode5-- 4.08 Hz. [C-814 bridge].

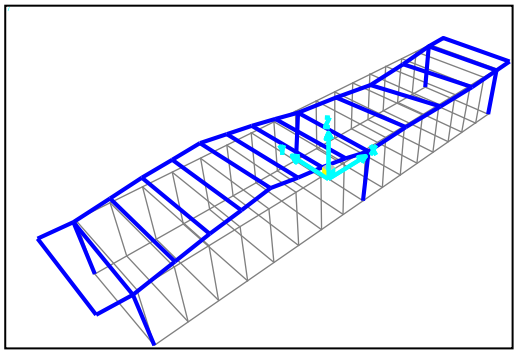

Mode6-- 4.20 Hz. [C-814 bridge].

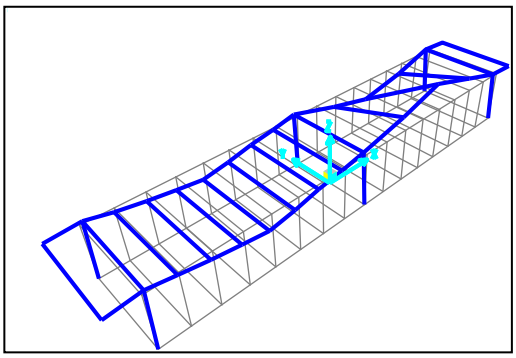

Mode7-- 5.21 Hz. [C-814 bridge].

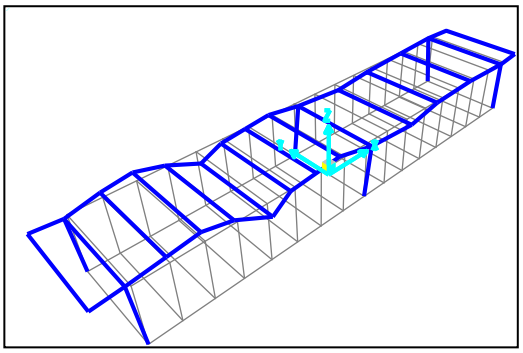

Mode8-- 6.04 Hz.[C-814 bridge].

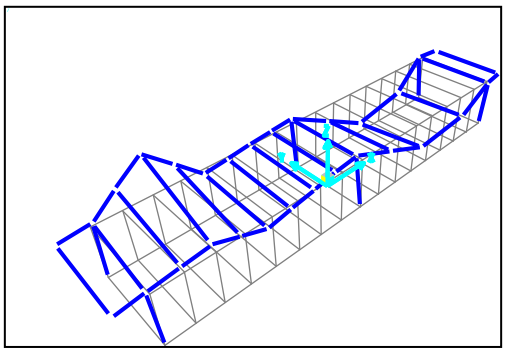

Mode9-- 6.39 Hz.[C-814 bridge].

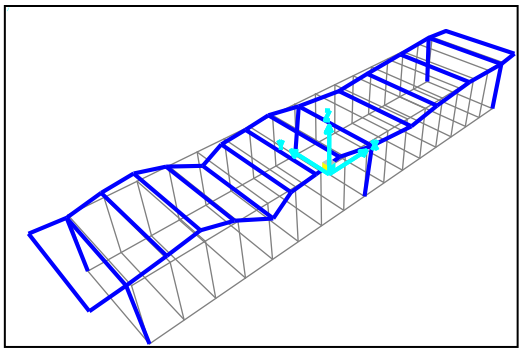

Mode10-- 7.03 Hz [C-814 bridge].

Figure 5.2 First ten mode shapes obtained by ERA.

Table 5.3 Natural frequencies and comparisons.

Mode	FEM (Hz) (1)	ERA (Hz) (2)	ERA-OKID (Hz) (3)	Ratio (2)/(1)	Ratio (3)/(1)
1	1.84	1.64	1.71	0.89	0.93
2	2.05	2.05	2.05	1.00	1.00
3	2.94	2.96	2.96	1.01	1.01
4	3.13	3.05	3.05	0.97	0.97
5	4.40	4.07	4.08	0.93	0.93
6	4.48	4.17	4.20	0.93	0.94
7	5.05	5.20	5.21	1.03	1.03
8	6.43	6.04	6.04	0.94	0.94
9	6.59	6.40	6.39	0.97	0.97
10	7.02	7.03	7.03	1.00	1.00

CHAPTER 6

CHERRY HILL BRIDGE—C123

6.1 Bridge Description

The bridge tested for this study is located in Farmington, Utah and serves as the northbound off-ramp of I-89 into the Cherry Hill area of Kaysville and Fruit Heights. The bridge consists of two equal length spans, of nearly forty-eight meters (157 ft) per span. The bridge deck from each span was supported with ten prestressed concrete W1850MG/203 girders at 1.64 meters (5.40 ft) on center. The specified minimum concrete strength for the girders is called out as 48.3 MPa (7.0 ksi).

The girders themselves are straight but the structure as a whole has a radius of curvature of 764 meters (2610 ft). The orientation of the girders is skewed over the top of the bent. The bridge deck thickness was specified as 260 millimeters (10 in.) depending on the location. The contractor that worked on the bridge however, indicated that the differences in camber between the girders caused the bridge deck thickness to vary from 200 to 450 millimeters (7.9 to 17.7 inches).

The specified minimum concrete strength for the deck concrete was 31.0 MPa (4.5 ksi). The main pier cap which supports the girders was fabricated with a rectangular cross section of 2.45 by 3.05 meters (8 by 10 ft) and spans 18.0 meters (59 ft) between supports. It is supported on each end by an octagon shaped column that has a width of 2.5 meters (8 ft 2 in.) at the center of the cross-section. The column on the east is 9.2 meters (30 ft) and the one on the west is 10.3 meters (33 ft 10 in.) from the top of pile cap to the bottom of the beam. The minimum concrete strength of each was specified as 34.5 MPa.

Figure 6.1 Elevation view of Cherry Hill Bridge.

Figure 6.2 Skewed girder over bent.

6.2 Field Testing

Forced vibration was used as an excitation source to determine the dynamic properties of the bridge. The forced vibration was induced by means of an eccentric mass shaker (see Figure 6.3). The shaker was a model 4600A, manufactured by AFB Engineering Test Systems. This model consists of two rotating masses which spin in opposite directions, creating a horizontal sinusoidal forcing (AFB Engineering Test System and Engineering Services, 1997).

To mount the shaker on the bridge deck, ten, one-inch diameter holes were drilled into the bridge deck. The holes were then filled with epoxy and a threaded steel rod was inserted and the epoxy was allowed to dry. The shaker was bolted to the rods using one inch washers to level the shaker.

Figure 6.3 Eccentric mass shaker.

6.2.1 Instrumentation

A total of 36 velocity transducers were used to measure the dynamic response of the bridge. Of this total, 30 transducers were used to measure the velocity in the longitudinal and transverse directions at discrete locations on the deck and pier cap. Six other transducers were used to measure the velocity at discrete locations in the vertical direction. Each velocity transducer comes with a calibration sheet which includes the natural frequency of the instrument, damping factor, and a transformation factor to convert from the voltage output of the instrument to velocity units.

The application of the sensors was an essential part of accurately distinguishing the possible mode shapes of the bridge. Prior to testing, it was anticipated that the transverse motion along the bridge would vary more than the longitudinal motion. For this reason 24 of the 30 horizontal velocity transducers (see Figure 6.4) were applied to measure the transverse motion along the bridge. Twenty-two of these were placed on the deck and two were place on the pier cap, one at each end. The other six were used to measure the longitudinal motion at each abutment and one was placed on the east end of the beam.

Due to the fact that only six vertical velocity transducers were available, it was decided to place all six on half of the bridge at ¼, ½, and ¾ span locations. Three accelerometers were also used to determine the response of the other half of the bridge. The layout and numbering of each instrument location is shown in Figure 6.5.

Figure 6.4 Transverse and longitudinal seismometers.

Two different force vibration tests were conducted with the forcing frequency ranging between 0.6 hertz and 20 hertz. The first frequency sweep was done with the forcing purely in the transverse direction, while the second test was done at a 45° angle thus producing a forcing component in the transverse and longitudinal directions. To facilitate the analysis, two additional accelerometers were used. One accelerometer was placed on the shaker to measure the forcing frequency and the other was used as a marker in the data.

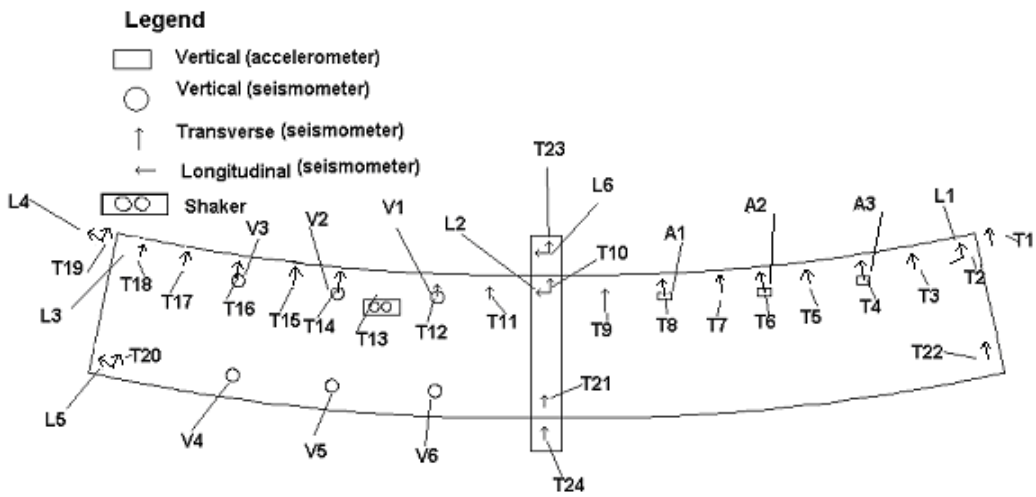

Figure 6.5 Instrument locations.

During testing an incremental increase of 0.05 hertz was used. After each increment, a settling time was allowed for the bridge to reach steady state. Once steady state was achieved the marker accelerometer located on the table was turned over and then placed back on the table, thus producing a spike which would be used to indicate usable data. The bridge was then allowed to respond for 15 to 30 seconds, depending on the forcing frequency and the sampling rate, before the forcing frequency was increased again.

6.3 Analytical Modeling

The forced vibration and ambient vibration data were collected and analyzed using system identification method. The forced vibration data was analyzed by FDD and ambient vibration data was analyzed by ERA-OKID. Finite element model was created to examine the dynamic properties of the testing bridge. Two different finite element models were generated and the results compared. The results comparisons are presented in the later section.

6.3.1 Finite Element Model

A finite-element model was developed using frame elements with the composite girder properties. The composite frame model was generated by taking each of the ten girders, adding a section of the slab on top of each girder and calculating the new properties of the combined section. The deck was divided into eight equally spaced

sections; each joint corresponded to the location of the transverse sensors that were positioned along the east side of the bridge.

This was done to allow the mode shapes of the frame model to be compared point by point with the measured forced vibration modes. The girders were divided into 8 frame sections each with the same properties, and the columns were each modeled as a single frame element.

To insure the girders and the slab moved rigidly, a frame element was placed between the two to add stiffness between each joint across the width of the bridge. The stiffeners were to add rigidity to the bridge, but at the same time not add mass; therefore a multiplier of zero was applied to the mass of the stiffeners. The moments of inertia for the stiffeners were increased until all members in the bridge deck responded as a whole.

The base of each column was assumed to be fixed and springs were applied to the joints located where the bridge attached to the abutments. The stiffness of the springs was adjusted until the desired mode shapes and frequencies were generated. The stiffness of the springs used was 1 MN/m in the longitudinal direction and 100 MN/m in the transverse direction.

A stick model and a beam model are the two different types of models generated to compare with forced vibration data and each will be described in detail below.

6.3.1.1 Stick Model

The stick model was designed with the idea of simplicity in mind. It contains relatively simple geometry and lumped properties for each frame section. It consists of 20 elements and 21 joints. Figure 6.6 is a typical picture of the stick model.

In this model the properties of each of the 10 girders and the slab were combined and the combined properties were assigned the sections labeled girders. Each span was separated into eight sections so there was a joint at each instrument location. The main beam was divided into two frame sections and each column represented one single frame section. The properties of each frame section can be found in later section and a picture of the cross-sections used along with the strength of concrete assumed in the model can be found in Figure 6.7.

Table 6.1 Stick model section properties.

Section	Area (m^2)	J (m^4)	Ix (m^4)	Iy (m^4)
Girders/slab	12.3	0.23	7.58	277
Beam	7.47	2.62	3.74	5.79
Column	5.18	0.0170	2.14	2.14

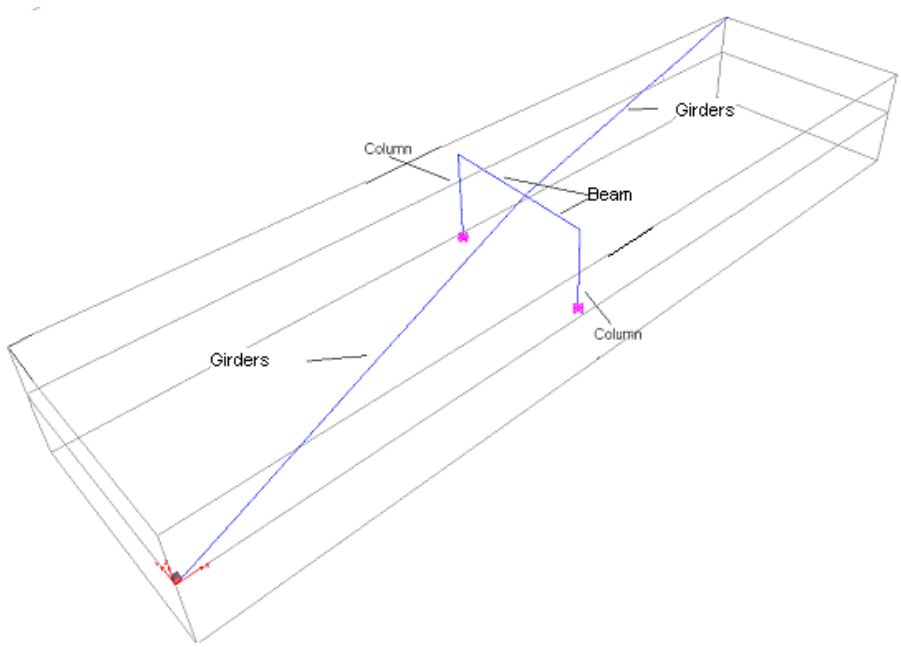

Figure 6.6 Stick model.

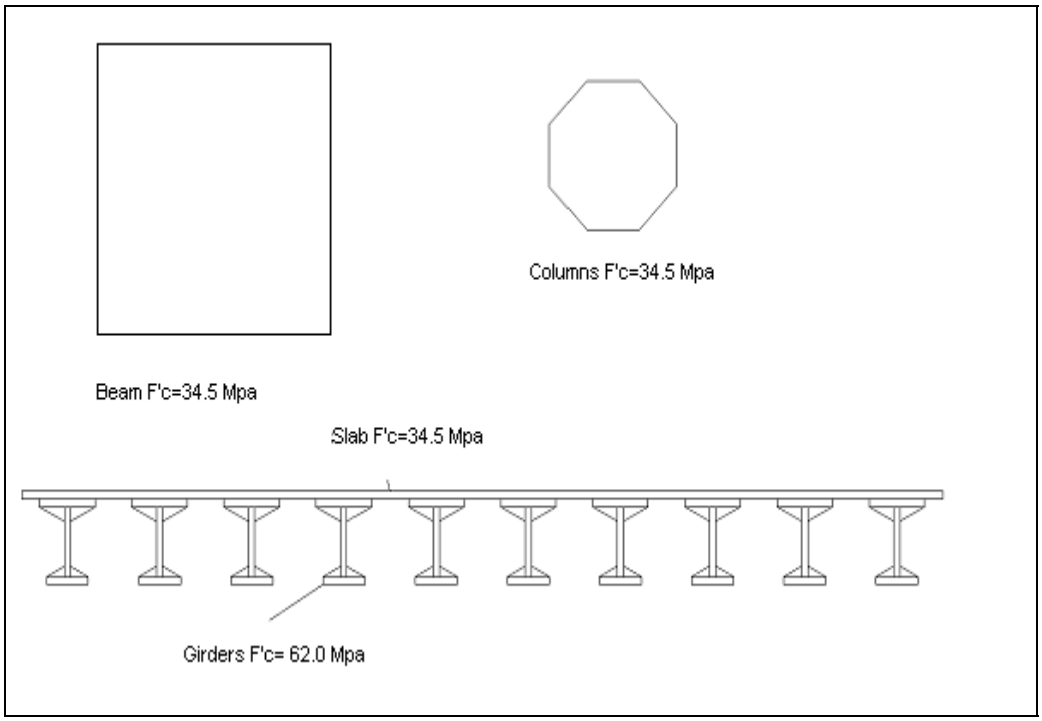

Figure 6.7 Stick model cross-sections.

The first time results were obtained from the model the frequencies obtained indicated the bridge was too soft. Because the concrete strengths specified in the plans are minimums and the equation used to calculate the modulus of elasticity of concrete is an under estimate, the actual concrete strengths used in the model were increased slightly to add stiffness and more accurately represent the structure.

Each frame element was assigned to a concrete material. This concrete material had a unit weight of 22.8 KN/m^3 and an assumed F´c of 62.0 Mpa. The modulus of elasticity was then calculated using equation 6.1. The modulus of elasticity used in the model was 37.3 Mpa.

$$E = 4735 * \sqrt{F'c} \tag{6.1}$$

The base of each column was assumed to be fixed from rotation and translation. In the forced vibration tests the abutments experienced some movement in the transverse and longitudinal directions, so fixing the end of the bridge at each abutment would not be realistic. Springs were used at each abutment to allow for movement. In the vertical direction it was assumed there was no vertical displacement in the forced vibration; therefore the same assumption was made in the model.

The stiffness of the springs was adjusted until the normal frequencies in the model were similar to the normal frequencies obtained from the forced vibration tests. The stiffness of the springs was 1E8 N/m.

The period, natural frequency, circular frequency, eigenvalues, and percent of participation mass of the first 10 modes can be found in Table 6.2. The 10 mode shapes generated form the stick models are shown in Figure 6.8.

Table 6.2 Stick model results.

Mode	Period	Frequency	CircFreq	Eigenvalue	Percent Mass Participation		
	Sec	Cyc/sec	rad/sec	rad2/sec2	Long	Trans	Vert
1	0.723	1.38	8.70	75.6	98.00	0.00	0.01
2	0.537	1.86	11.69	136.7	0.00	99.00	0.39
3	0.458	2.19	13.73	188.6	2.06	0.04	0.01
4	0.433	2.31	14.52	210.7	0.08	0.00	0.00
5	0.339	2.95	18.51	342.8	0.01	0.41	78.00
6	0.141	7.10	44.58	1987.7	0.00	0.05	5.15
7	0.120	8.33	52.33	2738.4	0.02	0.00	0.00
8	0.116	8.65	54.36	2955.0	0.00	0.01	0.00
9	0.110	9.09	57.11	3261.5	0.01	0.00	0.00
10	0.075	13.30	83.53	6978.0	0.00	0.00	6.73

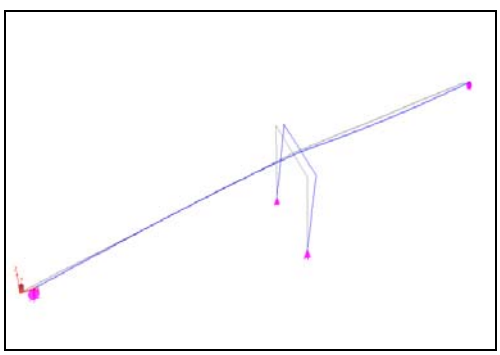

Mode 1 (1.38 Hz)

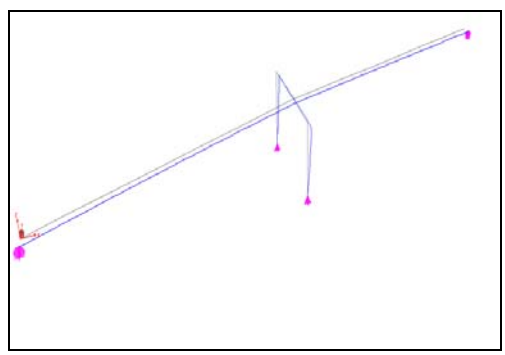

Mode 2 (1.86 Hz)

Figure 6.8 Selected modal shapes (continued on page 60).

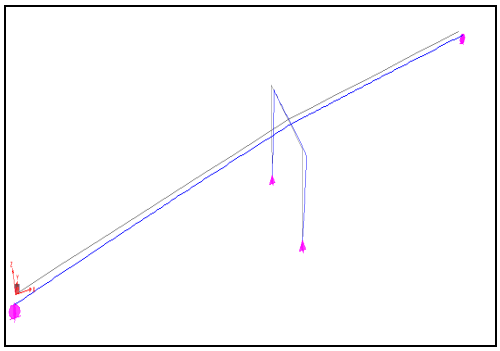

Mode 3 (2.19 Hz)

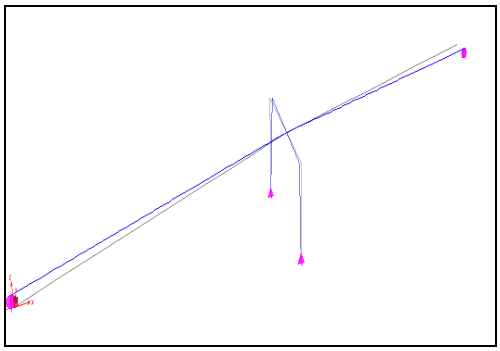

Mode 4 (2.31 Hz)

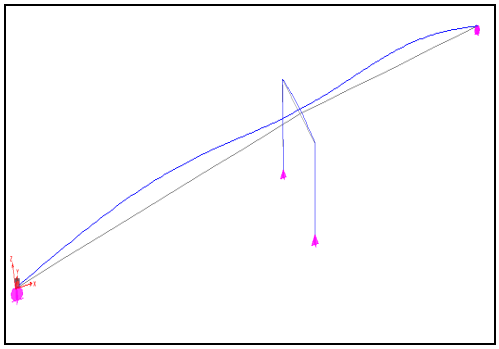

Mode 5 (2.95 Hz)

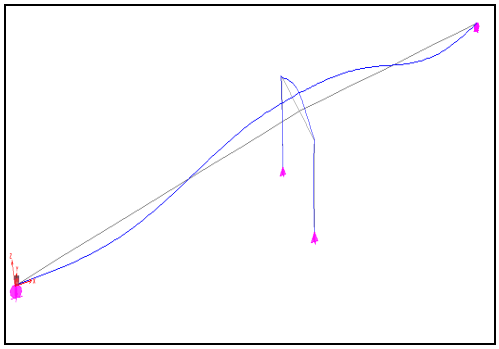

Mode 6 (7.10 Hz)

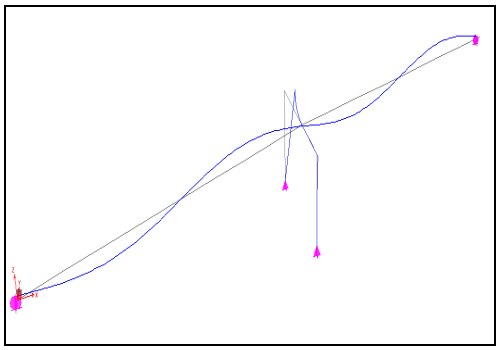

Mode 7 (8.33 Hz)

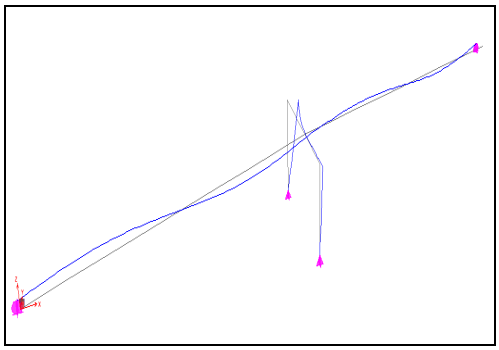

Mode 8 (8.65 Hz)

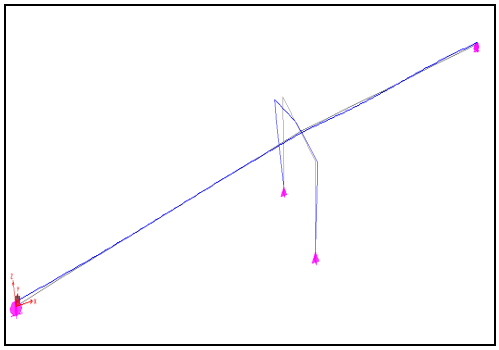

Mode 9 ((9.09 Hz)

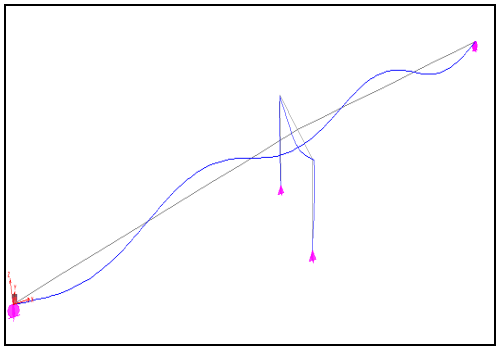

Mode 10 (13.30 Hz)

Figure 6.8 Selected modal shapes (continued from page 59).

6.3.1.2 Beam Model

The purpose of the beam model was to generate a more complicated model that would more accurately match the actual geometry of the bridge, but at the same time retain its simplicity. It contains 172 joints and 315 frame elements. Figure 6.9 is a diagram of the beam model.

The beam model was generated by taking each of the ten girders, adding a section of the slab on top of each girder and calculating the new properties of the combined section. Figure 6.10 shows the shape of the cross section of each girder frame.

Once again because of the difference in concrete strengths between the deck and the beams it was necessary to transform the slab into an equivalent 62.0 Mpa concrete to calculate the properties of the girder cross section. The spans were divided into eight equally spaced sections; each joint corresponded to the location of the transverse instruments that were positioned along the east side of the bridge.

Table 6.3 shows the periods, natural frequencies, circular frequencies, eiganvalues, and the percent mass participation of the first 10 modes. The period, natural frequency, circular frequency, eigenvalues, and percent of participation mass of the first 10 beam modes can be found in Table 6.4. The mode shapes of the first 10 modes are found in Figure 6.11.

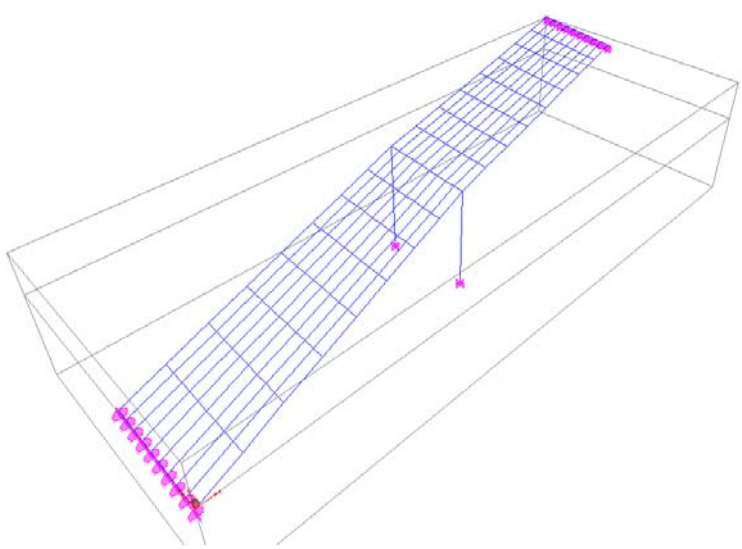

Figure 6.9 Beam model.

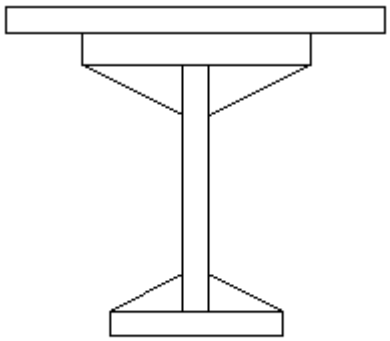

Figure 6.10 Girder frame cross-section.

Table 6.3 Beam model sectional properties.

Section	Area (m^2)	J (m^4)	Ix (m^4)	Iy (m^4)
Girders	1.22	0.008	1.35	0.257
Beam	7.47	2.62	3.74	5.79
Columns	5.18	0.167	2.14	2.14
Stiffeners	0.554	0.010	0.010	0.010

Table 6.4 Beam model results.

Mode	Period	Frequency	CircFreq	Eigenvalue	Percent Mass Participation		
	Sec	Cyc/sec	rad/sec	rad2/sec2	Long	Trans	Vert
1	0.652	1.53	9.63	92.8	94.00	0.00	0.00
2	0.351	2.85	17.90	320.5	0.02	90.00	0.22
3	0.315	3.18	19.97	398.9	5.34	0.04	0.00
4	0.282	3.55	22.29	497.0	0.09	0.01	0.10
5	0.234	4.28	26.90	723.4	0.00	0.16	71.00
6	0.227	4.41	27.74	769.3	0.00	0.00	0.82
7	0.183	5.47	34.36	1180.6	0.01	0.00	0.01
8	0.119	8.42	52.92	2800.5	0.01	8.30	0.24
9	0.087	11.55	72.57	5266.4	0.08	0.00	0.00
10	0.082	12.15	76.33	5825.5	0.00	0.00	1.72

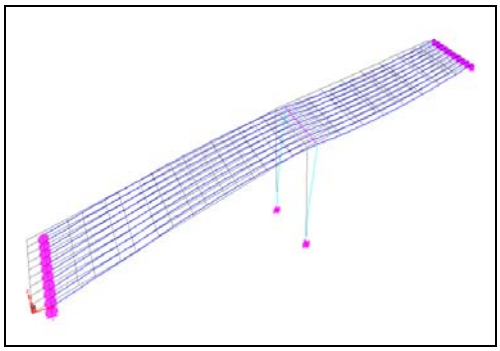

Mode 1 (1.53 Hz)

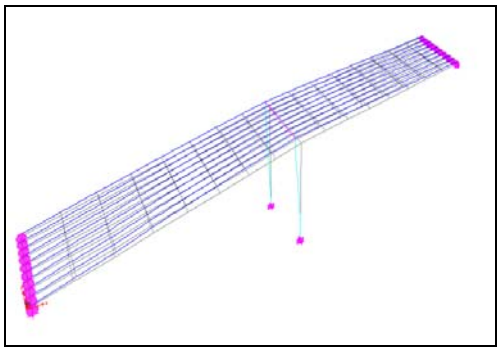

Mode 2 (2.85 Hz)

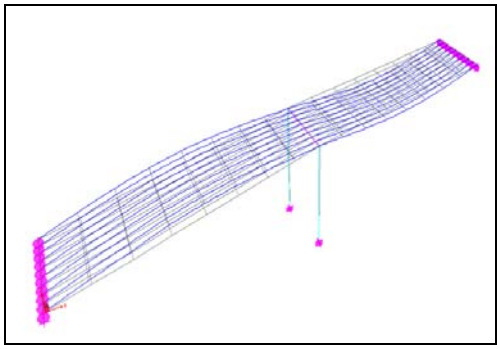

Mode 3 (3.18 Hz)

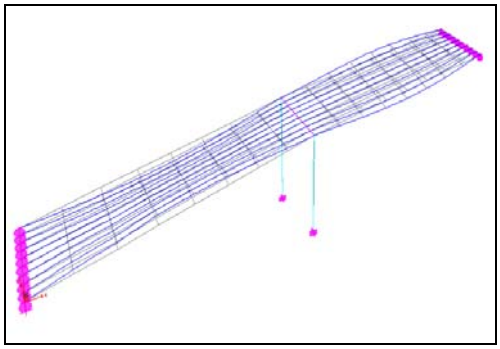

Mode 4 (3.55 Hz)

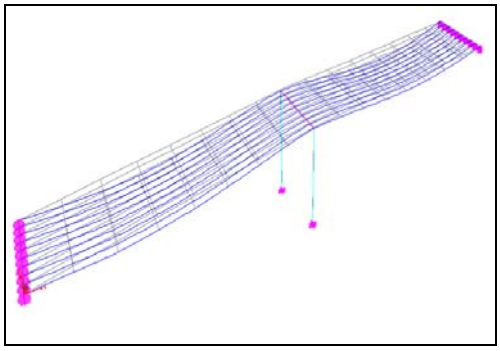

Mode 5 (4.28 Hz)

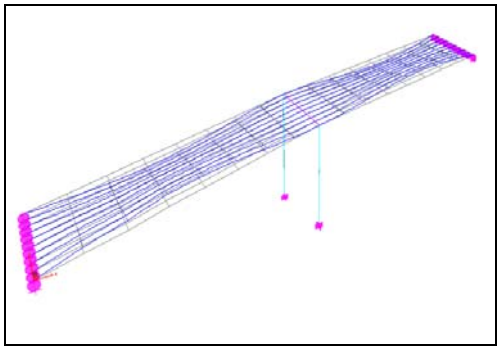

Mode 6 (4.41 Hz)

Figure 6.11 Selected modal shapes (continued on page 64).

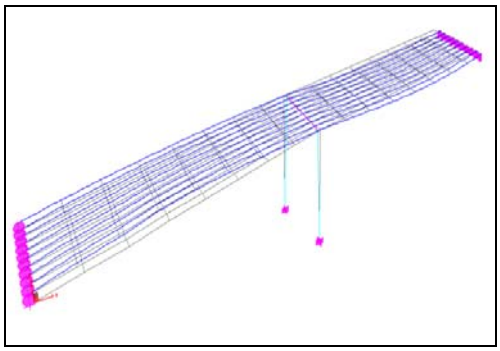

Mode 7 (5.41 Hz)

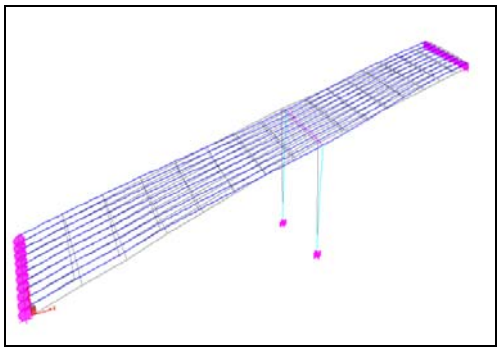

Mode 8 (8.42 Hz)

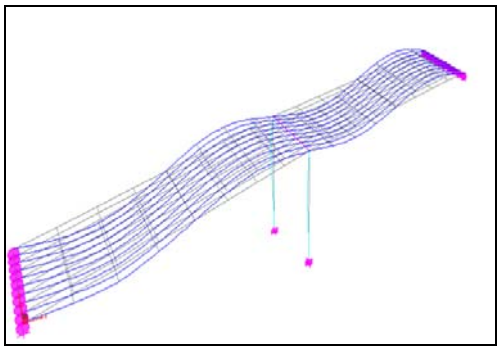

Mode 9 (11.55 Hz)

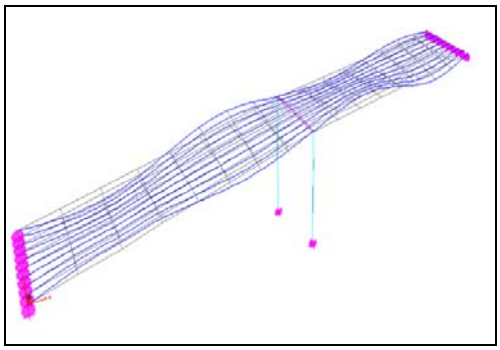

Mode 10 (12.15 Hz)

Figure 6.11 Selected modal shapes (continued from page 63).

6.3.2 System Identification Method

After the field testing was completed, the data was analyzed in order to determine the natural frequencies of the bridge. The first step was to generate normalized displacement versus frequency plots for each channel.

The displacements were then normalized by the amount of force being applied to the bridge. With the normalized displacement it was possible to locate the natural frequencies of the bridge. A plot of displacement versus frequency was produced for each sensor. The peaks of these plots, which correspond to the natural frequency of the bridge, were noted and six frequencies which appeared on the majority of the plots were selected as the natural frequencies. One other natural frequency, which did not appear on the majority of the plots, was also selected.

During the second frequency sweep, when the forcing was in the transverse and longitudinal directions, a peak appeared on some of the plots around 1.4 hertz. This peak was more prominent on the longitudinal channels. When looking at 1.4 hertz on the other plots in the transverse frequency sweep, a slight peak could be picked out when zoomed in. It was assumed that this was the natural frequency of a longitudinal mode which

received very limited excitation during the transverse forcing frequency sweep. Figure 6.12 shows the normalized displacement versus frequency for a typical sensor.

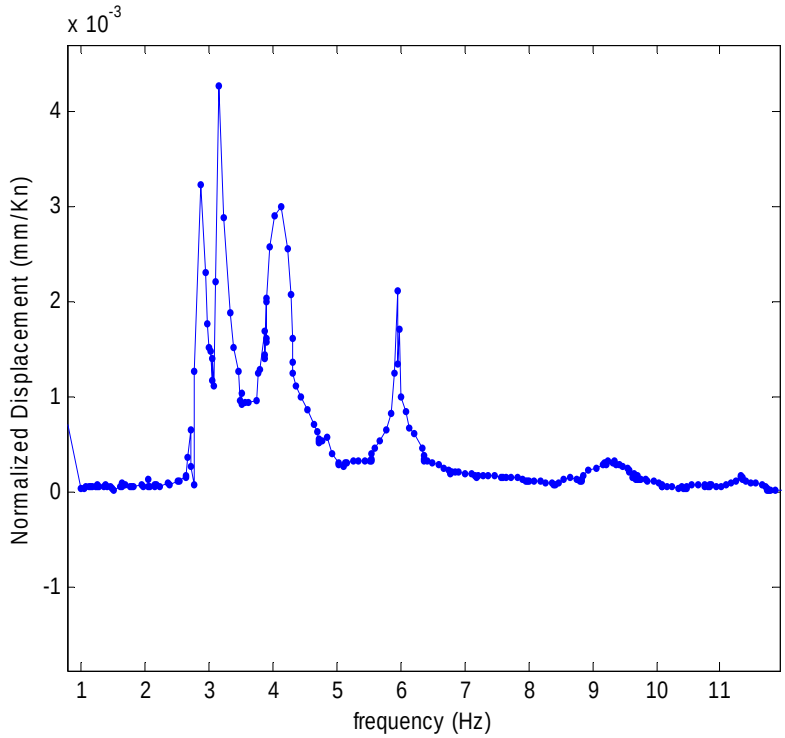

Figure 6.12 Typical normalized displacement plot.

6.4 Results

As mentioned previously, field collected forced and ambient vibration data were analyzed using two different system identification methods. Table 6.5 lists a comparison of the natural frequencies of the bridge as determined by the field test and the analytical model. Table 6.5 shows that the comparison between the measured and computer modeled frequencies are close for each of the first four measured frequencies. For the analytical model, modes 5 and 6 were not recorded during the field test. The omission of these two modes using the field data were due to the sparse distribution of vertical sensors. Overall, the frequencies calculated using the analytical modes were within 14% of the measured modes. This reasonably close correlation with this simplistic model is an encouraging indication for the feasibility of structural health monitoring.

In addition, the frequency results obtained using peak-picking method were compared to another system identification method (ERA-OKID). It is observed that the averaged identified natural frequencies are in good agreement. It is believe that the not applicable (NA) problem at the first mode is due to averaging or it may not be a dominant mode, and therefore is not identified.

Once the natural frequencies were known, mode shapes were generated for each frequency of vibration by picking the normalized displacement off each plot at the natural frequency. A Matlab routine was used to pick off these points, then each one was checked to ensure the correct point was selected.

Table 6.5 Cherry Hill Bridge comparison summary.

	Field Testing		Analytical Mode	Ratio	Ratio
Mode	Forced Vibration (Hz) (1)	Ambient Vibration (Hz) (2)	FEM (Hz) (3)	(2)/(1)	(3)/(1)
1	1.42	NA	1.53	NA	1.08
2	2.88	2.88	2.85	1.00	0.99
3	3.12	3.26	3.18	1.04	1.02
4	4.13	4.28	3.55	1.04	0.86

CHAPTER 7

CONCLUSIONS

This report has documented the performance of the bridges C-846, C-814, and C-123, which are located in the Salt Lake City, Utah area. These three instrumented and tested bridges are relatively new highway bridges. The three bridges were selected because they are representative bridges along the new alignment of the I-15 in the Salt Lake City area. The ability to model highway bridges to closely correspond with field measurements has been shown.

These bridges were tested and analyzed using finite element modeling and system identification methods. The different computer models were created based on different assumptions. Using the finite element model, the dynamic properties of the bridges were obtained. These parameters were then compared with the analysis results using system identification methods with forced and ambient vibration field collected data. Based on the analysis results for three bridges, the results between the finite element models and system identification method are in good agreement. In addition, this study addresses the success of the applications of finite element models and system identification methods.

I-15 Flyover Bridge, C846

Based on the comparison between the field testing and computed finite element model, the stick model provides some basic geometry and material properties for the structures being tested. In general, the frame model provides results with enough accuracy to be used to quickly verify the structural dynamic parameters. For research purposes, the shell model is recommended because it provides better precision of the testing structures. Mode shapes and modal frequencies for 10 modes were determined using each of the three models discussed. The field testing consisted of sinusoidal forced vibration testing and ambient vibration testing.

When comparing the first five modal frequencies of the more detailed shell model with the results from the forced vibration testing, the largest difference in frequencies was 14%. The first three modes were within 4% when comparing the model with the field results.

Vine Street Bridge, C814

This bridge was field-tested using both forced vibration testing as well as ambient vibration testing. The forcing used was a 4000 lb drop weight normally used for geotechnical site testing. This study is the first time that the authors are aware of this type of testing on a healthy, in-service highway bridge. In order to not damage the bridge or the bridge deck, the drop weight was lifted only approximately 4 inches off the deck and was dropped on a one inch thick neoprene pad.

The finite element model was compared with the results of both the forced vibration testing as well as the results of the ambient vibration testing. Each comparison was made with the first 10 identified modes. The identified modal frequencies from the forced vibration testing differed from the model by at most 11% whereas the same comparison with the ambient data differed by at most 7%. These modal correlations are extremely good, particularly since the drop weight excited predominantly vertical modes.

Cherry Hill Bridge, C123

The Cherry Hill bridge was field-tested using the sinusoidal shaker as well as ambient vibration. The bridge was modeled using both a stick as well as a beam type model. The first 4 modal frequencies obtained from the forced vibration testing differed by up to 14% from those obtained from the beam finite element model. The relatively large differences may be attributed to concrete deck thicknesses that differed substantially from the specified thicknesses and affected both the bridge stiffness as well as the mass.

The ability of using different system identification methods have been demonstrated in this report. The natural frequencies and mode shapes can be identified using many system identification methods. ERA and peak picking methods have been successfully applied to forced vibration data. On the other hand, the dynamic properties of the testing structure can be extracted using ERA-OKID and FDD methods.

Based on the results presented in this research, it was found that both methods (ERA-OKID and FDD) can be applied to ambient and forced vibration data. Also, these methods provide similar results in modal frequencies using field collected data.

Based on the results presented on the I-15 Flyover, Chapter 4, it appears that using an overlap in digital data processing did not produce better results. The results between the tests using the overlap compared to the results without the overlap are very similar. Some normalized variations were slightly higher while others were slightly lower. The difference was so insignificant that there were no benefits found to use an overlap in future analysis.

Statistical analysis was also done to determine if temperature has an effect in the ranges of the natural frequencies. The temperatures ranged from -6°C to 28°C. The average natural frequencies were found for files with temperatures from -6°C to 0°C, from 0°C to 14°C, and from 14°C to 28°C. According to the results presented in the third chapter, the effect of temperature on the natural frequencies of the bridges is inconclusive at this time.

This research has been able to better identify the natural frequencies of the bridge while giving future researchers a better idea of the ranges of natural frequencies that can be expected over the course of a year. The natural frequencies determined here will be

used in future analysis to identify changes to the dynamics of the structures. Although it appears that some natural frequencies have slight shifting, further analysis is needed to identify whether the shifts are due to the normal ranges of natural frequencies or to changes in the structural dynamics of the bridge. Some variations in natural frequencies may be due to white noise, or the lack of ambient excitation to the bridge. These natural frequencies will give a good basis for future testing and analysis of these bridges.

For computer modeling, many different assumptions were used to create the models as explained throughout the text. Variations of these assumptions caused slight variations in the modal characteristics of each of the models. Many of the assumptions are based on the geometry and material properties of the structure. While the geometry and material properties were derived from the as-built plans, it is likely that the actual geometry and material properties vary slightly from the assumed design values.

THIS PAGE INTENTIONALLY LEFT BLANK

CHAPTER 8

ACKNOWLEDGEMENTS

The authors would like to thank the Utah Department of Transportation and Civil and Environmental Engineering Department at Utah State University for the funding provided for these research projects. Special thanks to FHWA and UDOT for their support on the instrumentation. Mr. Blaine Leonard of the UDOT Research Division has been the administrative contact for this research and has been very helpful in all aspects.

The authors would like to express their appreciation to graduate and undergraduate students who spent tremendous amounts of time on helping with these projects.

THIS PAGE INTENTIONALLY LEFT BLANK

CHAPTER 9

REFERENCES

Abdel-Ghaffar, A. M., and Robert, H. S. (1985a). “Ambient vibration studies of Golden Gate Bridge I. Suspended structure.” J. Engrg. Mech., 111(4), 463-482.

Abdel-Ghaffar, A. M., and Robert, H. S. (1985b). “Ambient vibration studies of Golden Gate Bridge II. Pier-tower structure.” J. Engrg. Mech., 111(4), 483-499.

AFB Engineered Test Systems and Engineering Services. 1997. Eccentric Mass Shaker Model 4600A.

Aktan, A. E., Farhey, D. N., Helmicki, A. J., Brown, D. L., Hunt, V. J., Lee, K-. L., and Levi, A. (1997). “Structural identification for condition assessment: experimental arts.” J. Struct. Engrg., 123(12), 1674-1684.

Alampalli, S., G. Fu, and E. W. Dillon. 1995. Measured bridge vibration for detection of structural damage. Research Report. No. 165, Transportation R&D Bureau, New York City DOT, New York.

Ball, A. 2005. Modal analysis of a multi-span reverse curve steel girder bridge using computer modeling. M.S. Thesis. Utah State University, Logan, Utah. 124 p.

Bachmnann, H. B. (1992). “Case studies of structures with man-induced vibrations.” J. Struct. Engrg., 118(3), 631-647.

Benavent-Climent, A. (2005). “Shaking table tests of reinforced concrete wide beam-column connections.” Earthquake Engrg. Struct. Dyn. 34(15), 1833-1839.

Calcada, R., Cunha, A., and Delgado, R. (2002). “Dynamic analysis of metallic arch railway bridge.” J. Bridge Engrg., 7(4), 214-222.

Cawley, P., and R. D. Adam. 1979. The location of defects in structures from measurements of natural frequencies. Journal of Strain Analysis, 14(2):49-57.

Chang, C. C., Chang, T. Y. P., and Zhang, Q. W. (2001). “Ambient vibration of long-span cable-stayed bridge.” J. Bridge Engrg., 6(1), 46-53.

Chang, K-. C., and Lin, Y-. Y. (2004). “Seismic response of full-scale structures with added viscoelastic dampers.” J. Struct. Engrg., 130(4), 600-608.

Catbas, F. N., and Aktan, A. E. (2002). “Condition and damage assessment: issues and some promising indices.” J. Struct. Engrg., 128(8), 1026-1036.

Chen, X. and Kareem, A. (2005). “Validity of wind load distribution based on high frequency force balance measurements.” J. Struct. Engrg., 131(6), 984-987.

Chen, Z. M., and Yuan, G. (2000). “Design analysis of an integral lifting scaffold for super-high buildings.” Proc., Int. Symp., Civil Engineering in the 21st Century, Chinese Academy of Engineering, Beijing, 227-232.

Chotickai, P. and Bowman, M. D. (2006). “Truck models for improved fatigue life predictions of steel bridges.” J. Bridge Engrg., 11(1), 71-80.

Computers and Structures, Inc. (CSI). 1997. SAP2000 analysis reference. Volume I, Version 6.1. Computers and Structures, Inc., Berkeley, California. 417 p.

Cunha, A., Caetano, E., and Delgado, R. (2001). “Dynamic tests on large cable-stayed bridge.” J. Bridge Engrg., 6(1), 54-62.

Degrande, G. and Schillemans, L. (2001). “Free-field vibrations during the passage of a Thalys high-speed train at variable speed.” J. Sound. Vib., 247, 131-144.

DeWolf, J. T., Culmo, M. P., and Lauzon, R. G. (1998). “Connecticut’s bridge infrasturcture monitoring program for assessment.” J. Infrastruct. System, 4(2), 86- 90.

Dolce, M., Cardone, D., Ponzo, F. C., and Valente, C. (2005). “Shaking table tests on reinforced concrete frames without and with passive control systems.” Earthquake Engrg. Struct. Dyn. 34(14), 1687-1717.

Dye, T. 2002. Forced and ambient vibration testing of a permanently instrumented full scale bridge. M.S. Thesis, Utah State Univ., Logan, Utah.

Eberhard, M. O., and Marsh, M. L. (1997a). “Lateral-load response of a reinforced concrete bridge.” J. Bridge Engrg., 123(4), 451-460.

Eberhard, M. O., and Marsh, M. L. (1997b). “Lateral-load response of two reinforced concrete bents.” J. Bridge Engrg., 123(4), 461-468.

Farrar, C. R., and S. C. Doebling. 1998. Damage detection II. Field application to a large structure. Proceedings of Modal Analysis & Testing Conference, NATO Advanced Study Institute, Sesimbra, Portugal, 427-443.

Fujino, Y., Pacheco, B.M., Nakamura, S. I., and Warnitchai, P. (1993). “Synchronization of human induced walking observed during lateral vibration of a congested pedestrian bridge.” Earthquake Engrg. Struct. Dyn., 22, 741-758.

Gentile, C., and Cabrera, F. (1997). “Dynamic investigation of a repaired cable-stayed bridge.” Earthquake Engrg. and Struc. Dyn., 26(1), 41- 59.

Gioffre, M., Grigoriu, M., Kasperski, M, and Simiu, E. (2000). “Wind induced peak bending moments in low-rise building frames.” J. Engrg. Mech., 126(8), 879-881.

Gottipati, A. 2002. Finite element modeling of a six-span bridge. M.S. Thesis. Utah State University, Logan, Utah. 107 p.

Halling, M., Ball, A., Esplin, R., and Hsieh, K. H. (2004). “Forced and ambient vibration testing and modeling of highway bridges.” Proc., 13WCEE, Vancouver B.C., Canada.

Halling, M. W., I. Muhammad, and K.C. Womack. 2001. Dynamic Field Testing for condition Assessment of Bridge Bents. Journal of Structural Engineering, 127:161-167.

Hales, M. B. 2002. Long term vibration monitoring of a full-scale bridge using a permanent accelerometer array. M.S. Thesis. Utah State University, Logan, Utah. 179 p.

Hanagan, L. M. (2005). “Walking-induced floor vibration case studies.” J. Architectural Engrg., 11(1), 14-18.

Hanzlik, P., Diniz, S., Grazini, A., Grigoriu, M., and Simiu, E. (2005). “Building orientation and wind effects estimation.” J. Engrg. Mech., 131(3), 254-258.

Harik, I. E., Allen, D. L., Street, R. L., Guo, M. W., Graves, R. C., Harrison, J., and Gawry, M. J. (1997). “Free and ambient vibration of Brent-Spence Bridge.” J. Struct. Engrg., 123(9), 1262-1268.

Heckl, M., Hauck, G., and Wettschureck, R. (1996). “Structure-borne sound and vibration from rail traffic,” J. Sound Vib., 193, 175-184.

Hodson, J. D. 2001. Modal analysis of a three-span bridge using forced and ambient vibration techniques. M.S Thesis. Utah State University, Logan, UT. 176 p.

Huang, D. (2001). “Dynamic analysis of steel curved box girder bridges.” J. Bridge Engrg., 6(4), 506-513.

Jennings, P. C., Matthiesen, R. B., and Hoerner, J. B. (1971). “Forced vibration of a 22-story steel frame building.” Technical Rep No. Caltech EERL:1971.EERL-71-01., California Institute of Technology, Pasadena, California.

Jones, N. P., and Scanlan, R. H. (2001). “Theory and full-bridge modeling of wind response of cable-supported bridges.” J. Bridge Engrg., 6(6), 365-375.

Juang, J-. N. (1994). Applied System Identification. Prentice-Hall, Inc. Englewood Cliffs, New Jersey, 1994.

Kaynia, A. M., Madshus, C., and Zackrisson, P. (2000). “Ground vibration from high-speed trains: Prediction and countermeasure.” J. Geotech. Geoenviron. Eng., 126(6), 531-537.

Kim, J-. T., and Stubbs, N., (2003). “Nondestructive crack detection algorithm for full-scale bridges.” J. Struct. Engrg., 129(10), 1358-1366.

Kou, J-. W., and DeWolf, J. T. (1997). “Vibrational behavior of continuous span highway bridge-influencing variables.” J. Struct. Engrg., 123(3), 333-344.

Kramer, C., De Smet, C. A. M., and Peeters, B. (1999a). “Comparison of ambient and forced vibration testing of civil engineering structures.” Proc., 17th Int. Modal Analysis Conf. (IMAC XVII), Kissmmee, Florida.

Kramer, C., De Smet, C. A. M., and De Roeck. G. (1999b). “Z24 bridge damage detection tests.” Proc., 17th Int. Modal Analysis Conf. (IMAC XVII), Kissimmee, Florida.

Li, J., and Su, M. (1999). “The resonant vibration for a simply supported girder bridge under high-speed trains.” J. Sound Vib., 224(5), 897-915.

Li, J., Su, M., and Fan, L. (2003). “Natural frequency of railway girder bridges under vehicle loads.” J. Bridge Engrg., 8(4), 199-203.

Liu, P. L. 1995. Indentification and damage detection of trusses using modal data. Journal of Structural Engineering 121(4):599-608.

Liu, S., and Yao, J. T. P. (1978). “Structural identification concept.” ASCE J. Struct. Div., 104(12), 1845-1857.

Loland, O., and Dodds, C. J. (1976). “Experiences in developing and operating integrity monitoring system in North Sea.” Proc., 8th Annual Offshore Technology Conf., Huston, Texas, 313-319.

McManus, P. S., Hamilton, H. R., and Puckett, J. A. (2003). “Damping in cantilevered traffic signal structures under forced vibration.” J. Struct. Engrg, 129(3), 373-382.

Museros, P. and Alarcon, E. (2005). “Influence of the second bending mode on the response of high-speed bridges at resonance.” J. Struct. Engrg., 131(3), 405-415.

Nakashima, M., Matsumiya, T., Suita, K., and Liu, D. (2006). “Test on full-scale three-story steel moment frame and assessment of ability of numerical simulation to trace cyclic inelastic behavior.” Earthquake Engrg. Struct. Dyn. 35(1), 3-19.

Nielson, B. G., K. C. Womack, and M. W. Halling. 1999. Feasibility of system identification of multi-degree-of-freedom structures: Nine-span bridge case study. Transportation Research Board pre-print, January.

Oh, B. H., and B. S. Jung. 1998. Structural damage assessment with combined data of static and modal tests. Journal of Structural Engineering 124(8):956-965.

Pandey, A. K., and M. Biswas. 1994. Damage detection in structures using changes in flexibility. Journal of Sound and Vibration 169(1):3-17.

Paolucci, R. and Spinelli, D. (2006). “Ground motion induced by train passage.” J. Engrg. Mech. 132(2), 201-210.

Petty, T.S. 2002. Permanent instrumentation and testing of I-15 bridge. M.S. Thesis. Utah State University, Logan, Utah.

Ren, W. X., and G. D. De Roeck. 2002. Structural damage identification using modal data II: test verification. Journal of Structural Engineering 128(1):96-103.

Ren, W-, X., Zatar, W., and Harik, I. E. (2004). “Ambient vibration-based seismic evaluation of a continuous girder bridge.” Engrg. Struct., 26(5), 631-640.

Rigato, A., Chang, P., and Simiu, E. (2001). “Database-assisted design, standardization, and wind direction effects.” J. Struct. Engrg., 127(8), 855-860.

Salane, H. J., and J. W. Baldwin. 1990. Identification of modal properties of bridges. Journal of Structural Engineering 116(7):2008-2021.

Salawu, O. S. 1997. Detection of structural damage through changes in frequency: a review. Engineering Structure 19(9):718-723.

Salawu, O. S., and Williams, C. (1995). “Bridge assessment using forced-vibration testing.” J. Struct. Engrg., 121(2), 161-173.

Stubbs, N., and R. A. Osegueda. 1990. Global non-destructive damage evaluation

In solids. International Journal of Analytical and Experimental Modal Analysis, 5(2):67-80.

Stubbs, N., and J. T. Kim. 1996. Damage localization in structures without baseline modal parameters. American Institute of Aeronautics and Astronautics Journal 34(8):1644-1649.

Tsai, W. H., and J. C. S. Yang. 1988. Nondestructive evaluation of composite structures using system identification technique. Journal of Engineering Material and Technology, Transactions of ASME, 110(2):134-139.

Tschanz, T., and Davenport, A. G. (1983). "The base balance technique for the determination of dynamic wind loads." J. Wind. Eng. Ind. Aerodyn., 13(1-3), 429-439.

Vandiver, J. K. 1975. Detection of structural failure on fixed platforms by measurements of dynamic response. Proceedings of the 7th Annual Offshore Technology Conference, Huston, Texas, 2:243-252.

Vickery, P. J., and Skerlj, P. F. (2005). "Hurricane gust factors revisited." J. Struct. Engrg., 131(5), 825-832.

Wang, T-. L., Liu, C., Huang, D., and Shahawy, M. (2005). "Truck loading and fatigue damage analysis for girder bridges based on weight-in-motion data." J. Bridge Engrg., 10(1), 12-20.

Wheeler, J. E. (1982). "Prediction and control of pedestrian-induced vibrations in footbridges." J. Struct. Div., 108(9), 2045-2065.

Wilkinson, S. M. and Knapton, J. (2006). "Analysis and solution to human-induced lateral vibrations on a historic footbridge," J. Bridge Engrg., 11(1), 4-12.

Womack, K. C., Halling, M. W., and Bott, S. P. (2001). "Static and dynamic testing of a curved steel girder bridge in Salt Lake City, Utah." Utah DOT Research Rep. No. UT-00.13, Utah State Univ., Logan, Utah.

Wu, J. C., Lu, W. C, and Hsu, W. C. (2006). "Implementation of a feasible control design process incorporating robustness criteria for wind-excited high-rise buildings." J. Struct. Engrg. 132(1), 89-101.

Wu, J. C. and Pan, B. C. (2002). "Wind tunnel verification of actively controlled high-rise building in along-wind motion." J. Wind. Eng. Ind. Aerdyn., 90(12-15), 1933-1950.

Xu, Y. L., Ko, J. M., and Zhang, W. S. (1997). “Vibration studies of Tsing Ma suspension bridge.” J. Bridge Engrg., 2(4), 149-56.

Xu, Y. L., and Kwok, K. C. S. (1993). Mode shape corrections for wind tunnel tests of tall buildings.” Eng. Struct., 15, 618-635.

Xu, Y. L., Xia, H., and Yan, Q. S. (2003). “Dynamic response of suspension bridge to high wind and running train.” J. Bridge Engrg., 8(1), 46-55.

Yang, J. N., Agrawal, A.K., Samali, B., and Wu, J. C. (2004a). “Benchmark problem for response control of wind-excited tall buildings.” J. Engrg. Mech., 130(4), 437-446.

Yang, Y. B., Lin, C. L., Yau, J. D., and Chang, D. W. (2004b). “ Mechanism of resonance and cancellation for train-induced vibrations on bridges with elastic bearings.” J. Sound Vib., 269(1-2), 345-360.

Yang, Y. B., Yau, J. D., and Hsu, L. C. (1997). “Vibration of simple beams due to trains moving at high speeds.” Eng. Struct., 19(11), 936-944.

Yu, E., Whang, D. H., Conte, J. P., Stewart, J. P., and Wallace, J. W. (2005). “Forced vibration testing of buildings using the linear shaker seismic simulation (LSSS) testing method.” Earthquake Engrg. Struct. Dyn. 34(7), 737-761.

Yue, F., Yuan, G., Li, K., Chen, Z. M., and Wang, Z. P. (2005). “Wind load on intergral-lift scaffolds for tall building construction.” J. Struct. Engrg., 131(5), 816-824.

Zhao, J., and J. T. DeWolf. 1999. Sensitivity study for vibrational parameters used in damage detection. Journal of Structural Engineering 125(4):410-416.

THIS PAGE INTENTIONALLY LEFT BLANK

APPENDICES

THIS PAGE INTENTIONALLY LEFT BLANK

APPENDIX A

Summary of Test Instruments

To obtain the moments of inertia for this composite section, the concrete was transformed into an equivalent area of steel based on the modular ratio of the concrete to the steel. The modulus of the steel is given as 200 GPa. The modulus of elasticity of the concrete can be found using the equation:

$E_c=4{,}730\sqrt{f'c}$
Where
E_c = Modulus of elasticity of Concrete (GPa)
f'_c = Concrete Strength (MPa)

The modulus of elasticity of concrete is calculated using the formula above and found to be 25 GPa. The modular ratio, 'n,' of concrete to steel is found by using the equation:
$n= E_c / E_s$
Where
E_s = Modulus of Steel

A modular ratio of 0.125 is obtained from the equations above. The properties of the superstructure of this model were then calculated and are shown in Table A.1.

The properties for the bents were determined in a similar manner. An average of the bent dimensions shown in Appendix B was used to calculate average values for the stick model. The properties of the substructure of this model are shown in Table A.2.

The section property values for an individual column were modified by a factor of 2 to estimate the properties of the two columns at each bent with the exception of Bent 4, which has only one column.

Table A.1 Stick Model Superstructure Properties

Stick Model Superstructure Properties	
Depth	2.896 m
Width	12.924 m
Cross-sectional area	1.458 m^2
Torsional Constant	416.2 m^4
Moment of Inertia about Z	0.762 m^4
Moment of Inertia about Y	0.894 m^4
Section Modulus	475.2 m^3

Table A.2 Stick Model Substructure Properties

Stick Model Substructure Properties	
Diameter	2.200 m
Cross-sectional area	3.801 m^2
Torsional Constant	2.30 m^4
Moment of Inertia about Z	1.150 m^4
Moment of Inertia about Y	1.150 m^4
Section Modulus	1.05 m^3

Table A.3 Bridge locations of each instrument

TRANSVERSE

	JOINT #	X	Y	Z
T1	1	0	0	20
T2	5	0	13.34	20
T3	7	0	20	20
T4	10	10	26.67	20
T5	12	10	33.34	20
T6	14	10	40	20
T7	16	10	46.67	20
T8	18	10	53.34	20
T9	20	10	60	20
T10	22	10	66.67	20
T11	24	10	73.34	20
T12	26	10	80	20
T13	34	10	92.54	20
T14	36	10	98.37	20
T15	38	10	104.2	20
T16	40	10	110	20
T17	42	10	115.83	20
T18	44	10	121.7	20
T19	46	10	128.56	20
T20	48	10	135.43	20
T21	50	10	142.3	20
T22	52	10	149.17	20
T23	54	10	156.04	20
T24	56	10	162.91	20
T25	58	10	169.78	20
T26	60	10	176.65	20
T27	62	10	183.52	20
T28	44	17	121.7	17
T29	16	17	46.67	17
T30	20	17	60	17
T31	22	17	66.67	17
1-4	59	0	176.65	17
1-7	21	0	66.67	20
1-9	15	0	46.67	20
1-11	16	10	46.67	20
2-1	29	0	86.67	17
2-4	31	0	87.67	20
2-6	25	0	85.67	20
2-8	3	0	6.67	20

SHAKER LOCATION

JOINT #	X	Y	Z
30	10	86.67	17

VERTICAL

	JOINT #	X	Y	Z
V1	1	0	0	20
V2	5	0	13.34	20
V3	7	0	20	20
V4	19	0	60	20
V5	23	0	73.34	20
V6	37	0	104.2	20
V7	51	0	149.17	20
V8	10	10	26.67	20
V9	12	10	33.34	20
V10	20	10	60	20
V11	22	10	66.67	20
V12	24	10	73.34	20
V13	36	10	98.37	20
V14	38	10	104.2	20
V15	48	10	135.43	20
V16	52	10	149.17	20
1-5	59	0	176.65	17
1-6	59	0	176.65	20
1-8	21	0	66.67	20
1-10	15	0	46.67	20
1-12	16	10	46.67	20
2-3	31	0	86.67	17

LONGITUDINAL

	JOINT #	X	Y	Z
L1	31	0	87.67	20
L2	29	0	86.67	17
L3	44	10	121.7	20
L4	44	10	121.7	17
2-2	29	0	86.67	17
2-5	31	0	87.67	20
2-7	25	0	85.67	20
2-9	3	0	6.67	20

BENTS

	JOINT #	X	Y	Z
6	3 4 63 64	0 to 10	6.67	17
7	29 30 65 66	0 to 10	86.67	17
8	43 44 67 68	0 to 10	121.7	17
9	59 60 69 70	0 to 10	176.65	17

NOTE: All measurements are in meters.

THIS PAGE INTENTIONALLY LEFT BLANK

APPENDIX B

Mass Participation Ratios and Mode Shapes for Stick Model

Table B.1. Stick Model Modal Periods and Frequencies.

Stick Model Modal Periods And Frequencies					
StepNum	Period	Frequency	UX	UY	UZ
Unitless	Sec	Cyc/sec	Unitless	Unitless	Unitless
1	1.116	0.896	40.000%	38.000%	0.000%
2	0.968	1.033	53.000%	40.000%	0.000%
3	0.827	1.209	0.794%	2.824%	0.000%
4	0.758	1.320	2.226%	17.000%	0.000%
5	0.613	1.632	0.962%	0.280%	0.000%
6	0.586	1.706	0.090%	0.103%	0.000%
7	0.581	1.721	0.042%	0.012%	0.000%
8	0.564	1.773	0.016%	0.092%	0.000%
9	0.556	1.798	0.076%	0.002%	0.000%
10	0.518	1.931	0.052%	0.016%	0.000%
11	0.500	2.000	0.093%	0.009%	0.000%
12	0.474	2.109	0.012%	0.002%	0.000%
13	0.388	2.577	2.387%	0.750%	0.000%
14	0.359	2.788	0.410%	0.020%	0.000%
15	0.338	2.954	0.033%	0.008%	0.000%
16	0.262	3.820	0.098%	0.022%	0.000%
17	0.146	6.852	0.002%	0.000%	0.000%
18	0.102	9.769	0.000%	0.001%	0.000%
19	0.090	11.157	0.000%	0.000%	8.516%
20	0.088	11.334	0.000%	0.000%	7.801%

Mode 1. 0.896 Hz

Mode 2. 1.033 Hz

Mode 3. 1.209 Hz

Mode 4. 1.320 Hz

Mode 5. 1.632 Hz

Mode 6. 1.706 Hz

Mode 7. 1.721 Hz

Mode 8. 1.773 Hz

Mode 9. 1.798 Hz

Mode 10. 1.931 Hz

Mode 11. 2.000 Hz

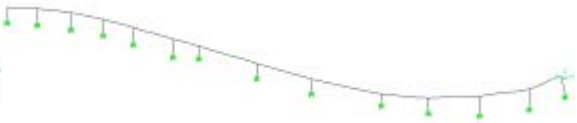

Mode 12. 2.109 Hz

Mode 13. 2.577 Hz

Mode 14. 2.788 Hz

Figure B.1 Mode shapes of Stick Model (continued on page 89).

Mode 15. 2.954 Hz

Mode 16. 3.820 Hz

Mode 17. 6.852 Hz

Mode 18. 9.769 Hz

Mode 19. 11.157 Hz

Mode20. 11.334 Hz

Figure B.1 Mode shapes of Stick Model (continued from page 88).

THIS PAGE INTENTIONALLY LEFT BLANK

APPENDIX C

General Testing Procedure and Summary of Collected Data Files

Table C.1 General testing procedure followed for each setup

Testing Procedure								
Frequency				Rate	Block Size	Settling	%	
Start	End	# Steps	Step	(sps)	(samples)	Time	Ecc	Filename
0.75	1.55	17	0.05	200	2048	10	100	0750_0155
1.55	1.8	26	0.01	200	2048	10	100	0155_0180
1.8	2.35	12	0.05	200	2048	10	100	0180_0235
2.35	2.65	31	0.01	200	2048	10	100	0235_0265
2.65	3.35	15	0.05	200	2048	10	100	0265_0335
3.35	3.75	41	0.01	200	2048	10	100	0335_0375
3.75	4.2	10	0.05	200	2048	10	100	0375_0420
4.2	4.45	26	0.01	200	2048	10	100	0420_0445
4.45	4.8	8	0.05	200	2048	10	100	0445_0480
4.8	4.95	16	0.01	200	2048	10	100	0480_0495
4.95	5.15	5	0.05	200	2048	10	100	0495_0515
5.1	5.5	41	0.01	200	2048	10	30	0510_0550
5.5	6.05	12	0.05	200	2048	10	30	0550_0605
6.05	6.3	26	0.01	200	2048	10	30	0605_0630
6.3	7.25	20	0.05	200	2048	10	30	0630_0725
7.25	7.5	26	0.01	200	2048	10	30	0725_0750
7.5	8.75	26	0.05	200	2048	10	30	0750_0875
8.75	8.95	21	0.01	200	2048	10	30	0875_0895
8.95	9	2	0.05	200	2048	10	30	0895_0900
9	9.45	46	0.01	200	2048	10	30	0900_0945
9.45	10	12	0.05	200	2048	10	30	0945_1000
9.95	10.6	66	0.01	200	2048	10	10	0995_1060
10.6	11.05	10	0.05	200	2048	10	10	1060_1105
11.05	11.3	26	0.01	200	2048	10	10	1105_1130
11.3	11.5	5	0.05	200	2048	10	10	1130_1150
11.5	11.85	36	0.01	200	2048	10	10	1150_1185
11.85	12	4	0.05	200	2048	10	10	1185_1200
12	12.4	41	0.01	200	2048	10	10	1200_1240
12.4	12.75	8	0.05	200	2048	10	10	1240_1275
12.75	12.9	16	0.01	200	2048	10	10	1275_1290
12.9	13.3	9	0.05	200	2048	10	10	1290_1330
13.3	13.65	36	0.01	200	2048	10	10	1330_1365

Table C.1 (continued from page 91).

Testing Procedure								
Frequency				Rate	Block Size	Settling	%	
Start	End	# Steps	Step	(sps)	(samples)	Time	Ecc	Filename
13.65	14.1	10	0.05	200	2048	10	10	1365_1410
14.1	14.6	51	0.01	200	2048	10	10	1410_1460
14.6	15.55	20	0.05	200	2048	10	10	1460_1555
15.55	15.8	26	0.01	200	2048	10	10	1555_1580
15.8	16.35	12	0.05	200	2048	10	10	1580_1635
16.35	16.7	36	0.01	200	2048	10	10	1635_1670
16.7	16.75	2	0.05	200	2048	10	10	1670_1675
16.75	17	26	0.01	200	2048	10	10	1675_1700
17	18.1	23	0.05	200	2048	10	10	1700_1810
18.05	19.15	45	0.025	200	2048	10	5	1805_1915
19.15	19.8	14	0.05	200	2048	10	5	1915_1980
19.8	20	21	0.01	200	2048	10	5	1980_2000
TOTALS			Steps	982	Minutes	360.07	Hours	6

Table C.2 List of data files recorded during forced vibration testing

FORCED DATA FILES

TEMPORARY ARRAY

SETUP 1	SETUP 2	SETUP 3
0750_0145	0750_0155	0750_0155
0145_0165	0155_0180	0155_0180
0165_0225	0180_0235	0180_0235
0225_0250	0235_0265	0235_0265
0250_0325	0265_0335	0265_0335
0325_0360	0335_0375	0335_0375
0360_0410	0375_0420	0375_0420
0410_0430	0420_0445	0420_0445
0430_0470	0445_0480	0445_0480
0470_0480	0480_0495	0480_0495
0480_0505	0495_0515	0495_0515
0510_0550	0510_0550	0510_0550
0550_0605	0550_0605	0550_0605
0605_0630	0605_0630	0605_0630
0630_0725	0630_0725	0630_0725
0725_0750	0725_0750	0725_0750
0750_0875	0750_0875	0750_0875
0875_0895	0875_0895	0875_0895
0895_0900	0895_0900	0895_0900
0900_0945	0900_0945	0900_0945
0945_1000	0945_1000	0945_1000
0995_1060	0995_1060	0995_1060
1060_1105	1060_1105	1060_1105
1105_1130	1105_1130	1105_1130
1130_1150	1130_1150	1130_1150
1150_1185	1150_1185	1150_1185
1185_1200	1185_1200	1185_1200
1200_1240	1200_1240	1200_1240
1240_1275	1240_1275	1240_1275
1275_1290	1275_1290	1275_1290
1290_1330	1290_1330	1290_1330
1330_1365	1330_1365	1330_1365
1365_1410	1365_1410	1365_1410
1410_1460	1410_1460	1410_1460
1460_1555	1460_1555	1460_1555
1555_1580	1555_1580	1555_1580
1580_1635	1580_1635	1580_1635
1635_1670	1635_1670	1635_1670
1670_1675	1670_1675	1670_1675
1675_1700	1675_1700	1675_1700
1700_1810	1700_1810	1700_1810
1805_1915	1805_1915	1805_1915
1915_1980	1915_1980	1915_1980
1980_2000	1980_2000	1980_2000

PERMANENT ARRAY

SETUP 1	SETUP 2	SETUP 3
0750_0145p**	0750_0155p	0750_0155p
0145_0165p**	0155_0180p	0155_0180p
0160_0165p**	0180_0235p	0180_0235p
0165_0225p**	0235_0265p	0235_0265p
0225_0250p**	0265_0335p	0265_0335p
0250_0325p**	0335_0375p	0335_0375p
0325_0360p**	0375_0420p	0375_0420p
0360_0410p**	0420_0445p	0420_0445p
0410_0430p**	0445_0480p	0445_0480p
0430_0470p**	0480_0495p	0480_0495p
0470_0480p**	0495_0515p	0495_0515p
0480_0505p**	0510_0550p	0510_0550p
0510_0550p	0550_0605p	0550_0605p
0550_0605p	0605_0630p	0605_0630p
0605_0630p	0630_0725p	0630_0725p
0630_0725p	0725_0750p	0725_0750p
0725_0750p	0750_0875p	0750_0875p
0750_0875p	0875_0895p	0875_0895p
0875_0895p	0895_0900p	0895_0900p
0895_0900p	0900_0945p	0900_0945p
0900_0945p	0945_1000p	0945_1000p
0945_1000p	0995_1060p	0995_1060p
0995_1060p	1060_1105p	1060_1105p
1060_1105p	1105_1130p	1105_1130p
1105_1130p	1130_1150p	1130_1150p
1130_1150p	1150_1185p	1150_1185p
1150_1185p	1185_1200p*	1185_1200p
1185_1200p*	1200_1240p	1200_1240p
1200_1240p*	1240_1275p	1240_1275p
1240_1275p*	1275_1290p	1275_1290p
1275_1290p*	1290_1330p	1290_1330p
1290_1330p*	1330_1365p	1330_1365p
1330_1365p*	1365_1410p	1365_1410p
1365_1410p*	1410_1460p	1410_1460p
1410_1460p*	1460_1555p	1460_1555p
1460_1555p*	1555_1580p	1555_1580p
1555_1580p*	1580_1635p	1580_1635p
1580_1635*	1635_1670p	1635_1670p
1635_1670p*	1670_1675p	1670_1675p
1670_1675p*	1675_1700p	1675_1700p
1675_1700p*	1700_1810p	1700_1810p
1700_1810p	1805_1915p	1805_1915p
1805_1915p	1915_1980p	1915_1980p
1915_1980p	1980_2000p	1980_2000p
1980_2000p		

* Indicates that analysis could not be performed due to bad

** Indicates that files were sampled at 50 samples per second

Table C.3 Correlation of instrument channels and data column assignments

TEMPORARY ARRAY

SETUP 1

Column	Location
1	T1
2	T2
3	T3
4	T4
5	T5*
6	T6
7	T7
8	T8
9	T9
10	T10
11	T11
12	T12
13	T13
14	T14
15	T15
16	T16
17	T17
18	T18
19	T19
20	T20
21	T21
22	T22
23	T23
24	T24
25	T25
26	T26
27	T27
28	T28
29	L2*
30	L1
31	V4
32	V5
33	V8
34	V10
35	V11
36	V12
37	machine

SETUP 2

Column	Location
1	T2
2	T4
3	T6
4	T7
5	T8
6	T9
7	T10
8	T11
9	T12
10	T13
11	T14
12	T15
13	T16
14	T17
15	T18
16	T19
17	T20
18	T21
19	T22
20	T23
21	T24
22	T25
23	T26
24	T27
25	T28
26	L2*
27	L1
28	V2
29	V3
30	V8
31	V9
32	V11
33	V1
34	machine

SETUP 3

Column	Location
1	T1
2	Tground
3	Lground
4	T4
5	T7
6	T9
7	T10
8	T11
9	T12
10	T13
11	T14
12	T15
13	T16
14	T17
15	V6
16	T19
17	V16
18	T21
19	T23
20	T24
21	T25
22	T26
23	L2*
24	L1
25	T29
26	T30
27	T31
28	L3
29	L4
30	V7
31	V13
32	V14
33	V15
34	A1
35	A2
36	A4
37	A3
38	A5
39	A9*
40	machine

PERMANENT ARRAY

SETUPS 1, 2, 3

Column	Location
1	1-1
2	1-2
3	1-3
4	1-4
5	1-5
6	1-6*
7	1-7
8	1-8*
9	1-9
10	1-10*
11	1-11
12	1-12*
13	2-1
14	2-2
15	2-3
16	2-4
17	2-5*
18	2-6
19	2-7*
20	2-8
21	2-9*

* Indicates the instruments were installed so a positive reading is in the negative direction.

Table C.4 Data files recorded during ambient vibration testing

AMBIENT DATA

SETUP 1		
Array	Filename	Sampling Rate
PERM	ambient_061101_250sps	250
PERM	ambient_0612_200sps**	200
PERM	ambient_0614_200sps	200
TEMP	ambient_0614	1000
TEMP	ambient1_0612	1000
TEMP	ambient1000_0611	1000
TEMP	ambient2_0612	1000
TEMP	ambient3_0612	1000

SETUP 2		
Array	Filename	Sampling Rate
PERM	ambient_0613_200sps	200
TEMP	setup2*	Unknown

* This data was recovered from a saving error. Data was lost.

SETUP 3		
Array	Filename	Sampling Rate
PERM	ambient_0619_200sps	200
PERM	ambient_0620_200sps	200
TEMP	ambient_0619**	200
TEMP	ambient_0620	1000
TEMP	ambient_0627_500sps**	500

** Files were too large to be opened by Matlab. No analysis could be performed on these.

Table C.5 Ambient vibration data files after July 2001

Date	Start Time	Temp (°F)	Temp (°C)	Wind (mph)	Recorder 1 (.evt)	rate (sps)	Recorder2 (.evt)	rate (sps)
8/30/01	18:34	81.0	27.2	7	cj001	200	br001	200
8/30/01	20:05	80.0	26.7	7	cj003	200	br003	200
8/30/01	20:49	77.0	25.0	7	cj004	200	br004	200
9/6/01	21:30	53.5	11.9	9	ck001	200	bs001	200
9/6/01	21:55	53.0	11.7	9	ck002	200	bs002	200
9/6/01	22:30	52.5	11.4	9	ck003	200	bs003	200
9/6/01	22:54	52.0	11.1	9	ck004	200	bs004	200
9/13/01	19:00	79.0	26.1	10	cl001	200	bt001	200
9/13/01	19:25	77.0	25.0	12	cl002	200	bt002	200
9/13/01	19:52	70.0	21.1	16	cl003	200	bt003	200
9/13/01	20:20	72.0	22.2	12	cl004	200	bt004	200
9/20/01	19:30	83.0	28.3	3	cm001	200	bu001	200
9/20/01	19:55	78.0	25.6	3	cm002	200	bu002	200
9/20/01	21:25	70.0	21.1	3	cm003	200	bu003	200
10/4/01	20:11	71.0	21.7	3	cq001	100	bz001	200
10/4/01	20:32	20.0	68.0	3	cq002	100	bz002	200
10/4/01	20:53	19.4	67.0	3	cq003	100	bz003	200
10/4/01	21:15	20.6	69.0	3	cq004	100	bz004	200
10/19/01	19:30	17.2	63.0	2	cz001	100		
10/19/01	19:37	16.1	61.0	2	db001	100		
10/19/01	19:58	14.4	58.0	2	db002	100		
10/19/01	20:19	14.3	57.7	3	db003	100		
10/19/01	20:40	13.3	56.0	3	db004	100		
12/17/01	10:27	-5.8	21.6	5	dj002	250		
12/18/01	10:28	-5.8	21.6	5			co002	250
1/18/02	14:12	-2.1	28.2	6	dt001	250		
1/19/02		-2.1	28.2	6			cw002	251
1/30/02	14:10	-6.0	21.2	8	dy001	250	dc001	250
2/13/02	17:09	-0.4	31.3	8	ec002	250	df002	250
2/28/02	13:04	2.5	36.5	7	ee001	250	dh001	250
3/12/02	9:40	6.1	43.0	4	eg001a	250	dj001	250
4/4/02	18:53	15.8	60.5	4	fa005	200		
4/4/02	21:58	12.2	54.0	2	fa006	200		
4/9/02	21:40	13.0	55.4	2	fa007	200		
4/11/02	16:01	15.7	60.3	9	fa008	250		
4/26/02	11:11	14.2	57.5	2	fb001	250		

APPENDIX D

Information for Peak Picking, ERA and ERA-OKID, and FDD Methods.

D.1 Peak Picking Method

There are several identification techniques available for evaluating the dynamic characteristics of structures subjected to ambient vibrations. De Roeck, Peeters, and Ren (2000) performed a study comparing two of these identification techniques; the averaged normalized power spectral density method (also called the peak picking method) and the stochastic subspace identification method based on the singular value decomposition. It was determined that both techniques can identify the eigenfrequencies and the mode shapes. Damping ratios could only be determined from the stochastic subspace method. For real applications it is suggested to use the peak picking technique since this could be done on site to judge the overall dynamic characteristics of the structure.

The peak picking method is probably the simplest method used in extracting the modal parameters from vibration data. In this method the output signals are converted into frequency response functions using the Fourier Transform. The magnitude of the frequency response can then be plotted. Natural frequencies of the structure correspond to the peaks of these plots, allowing the natural frequencies to be read or picked off of the plots. In other words, the peak-picking method found peaks on the normalized displacement plot, which correlated with natural frequencies.

This method may be used in both forced and ambient vibration data as long as the output signals have been converted from the time domain to the frequency domain. The Peak Picking program finds the peak with the largest magnitude in a given range for each instrument channel. This frequency value is recorded and stored for use in the natural frequency statistical file.

D.2 ERA and ERA-OKID Methods

Juang and Pappa (1985) developed the Eigensystem Realization Algorithm (ERA) technique for modal parameter identification and model reduction of dynamic systems using test data. A state-space model for modal parameter identification is based on Markov process or Markov parameters.

The dynamic system basically modeled as Markov process which is the output of a stochastic linear differential or difference equation. The observer/Kalman filter identification algorithm (OKID) was developed to compute the Markov parameters in a linear system (Juang et al. 1993). The method of OKID is formulated entirely in the time-domain. Kalman filter is an optimal observer in the existence of noise smoothing and it also provides the best estimation of the state space vector. It also is a very fast deadbeat observer in the absence of noise.

In theory, the OKID method is a direct Kalman filter gain approach. It does not require any prior statistical information and does not rely on sample correlation or covariance calculations. The OKID method has the advantages associated with the direct Kalman filter gain approach. It has been successfully applied to identification of real systems (Juang 1992).

The time-domain methods for modal parameter identification in the field of structures are based on the transfer function matrix which yield pulse response or Markov parameters. A Hankel matrix is usually constructed using pulse response. Hankel matrix is then used as the basis for the realization of a discrete-time state-space model.

D.3 FDD Method

According to the information provided by Brincker et al. (2001), the Frequency Domain Decomposition (FDD) technique was an expansion of the traditional frequency domain approach. Signal processing utilizing a discrete Fourier transform is the typical and traditional approach of domain decomposition. More information about Fourier transform can be found in the appendix section.

One of the advantages is that FDD does not require inputs. The reference and input can be unknown. In other words, there is no need to setup sensors on the free field. The collected data is sufficient to provide insights of the testing structure. The major disadvantage of frequency domain method is that it is mainly used for single input single output (SISO) system. Both ERA-OKID and ERADC-OKID methods can be modified to apply to multiple inputs multiple outputs (MIMO) system. Therefore, all work done by FDD method is using SISO.

The Frequency Domain Decomposition (FDD) method finds the power spectral density (PSD) matrix from the output signals by using auto spectral density functions and cross spectral density functions. As can be seen in its name, FDD falls in the category of frequency domain analysis. The power spectral density matrix is decomposed at every discrete frequency line by Singular Value Decomposition (SVD). The diagonal singular value matrix is then plotted versus frequency where the natural frequencies are represented by the peaks of this plot.

More detailed descriptions of SVD and some of its applications can be found at Lay (1996), Maia et al. (1997), Heath (2002), and Shih et al. (1989). A more complete description of this method can be found in Brincker et al. (2000) and Brincker et al. (2001).

APPENDIX E

Frequencies for Forced and Ambient Vibration

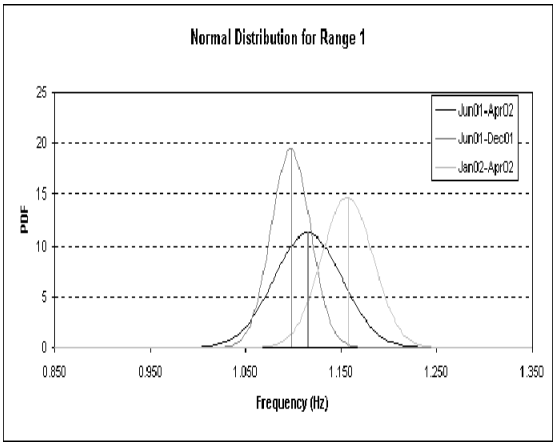

Figure E.1. Range 1.

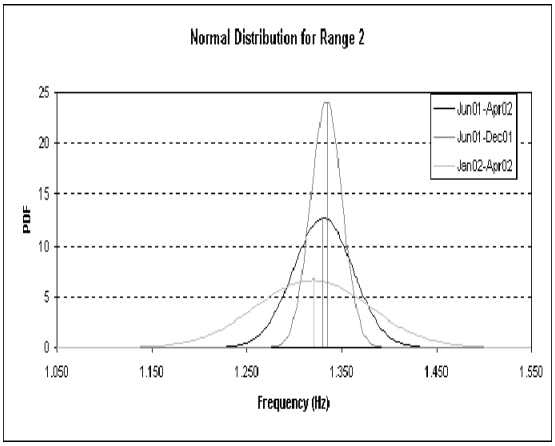

Figure E.2. Range 2.

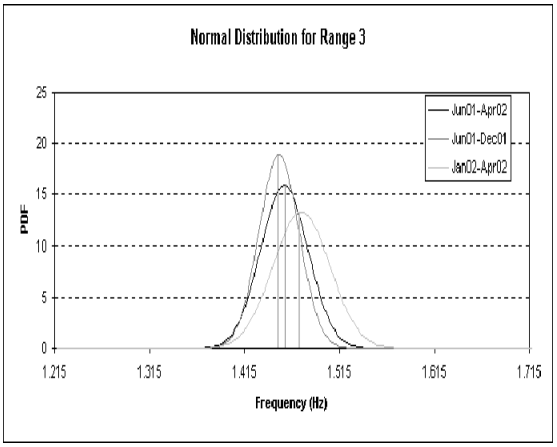

Figure E.3. Range 3.

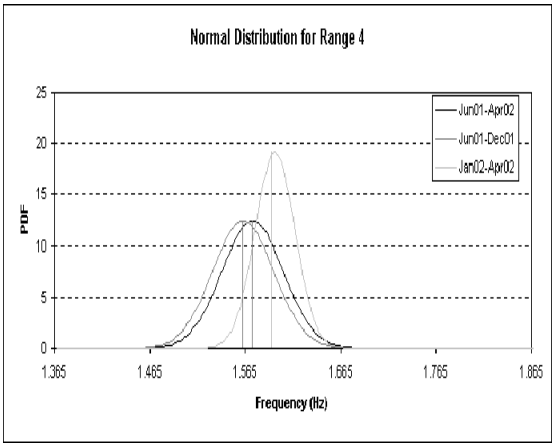

Figure E.4. Range 4.

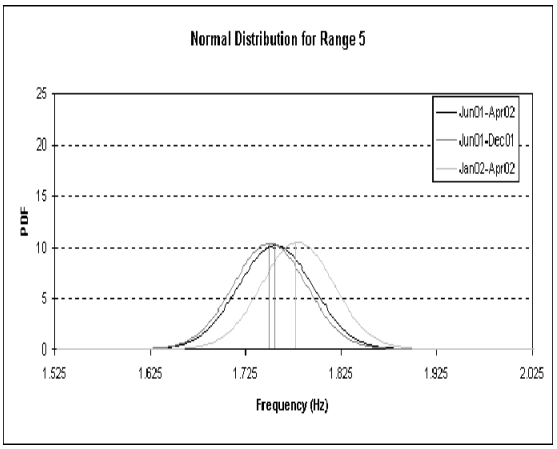

Figure E.5. Range 5.

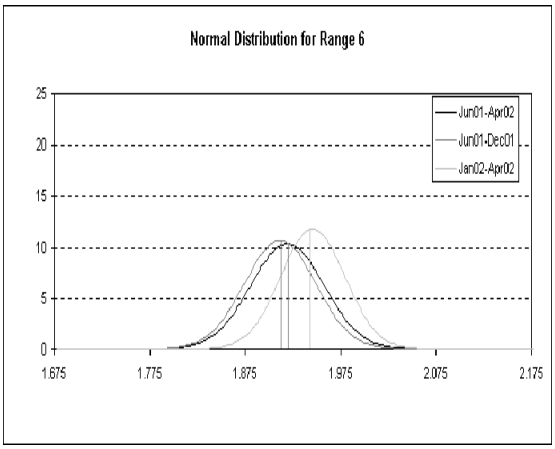

Figure E.6. Range 6.

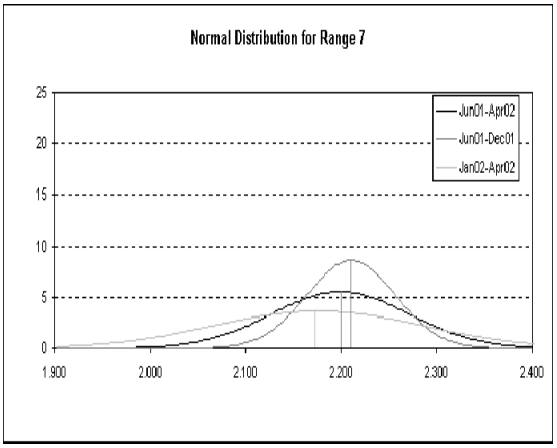

Figure E.7. Range 7.

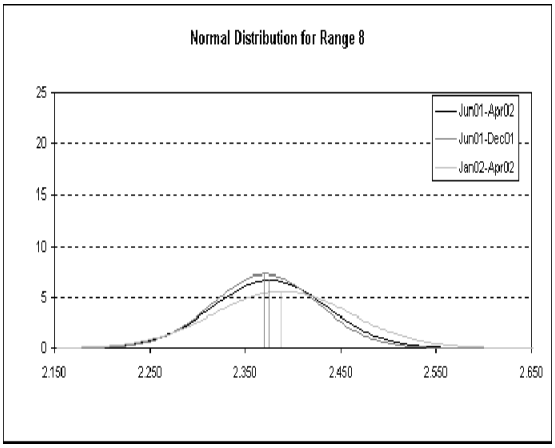

Figure E.8. Range 8.

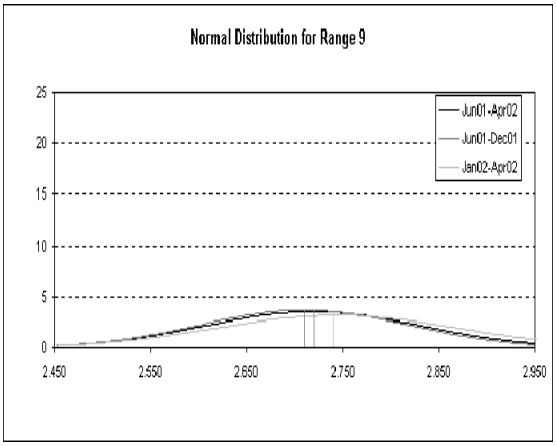

Figure E.9. Range 9.

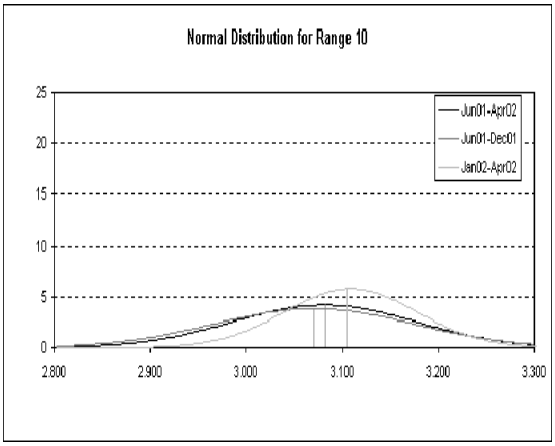

Figure E.10. Range 10.

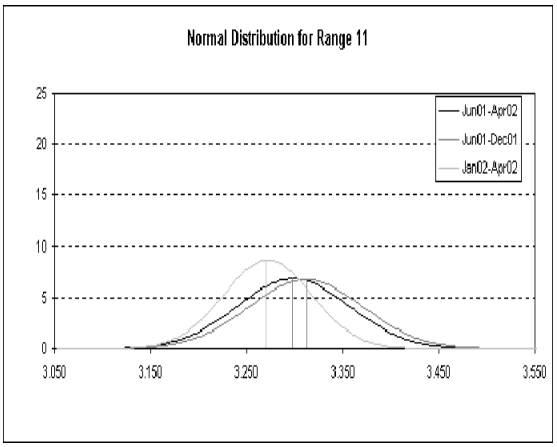

Figure E.11. Range 11.

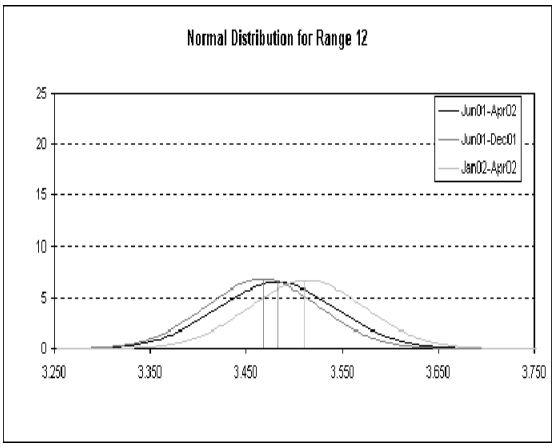

Figure E.12. Range 12.

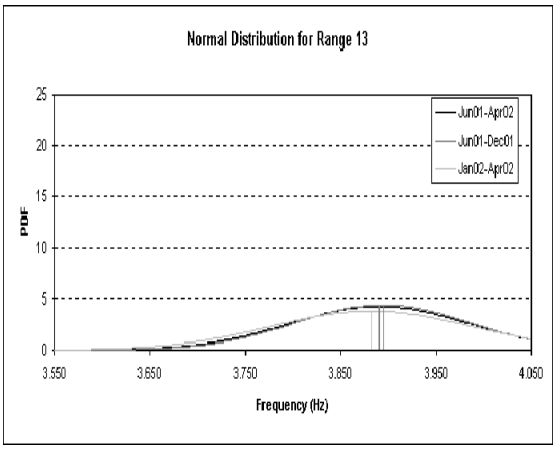

Figure E.13. Range 13.

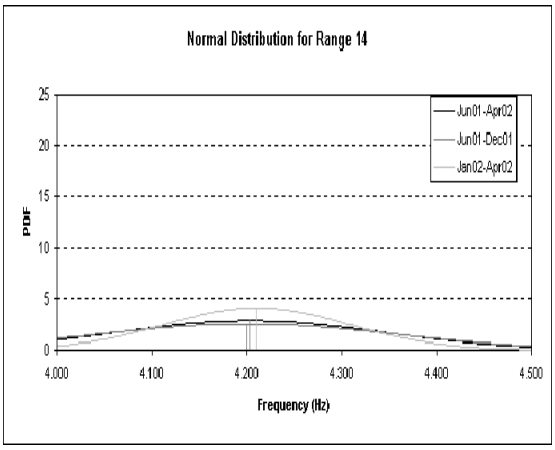

Figure E.14. Range 14.

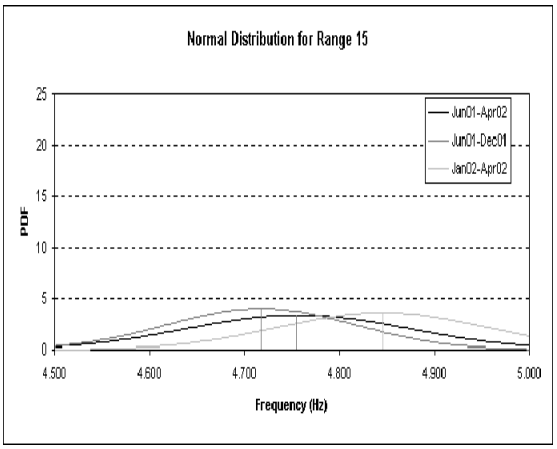

Figure E.15. Range 15.

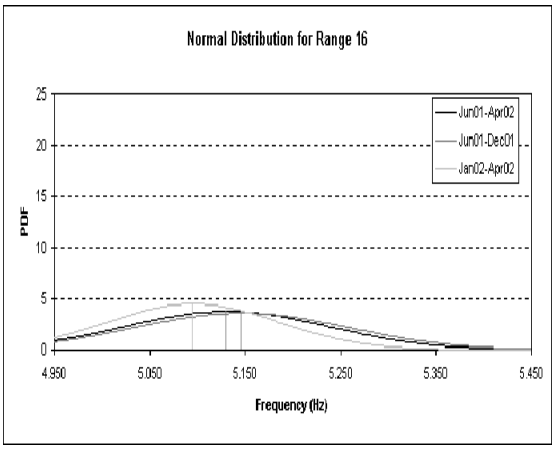

Figure E.16. Range 16.

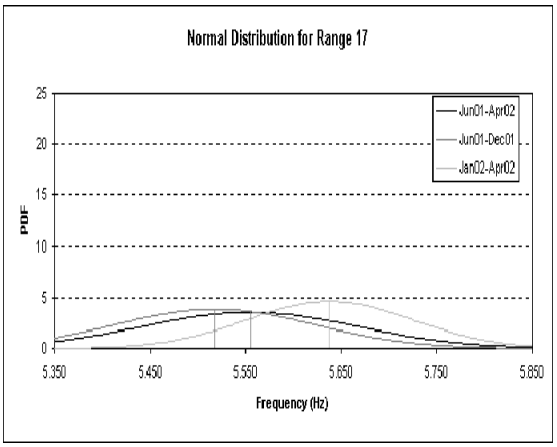

Figure E.17. Range 17.

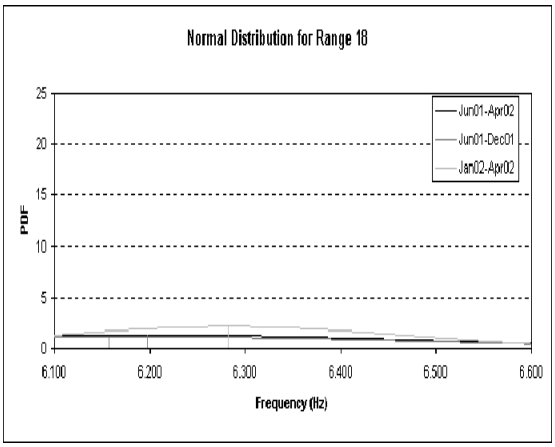

Figure E.18. Range 18.

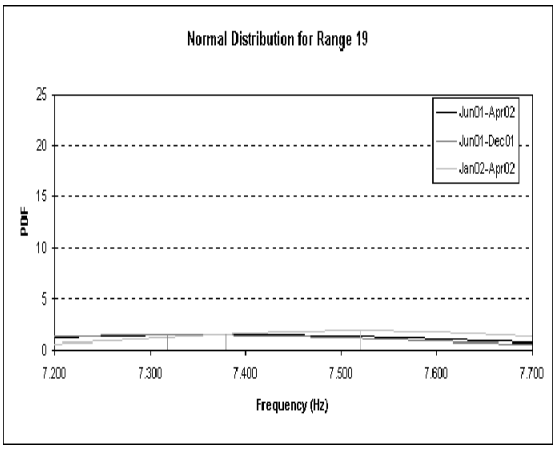

Figure E.19. Range 19.

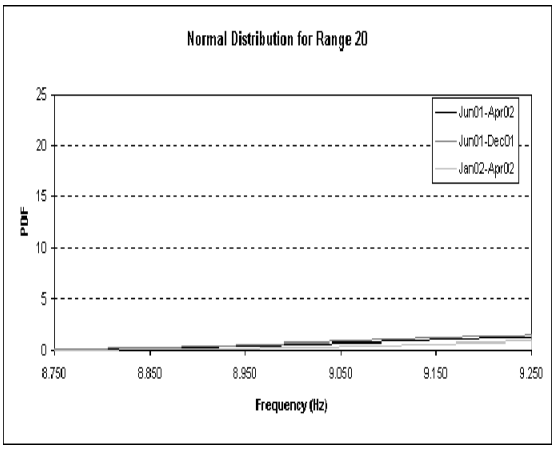

Figure E.20. Range 20

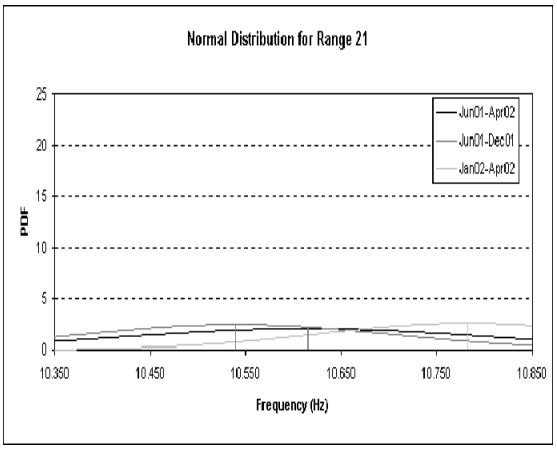

Figure E.21. Range 21.

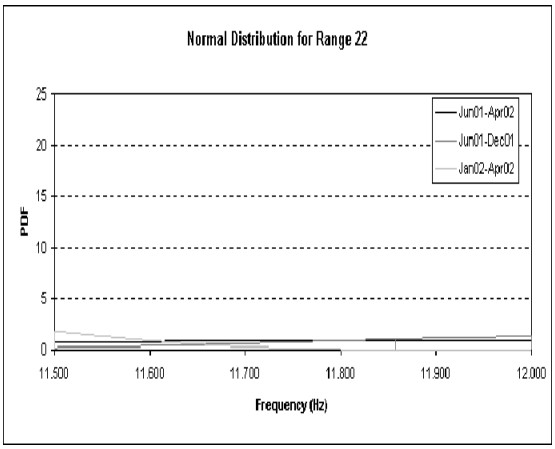

Figure E.22. Range 22.

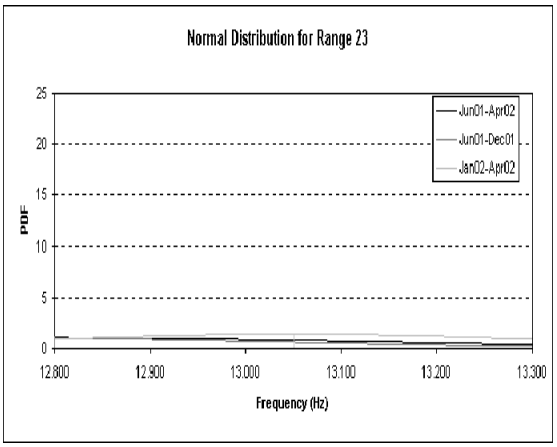

Figure E.23. Range 23.

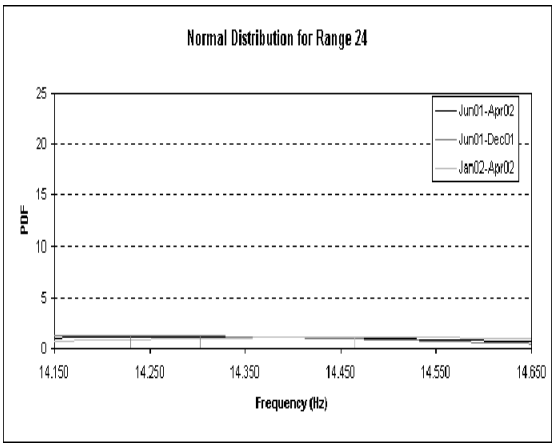

Figure E.24. Range 24.

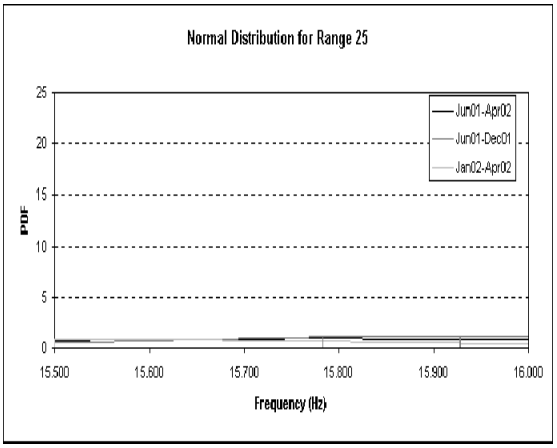

Figure E.25. Range 25.

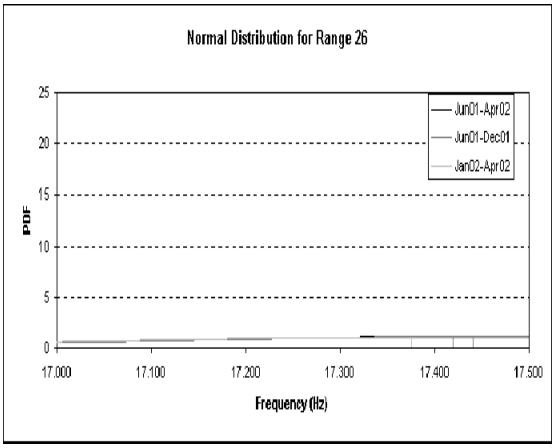

Figure E.26. Range 26.

THIS PAGE INTENTIONALLY LEFT BLANK

ACRONYMS

ERA	Eigensystem Realization Algorithm
OKID	Observer/Kalman Filter Identification Algorithm
FDD	Frequency Domain Decomposition
SISO	Single Input Single Output
MIMO	Multiple Inputs Multiple Outputs
PSD	Power Spectral Density
SVD	Single Valve Decomposition